UMTRI-92-7

AIRBAG-INDUCED SKIN ABRASIONS: DESIGN FACTORS AND INJURY MECHANISMS

FINAL REPORT

Matthew P. Reed
Lawrence W. Schneider
Richard E. Burney

The University of Michigan
Transportation Research Institute
2901 Baxter Road
Ann Arbor, Michigan 48109

Submitted To:
Honda Research and Development
1900 Harper's Way
Torrance, California 90501

May 1992

Technical Report Documentation Page

1. Report No.	2. Government Accession No.	3. Recipient's Catalog No.
UMTRI-92-7		

4. Title and Subtitle	5. Report Date
AIRBAG-INDUCED SKIN ABRASIONS: DESIGN FACTORS AND INJURY MECHANISMS	May 1992
	6. Performing Organization Code

7. Authors	8. Performing Organization Report No.
Matthew P. Reed Lawrence W. Schneider Richard E. Burney	UMTRI-92-7

9. Performing Organization Name and Address	10. Work Unit No.
The University of Michigan Transportation Research Institute 2901 Baxter Road Ann Arbor, Michigan 48109-2150	
	11. Contract or Grant No.

12. Sponsoring Agency Name and Address	13. Type of Report and Period Covered
Honda Research and Development North America 1990 Harper's Way Torrance, California 90501	Final Report
	14. Sponsoring Agency Code

15. Supplementary Notes

16. Abstract

Static laboratory deployments of driver-side airbags were conducted with human volunteers to investigate the mechanisms of airbag-induced skin abrasion and to determine the effects of several airbag design and deployment parameters on abrasion incidence and severity. Deployments were conducted with 60-L airbags, using two different airbag fabrics, two inflator capacities, and both tethered and untethered airbags. The male subjects were positioned with their anterior tibia regions located between 225 and 450 mm from the airbag module prior to the deployment. Additional tests were conducted with untethered, 40-L airbags with 190-kPa inflators at distances from 200 to 325 mm.

Higher capacity inflators were found to cause more severe abrasions than lower capacity inflators, and over a wider range of the deployment envelope. Abrasions were observed with tethered airbags between 225 and 300 mm from the airbag module and from 225 to 400 mm from the module with untethered airbags. Airbag tethering effectively eliminated abrasion at distances greater than 300 mm. Finer-weave (420-denier) fabric was not found to reduce the incidence or severity of abrasion compared with coarser-weave (840-denier) fabric.

Quantitative measurements of airbag fabric velocity and target surface pressures indicated that the primary cause of abrasions in these tests was high surface pressures resulting from the high-velocity impact of the airbag fabric with the skin. Patterns of peak surface pressure were found to correlate well with the patterns of injury, with higher surface pressures associated with greater depth of injury. Peak surface pressures greater than 175 kg/cm^2 on a rigid target surface exposed to an airbag deployment were associated with airbag fabric impacts capable of causing skin abrasion with immediate surface bleeding. Airbag deployment kinematics resulting from the fold technique were found to play an important role in determining abrasion severity. An experimental fold technique based on the findings from this study was found to reduce abrasion severity.

17. Key Words	18. Distribution Statement
Airbag, Skin Abrasion, Injury Mechanisms	

19. Security Classif. (of this report)	20. Security Classif. (of this page)	21. No. of Pages	22. Price
		126	

CONTENTS

ACKNOWLEDGMENTS

The authors would like to acknowledge the valuable contributions of Tomiji Sugimoto and James Mahern of Honda Research and Development to the conduct of the project. Their technical and administrative guidance was critical to the successful completion of the research. The authors would also like to thank Dr. Frank Filisko of the University of Michigan College of Engineering, who provided expertise in the effort to develop an abrasion-predictive surrogate skin.

Special thanks is due to Dr. Roger Haut and Cliff Beckett of Michigan State University, who offered assistance in the formulation of procedures for surface pressure measurement, and to Dr. Mats Öström, of the Institute of Forensic Medicine at the University of Umeå, Sweden, who assisted with testing of subjects and medical evaluation of injuries, as well as contributing to the development of abrasion severity rating systems.

The authors would like to recognize the important assistance provided during the testing phases of the project by Alex Wilson, Kurt Wise, and Brian Eby, who were responsible for building the test apparatus. Special recognition is due to Eric Olson for his excellent photographic documentation of the testing, and to Leda Ricci for assistance with the preparation of project reports.

Thanks also go to the researchers at outside firms who supplied expertise or product samples for the abrasion-predictive coating development effort: Dr. Louis Rua of Craig Adhesives, Inc., Bobby Johnson of Webcraft, Inc., Dr. Douglas Whittaker of Microscent, Inc., and Tony Limina of Moore Research, Inc.

LIST OF TABLES

LIST OF FIGURES

1.0 INTRODUCTION

Studies of automobile crashes in which a driver-side airbag was deployed have demonstrated that airbags can significantly reduce the incidence of severe injuries to the head and chest, particularly if a three-point belt system is also used. However, minor injuries induced by airbags have been reported. Digges, Roberts, and Morris (1989) cited field investigation data indicating that occupants had complained of abrasions to the neck and face and minor burns to the hands following airbag deployment. In a more recent study by Huelke, Roberts, and Moore (1992), similar injuries were reported, including abrasions to the face, neck, and forearms. Often these injuries were found to have occurred in low-speed crashes and with female drivers of small stature.

Airbag-induced abrasions have also been reported in laboratory tests in which human volunteers participated in dynamic tests of airbag systems. Smith, Gulash, and Baker (1974) tested young male volunteers with a driver-side airbag system on a laboratory sled over a range of impact severities. Although no significant injuries were reported, the volunteers sustained minor abrasions, ecchymosis, and erythema on the face, forearms, and hands. These skin injuries occurred even though the volunteers' faces and hands were coated with cold cream prior to testing to protect against abrasion. It should be noted that these tests were performed in the early 1970s with airbag systems that may have differed in important ways from current designs.

Research to quantify the effects of deploying airbag fabric on skin was conducted by Kikuchi *et al.* (1975) with an animal model. Using compressed air to deploy an unfolded airbag, skin and eye injuries were quantified for a range of deployment velocities. The authors recommended design guidelines for inflation velocity, impulse to the skin, and internal airbag pressure to reduce the potential for skin and eye injury. The airbag system design used in the Kikuchi study differed considerably from those

currently employed, and the use of an unfolded airbag produced airbag fabric kinematics substantially different from those of a folded airbag deployed from a steering wheel module.

To address the problem of airbag-induced skin abrasion with airbag systems similar to those currently used in vehicles, a study was conducted at UMTRI to investigate the effects of several airbag design and deployment factors on the incidence and severity of injury to human skin. The study was conducted in three phases.

1. Deployments were conducted into the anterior tibia regions of human volunteers* using eight different airbag module configurations and a range of distances between the airbag module and the skin surface. The resulting injury patterns were analyzed to determine the influence of distance, airbag tethering, inflator capacity, airbag fold techniques, and fabric material on skin injury.

2. Quantitative measurements of airbag fabric kinetics and kinematics associated with injury were made. These data were used to establish relationships between deployment parameters and skin injury and to describe the mechanisms by which the injuries observed with human skin were produced.

3. The findings from the first two phases were used to develop a method of assessing airbag skin injury potential through use of a surrogate "skin." Testing with a variety of candidate materials led to the selection of a pressure-sensitive film as the most suitable and quantitative abrasion-predictive

---

*The rights, welfare, and informed consent of the volunteer subjects who participated in this study were observed under guidelines established by the U.S. Department of Health, Education, and Welfare Policy (now Health and Human Services) on Protection of Human Subjects and accomplished under medical research design protocol standards approved by the Committee to Review Grants for Clinical Research and Investigation Involving Human Beings, Medical School, The University of Michigan.

material. A test procedure and fixture for utilizing the pressure-sensitive film to assess airbag skin injury potential was developed and is reported separately (Reed and Schneider 1992).

The methods and results of testing with human volunteers are presented in Section 2 of this report. The quantitative measurements and description of the abrasion mechanisms are presented in Section 3. The development of materials and procedures to evaluate the potential for airbag-induced abrasion using surrogates for human skin is presented in Section 4. Section 5 of the report summarizes the findings of the study and indicates directions for future research.

4

2.0 HUMAN VOLUNTEER TESTING

2.1 OVERVIEW

In this phase of the study, abrasion mechanisms and the influence of airbag design and deployment factors on the incidence and severity of skin injury were investigated using static laboratory deployments of airbags into the anterior tibia regions of male volunteers. Forty deployments were conducted using eight different airbag module configurations.

While the occupant is typically moving toward the airbag module when the airbag is deployed in a crash, this occupant velocity was believed to be small compared to the velocity of the airbag fabric exiting the module. Consequently, static laboratory tests, with the distance between the subject's skin and the airbag module fixed prior to airbag deployment, were considered suitable to examine the primary mechanisms of airbag-induced skin injury.

The anterior tibia region was chosen because of the composition of the underlying tissue and the suitability of the area for sustaining the forces applied by the airbag without serious injury. The tibia bone lies close to the skin in the medial area while the lateral aspect is comprised of skin supported by muscle. Airbag-induced abrasions in field reports are generally to the face and neck, particularly in the area of the jaw. In consideration of the tissue characteristics of these areas, it was hypothesized that the proximity of the tibia to the surface might allow observation of the effect of the airbag interaction with skin supported by bone, as well as with skin supported by softer muscle or adipose tissue.

2.2 PROCEDURES

2.2.1 Airbag Factors Investigated

Static deployment test conditions were established to investigate the influence of several airbag design and deployment parameters on the incidence and severity of skin abrasions. Standard-size (60-liter) driver-side airbags were tested for the following factors and levels, as shown in Table 1:

Factor	*Levels*
Airbag Fabric	840 / 420 denier
Tether	Present / Absent
Inflator Capacity	320 / 350 kPa
Distance	225 to 400 mm

Table 1
Matrix of Tests With Human Subjects

Airbag Fabric (denier)	Inflator Capacity (kPa)	Distance (mm)								
		200	225	250	275	300	325	350	375	400
420	320		●○ ●○ ●●			●○ ●○				
	350		●○ ●○	●○	●○	●○ ●○ ○○	●○	●○		○
840	320		○			○				
	350		○			○				
420	190	○	○	○	○	○	○			

● Tethered
○ Untethered

Airbag Fabric. All airbags tested were woven nylon with either 840- or 420-denier (D) fibers. Denier is a unit of fiber density related to the mass of the fiber per unit length. (One denier fiber has a weight of one gram per 9000 meters of fiber, or 111 μg per meter). The heavier nylon fiber has a larger diameter, producing a rougher-textured weave. It was hypothesized that fabric roughness, which is dependent on the fiber thickness, would play a role in abrasion mechanisms.

Tether. A tethered airbag has four strips of airbag material (67 x 250 mm) sewn inside the airbag between the centers of the front and rear of the airbag. From the outside of the airbag, only a 160-mm ring of stitching at the anchoring point around the center of the front of the bag is visible. These tethers restrain the maximum excursion of the center of the airbag during deployment and alter other aspects of airbag deployment kinematics. The effects of tethering on deployment kinematics were expected to influence abrasion mechanisms, especially at distances comparable to the tether length.

Inflator. Airbag inflators are commonly specified by a pressure value that corresponds to the maximum pressure attained in a sealed tank into which the inflator is deployed. The inflators used in this study were rated at 320 or 350 kPa by this method using a 28.3-liter (1-ft^3) tank. It was hypothesized that the inflator capacity would be related to the potential of the airbag to cause abrasions.

Distance. The distance from the undeployed airbag module to the skin surface was also expected to be an important variable. Tests were conducted with the target surface (*e.g.*, a subject's leg) positioned 225 to 400 mm from the center of the airbag module.

In addition to these tests, a limited number of tests were conducted with untethered, 40-liter airbags that are substantially smaller than the standard 60-liter airbags. For these smaller airbags, only the distance from the module cover to the skin was varied. Also, while most of the 60-L airbags were folded into the module cover

using the same fold technique, several tests were conducted with an experimental fold technique using the 420-D, tethered airbags. The fold technique was believed to be an important determinant of the deployment kinematics that were responsible for abrasion.

2.2.2 Airbag Laboratory

A dedicated laboratory space at UMTRI was established to meet the needs of static airbag testing, as shown in Figure 1. A 3/8-inch (9.5-mm) steel plate attached to a steel frame provides the basic platform for an airbag/steering-wheel support structure and an adjustable seat for the human volunteer. A specially designed fixture for photo documentation of the abrasions is located behind the seat, so that the volunteer can remain seated while being positioned for post-test photos. Lighting and facilities for high-speed filming deployments is provided, and an exhaust system with a capacity of 57 m^3/min (2000 ft^3/min) removes airbag inflation gases out of the laboratory through two 150-mm (6-in) ducts located near the airbag module.

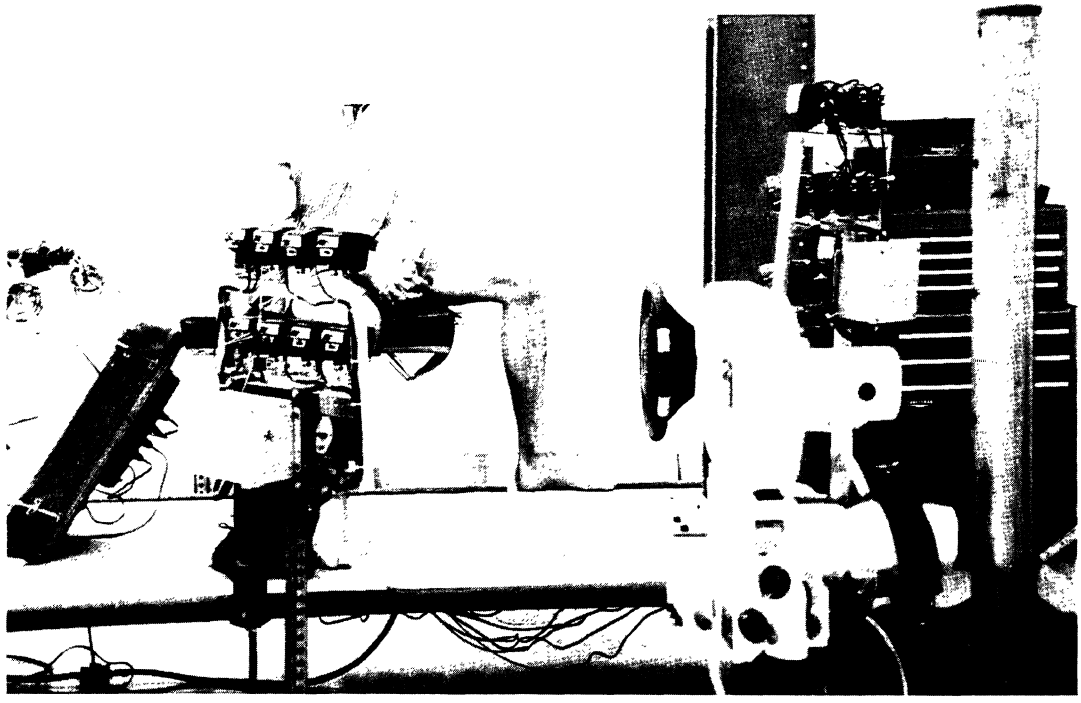

Figure 1. Airbag laboratory for static deployment testing.

2.2.3 Subjects

Nineteen male subjects participated in a total of 43 deployments. In general, two tests were conducted on each subject, with one test per leg, but some subjects volunteered for additional tests after one or both of the first two deployments caused no injury. The ages of the volunteers ranged from 20 to 40 years, with a median age of 23 years. Only four subjects were older than 30 years.

Informed consent of each subject was obtained prior to testing. Subjects were shown photos of injuries produced in previous testing and fully informed of the objectives and procedures. Preliminary deployments conducted with the investigators as subjects were used as illustrations. A physician was present during testing and provided first-aid treatment to subjects who received abrasions. The subjects were asked to participate in two deployments but were told that they could discontinue the testing at any time. Only one subject discontinued testing after the first deployment. One subject volunteered for a total of six deployments in three different test sessions separated by more than five weeks. In only one of the last two tests did substantial abrasion occur.

2.2.4 Test Protocol

The airbag module to be tested was installed in an appropriate steering wheel that was mounted to the support structure as shown in Figure 2. The steering wheel was rotated 90 degrees clockwise from the neutral position to align the predominant motion of the airbag fabric during deployment (described more fully in Section 3.1) with the long axis of the subject's leg, thereby maximizing exposure to the potentially injurious fabric motion.

Prior to testing, the anterior surfaces of the subject's lower legs were shaved with an electric razor to eliminate possible effects of hair on abrasion and to facilitate post-test evaluation of the skin condition. Also, the subject's legs were targeted on the skin along the medial, anterior edge of the tibia with colored marking pens, as shown in Figure 3.

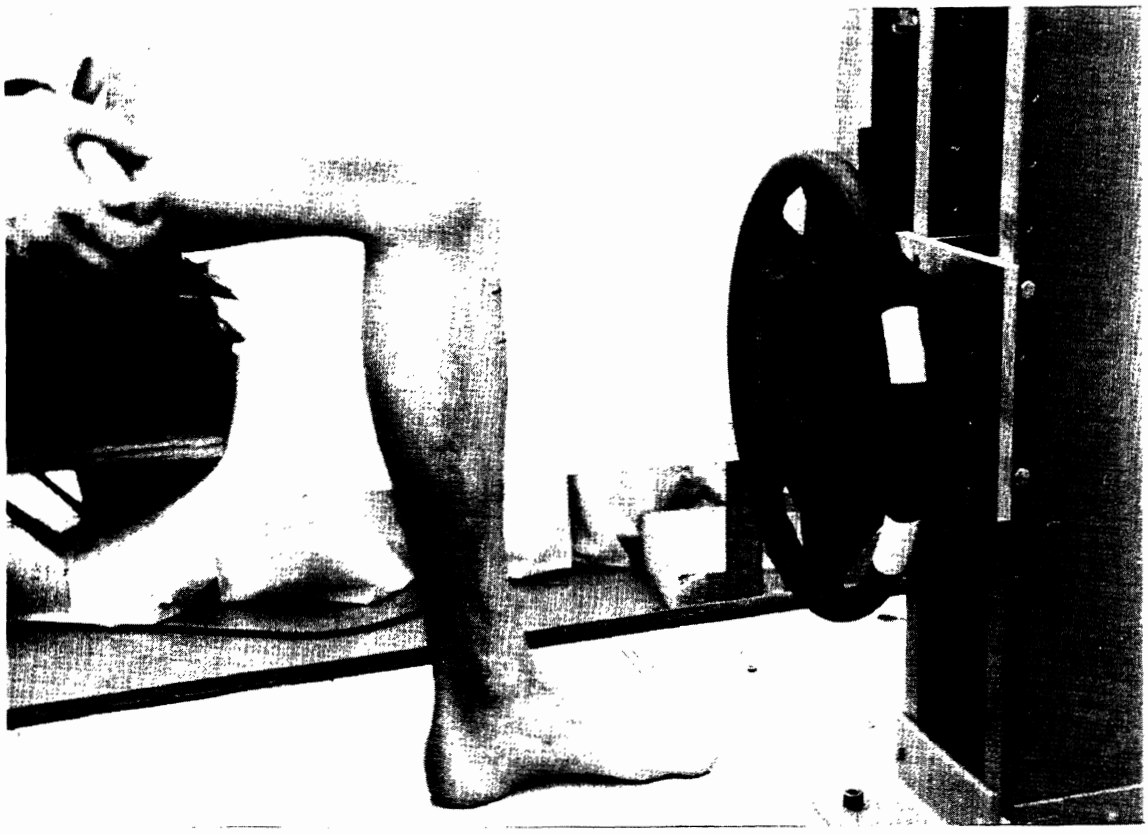

Figure 2. Airbag module and steering wheel mounted on support structure.

Four or five 20-mm-diameter circular targets were drawn at 40-mm intervals vertically along the front of the leg. During skin contact by the deploying airbag, these marks transferred to the airbag fabric, providing information on the portions of airbag fabric making contact with the leg and the type of contact (*e.g.*, stamping or smearing). A color photo of the subject's leg was taken to record the condition of the skin prior to the test.

The subject was seated on the platform so that one leg was positioned vertically in front of the airbag module at a specified distance from the undeployed module cover surface (Figure 2). The subject's leg was centered both vertically and horizontally relative to the airbag module with the subject's foot resting on a 100-mm-thick block of balsa wood. The leg was positioned so that it could easily flex at the knee during the deployment. The subject was supplied with ear protection and instructed to remain in

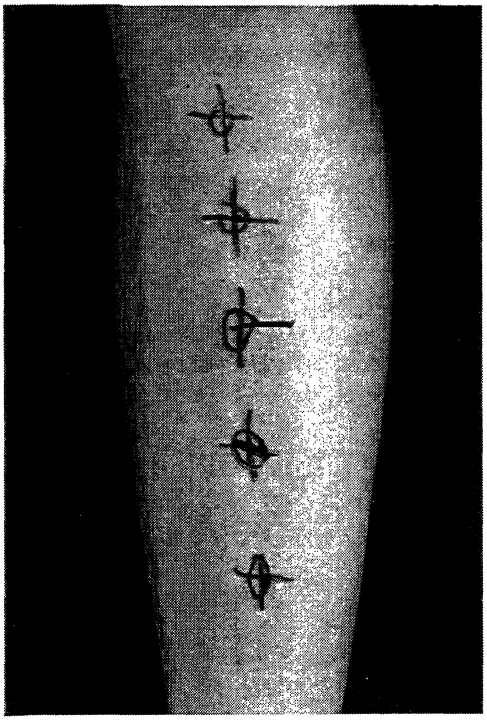

Figure 3. Pre-test photo of a subject's leg, showing marking-pen targets.

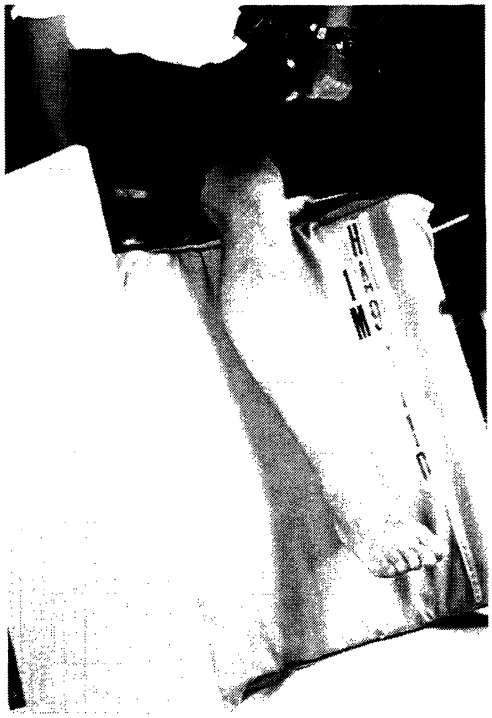

Figure 4. Subject positioned for post-test photo documentation of skin condition.

position until after the deployment. When the subject was ready, the airbag was deployed and the event recorded on high-speed film taken at a nominal speed of 3000 or 6000 frames per second.

Following the deployment, the subject rotated on the seat to place his leg in the photographic fixture on the back of the test buck, as illustrated in Figure 4. Post-test photos of the subject's leg were taken at intervals of one, five, fifteen, and thirty minutes after the deployment. First-aid treatment was provided to the subjects as necessary. In several instances, follow-up photos were taken days, weeks, or months after the test to document the condition and healing of the injuries.

2.2.5 Abrasion Severity Reporting Systems

Skin injury severities were quantified in two ways. An Abrasion Rating System (ARS) was developed to categorize the injuries according to depth, a measure of severity related to the subsequent healing of the injury. A second ranking system that provided better resolution among the injuries was used in the analysis and presentation of the injury data.

Abrasion Rating System. The ARS was developed through examination and treatment of the subjects in this study. Under the ARS, each test is assigned a number from 1 to 5 corresponding to the highest level of injury observed according to the guidelines in Table 2. This system considers only the maximum depth of injury, and does not take into account other potentially important variables such as the area of injury.

Table 2
ARS Categories

ARS Category	Description of Injury
1	No abrasion sufficiently severe to cause bleeding or seeping of fluid 24 hours or less after insult. Erythema or transient discoloration ot the skin.
2	Bleeding, weeping of fluid, or scab (eschar) formation occurring more than 30 minutes but less than 24 hours after insult.
3	Superficial partial thickness skin abrasion, characterized by damage to the upper dermal layer and fine, punctate (pin-point) bleeding from small vessels.
4	Deep partial thickness abrasion, characterized by damage to the lower layers of dermis and coarser bleeding.
5	Full thickness abrasion, extending through the dermis into the subcutaneous tissue in places.

Maximum injury depth was selected as the most important parameter for quantifying the severity of injury because of the association between injury depth and recovery time, the potential for infection, and the potential for scarring. Each of these important considerations in the prognosis of the injury is increased with increasing depth of injury. Additionally, the area of injury was found to be reasonably well correlated with the greatest depth of injury for the test. That is, tests for which a greater maximum depth of injury was observed also exhibited a larger area of injury. Figure 5 shows a schematic cross-section of human skin, indicating the relative depths of tissue damage corresponding to the various ARS levels.

The ARS has several advantages for application to airbag abrasion injuries over other categorical systems that rate an injury relative to a group of other injuries:

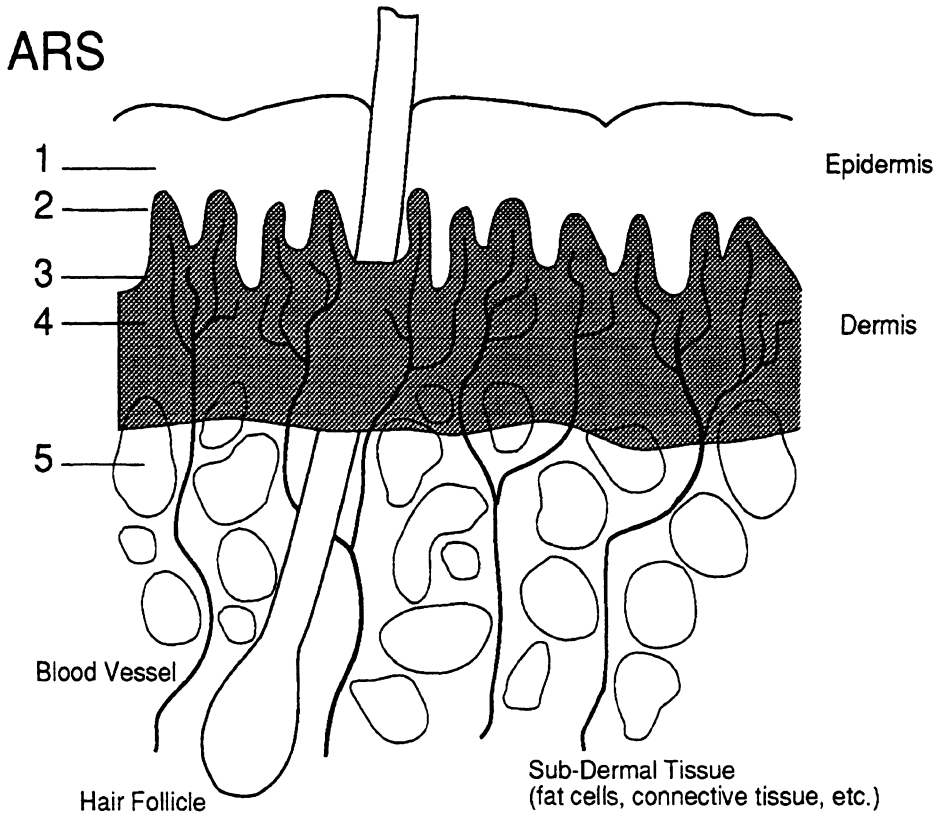

Figure 5. Schematic cross-section of human skin showing relative depth of ARS injury levels.

1. The scale may be applied by personnel who have not had experience with other airbag-induced abrasions.

2. The scale may be used to compare airbag injury severities among different researchers and studies.

3. Airbag-induced abrasion severities can be compared with the abrasions caused by other trauma.

4. The scale is objectively determined to a large extent (*i.e.*, bleeding and scab formation are readily identified) and contains categories defined without reference to other injuries.

5. The category definitions contain information that can be used to assess the clinical significance of the injuries (*e.g.*, the potential for scarring and required treatment).

One disadvantage of the ARS is the relative coarseness of the scale. Almost all of the tests in this study are classified as ARS 3 or 4. ARS 1 and 2 injuries are confined to the epidermis and have little or no clinical significance. No ARS 2 injuries are reported in this study because no follow-up was performed for subjects with less than ARS 3 injuries. ARS 5 injuries involve damage to the full dermal thickness and were not observed in this study.

Injury Rankings. Although the ARS is valuable for describing skin injuries because it is related to the physical depth of injury, the coarseness of the scale makes comparisons between the injuries produced by different airbag module configurations difficult. To facilitate these evaluations, a second injury measure was developed. The thirty-three tests performed with standard-fold, 60-L airbags were ranked from 1 (least injury) to 33 (greatest injury) on the basis of visual examination of photographs of the injuries and the notes and observations of the investigators. The primary criterion for these rankings was the area of injury, although, as noted before, the depth of injury was fairly well correlated with the area of injury for these tests. In eight of the thirty-three deployments, no skin injury was noted (ARS 1), producing a tie for least injury.

Consequently, each of the tests was assigned a ranking of 4.5 (average of ranks 1 through 8), and the least severe injury with ARS 3 was assigned a ranking of 9, following the ranking technique of Wilcoxon (Box *et al.* 1978).

Although these rankings were performed by the investigators, who were aware of the airbag configurations associated with each injury, the range of injuries was large enough that the rankings were quite easily performed. Another observer might rank the injuries slightly differently, but the results are sufficiently clear that conclusions drawn from the data would not be substantially different. The rankings are consistent with ARS levels, in that injury rankings of 25 and higher correspond to ARS 4, while those rankings between 9 and 24, inclusive, correspond to ARS 3. The photos used in the ranking process are shown in the Appendix in rank order.

2.3 RESULTS

2.3.1 Overview of Results

Skin abrasions were observed for all airbag module configurations, but with widely differing severities. No injury was noted in fourteen deployments while, in the remaining twenty-six tests, abrasions were observed with surface bleeding occurring within five minutes after the test. One subject who received particularly severe abrasions required treatment by a physician for two weeks after testing. This case is described more fully in Section 2.3.6.

The overall severity of the injuries produced in each test were quantified by two methods previously described in Section 2.2.5. Table 3 contains a complete list of human subject tests with the test configuration, ARS, and injury ranking. Three distinct types of abrasion caused by different airbag fabric motions were identified as described below.

Table 3
Results of Tests with Human Subjects

Test Number	Bag Fabric (denier)	Inflator (kPa)	Tethered/ Untethered	Distance (mm)	ARS (1 – 5)	Injury Rank (4.5 – 33)
HA91110	420	320	T	225	3	14
HA9152	420	320	T	225	3	24
HA9167	420	320	T	225	3	19
HA9168	420	320	T	225	3	21
HA9148	420	320	T	300	1	4.5
HA9169	420	320	T	300	1	4.5
HA91132	420	320	U	225	3	20
HA9153	420	320	U	225	4	27
HA9149	420	320	U	300	1	4.5
HA9170	420	320	U	300	1	4.5
HA9107	420	350	T	225	4	28
HA9150	420	350	T	225	4	32
HA9105	420	350	T	250	3	10
HA9124	420	350	T	275	3	18
HA9109	420	350	T	300	3	12
HA9146	420	350	T	300	3	13
HA9122	420	350	T	325	1	4.5
HA9111	420	350	T	350	1	4.5
HA9108	420	350	U	225	4	29
HA9151	420	350	U	225	4	33
HA9106	420	350	U	250	4	26
HA9125	420	350	U	275	3	17
HA9110	420	350	U	300	4	31
HA9147	420	350	U	300	3	22
HA9165	420	350	U	300	3	23
HA9166	420	350	U	300	3	11
HA9123	420	350	U	325	3	16
HA9112	420	350	U	350	4	30
HA9113	420	350	U	400	1	4.5
HA9126	840	350	U	300	3	9
HA9127	840	320	U	300	1	4.5
HA9154	840	350	U	225	4	25
HA9155	840	320	U	225	3	15
40-L Airbags						
HA91106	420	190	U	200	3	
HA91101	420	190	U	225	1	
HA91100	420	190	U	250	1	
HA9199	420	190	U	275	1	
HA9198	420	190	U	300	1	
HA91108	420	190	U	325	1	

2.3.2 Classification of Abrasion Types

The abrasions observed in these tests can be classified into three groups: wing abrasions, stamp abrasions, and slap abrasions. Table 4 shows the airbag configuration and portion of fabric material associated with each. Figure 6 shows examples of the three types of abrasion in post-test photos.

Wing abrasions refer to injuries produced by flaps of the unfolding airbag fabric impacting and wiping across the skin. Because of the shape and motion of these fabric flaps, they are described in this report as "wings." Figure 7 is a film frame taken from the high-speed film of a deployment, showing the airbag wings at the moment of contact with the skin. Wing abrasions occurred only for initial distances between the skin and the airbag module cover of 250 mm or less because swinging action of the airbag fabric flaps reached only to that distance. This injury type was produced by all standard-fold airbag configurations with varying degrees of severity.

Figure 8 shows an area of airbag material near the seam after a deployment that caused a wing abrasion. Colored markings from the subject's leg in the area of a wing abrasion have transferred to the portion of airbag fabric that formed the end of the upper airbag "wing" when the airbag first contacted the leg. The airbag seam was at or near the leading edge of the airbag when the wing contacted the leg, resulting in a distinctive abrasion corresponding to the pattern of the seam. A typical abrasion due to an airbag seam is visible in Figure 6a.

Table 4
Injury Types, Associated Deployment Conditions, and Region of Fabric Causing Injury

Abrasion Type	Airbag Configurations	Distances	Fabric Region
Wing	All Configurations	< 250 mm	Seam
Stamp	350-kPa Tethered	300 mm	Center
Slap	350-kPa Untethered	300 to 400 mm	Center

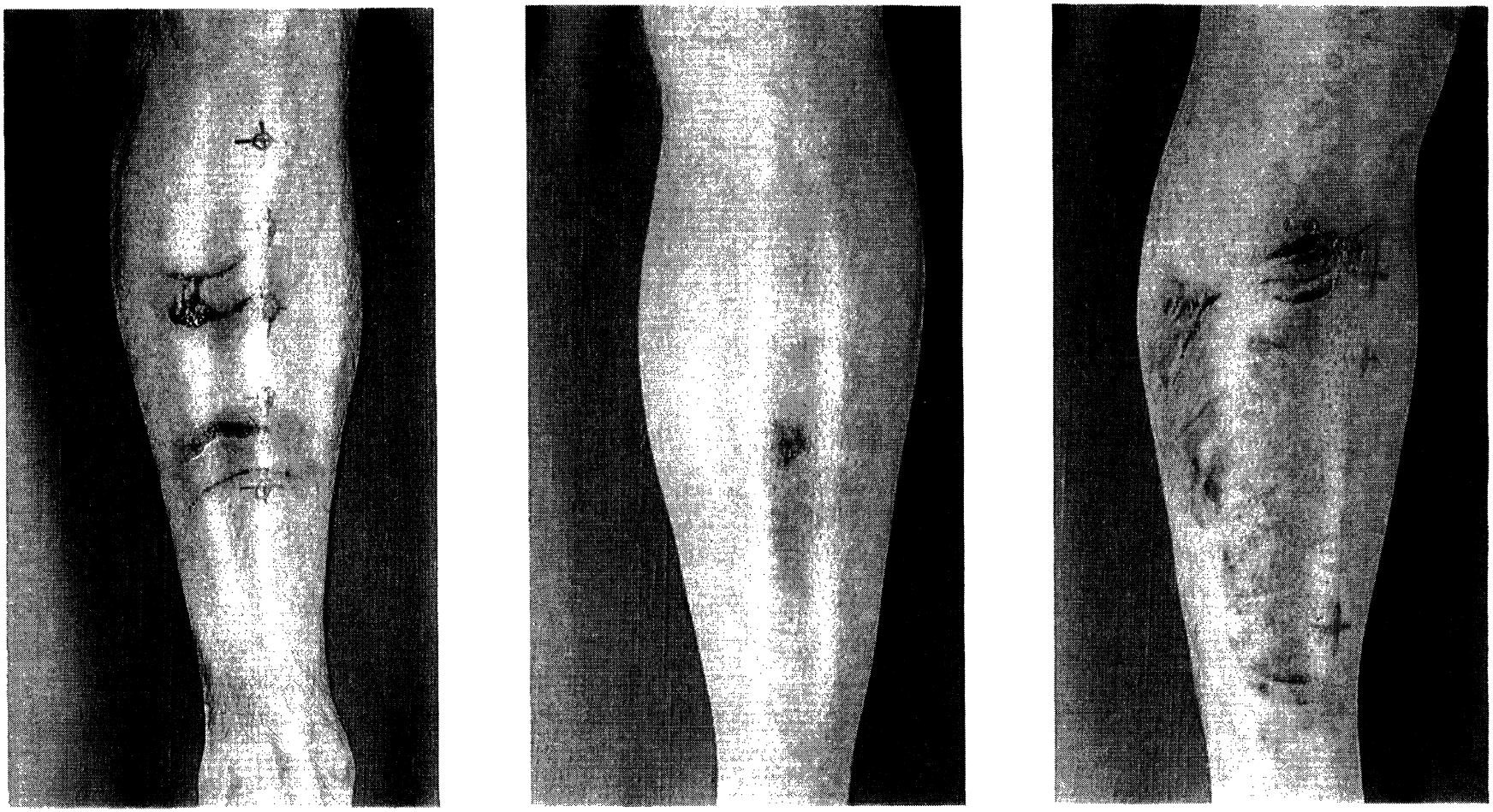

(a) (b) (c)

Figure 6. Post-test photos showing the three injury types: (a) wing abrasions, (b) stamp abrasions, and (c) slap abrasions.

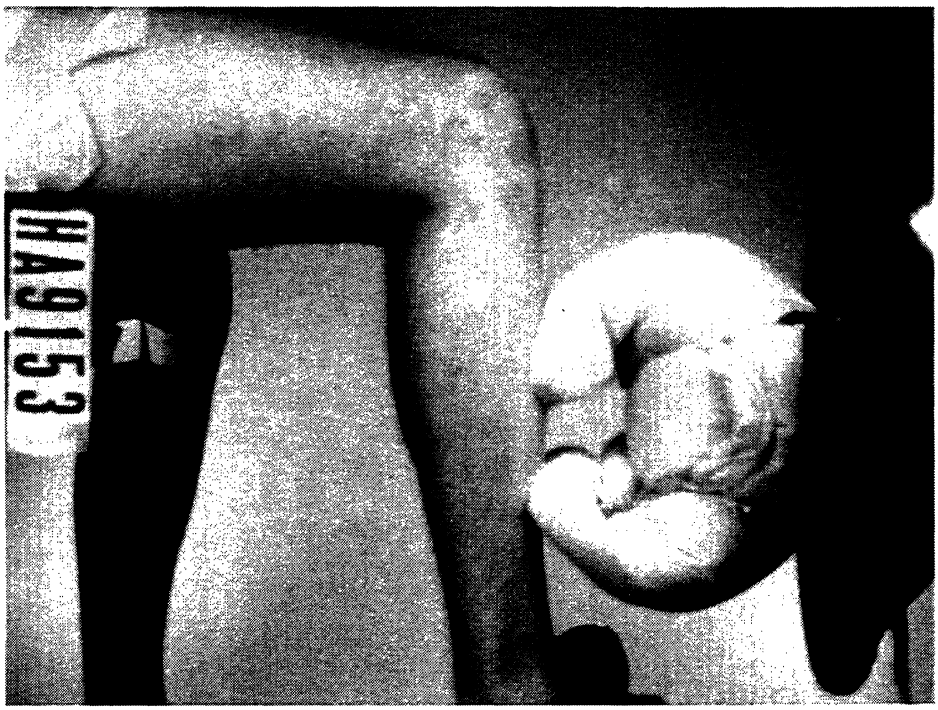

Figure 7. Film frame taken from high-speed film of a deployment showing airbag "wings."

Stamp abrasions were produced by a normal (*i.e.*, perpendicular) impact of the skin by the fabric at the center of the airbag. Because there was little lateral movement of the airbag fabric, much of the epidermis often remained intact over the injury, although it was subsequently shed during healing of the damaged dermal layers. These injuries became apparent through blood pooling immediately below the epidermis and subsequent surface bleeding as the blood broke through the epidermis. This injury type was observed with tethered airbags and 350-kPa inflators at 250 and 300 mm from the airbag module. The stamping action of the airbag responsible for this type of injury can be observed in the colored markings transferred from the subject's leg to the airbag during the deployment. Figure 9 shows a tethered airbag that produced a stamp abrasion, showing cleanly defined markings that indicate an airbag fabric motion perpendicular to the skin during contact.

Slap abrasions were observed with untethered airbags at distances from 250 to 400 mm. This type of abrasion is less clearly understood, but the injuries appear to be caused by approximately normally-directed impacts of airbag fabric with the leg (see

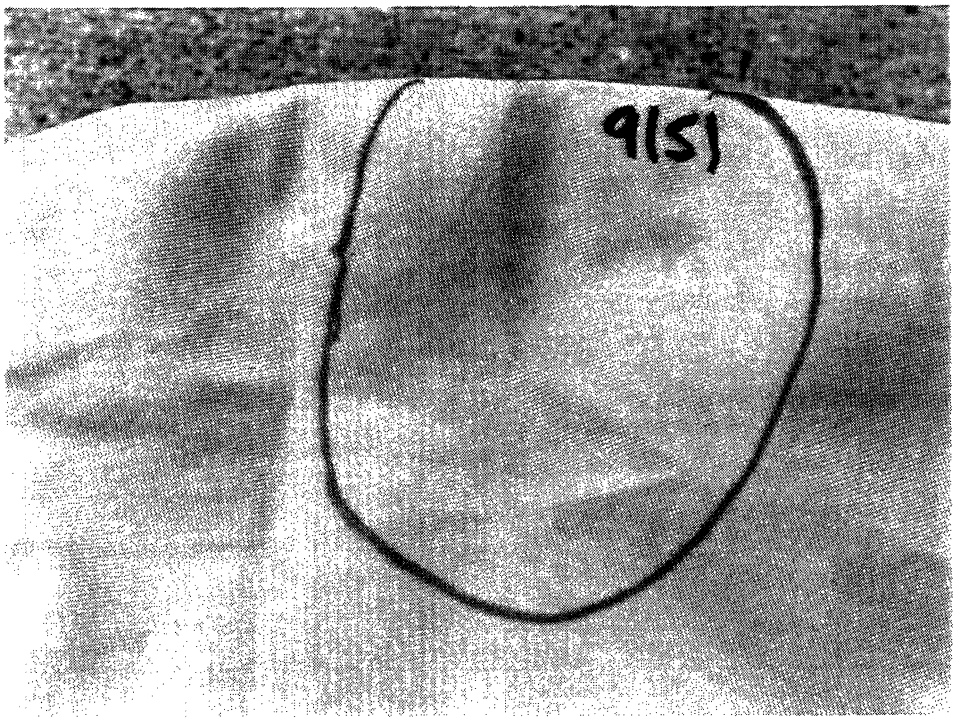

Figure 8. Section of airbag material near seam after a wing abrasion event showing markings transferred from the subject's leg.

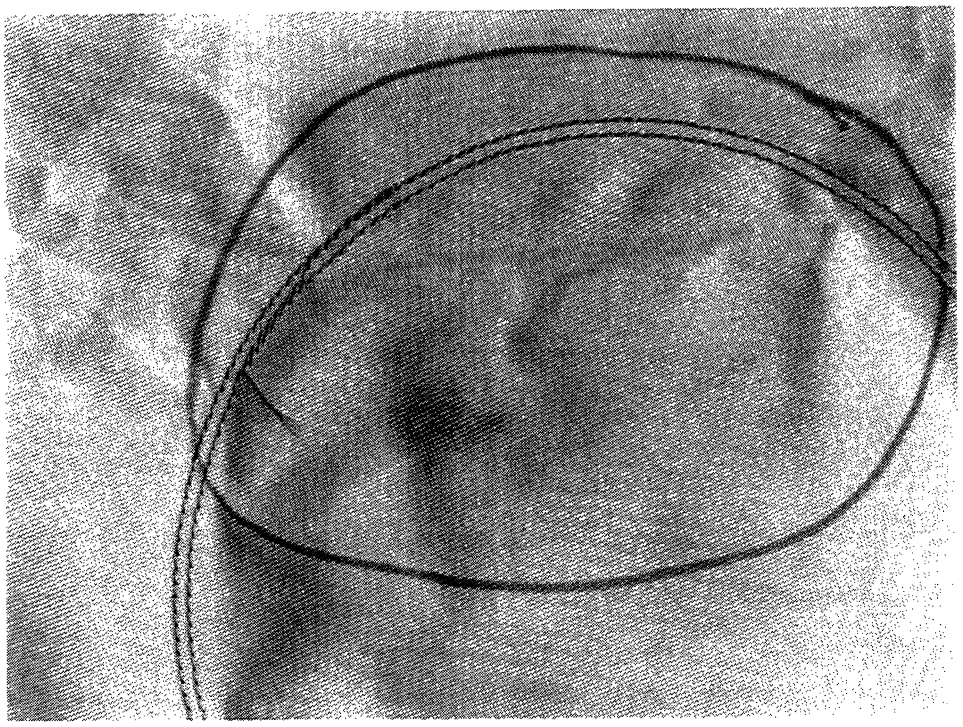

Figure 9. Section of airbag material near center of airbag after a stamp abrasion event showing markings transferred from the subject's leg.

Section 3.4). However, these injuries were often observed at the side of the leg because of a tendency of the airbag fabric of untethered airbags to wrap around the leg as the airbag deploys. The abrasions are similar in appearance to the stamp abrasions, often leaving much of the epidermis intact but with blood pooling immediately underneath it. Markings that transferred to the airbag fabric during slap abrasion events were generally smeared, as shown in Figure 10, indicating that the fabric was moving laterally relative to the skin at the time of fabric contact, although the normally-directed impact is believed to be the primary mechanism of injury (see Section 3.5).

2.3.3 Effects of Design and Deployment Factors

Airbag Fabric. Four 60-L airbag tests were conducted with human subjects and 840-D airbags, while the remaining 29 tests were conducted with 420-D fabric. It had been hypothesized that the 840-D fabric would cause more frequent and more severe

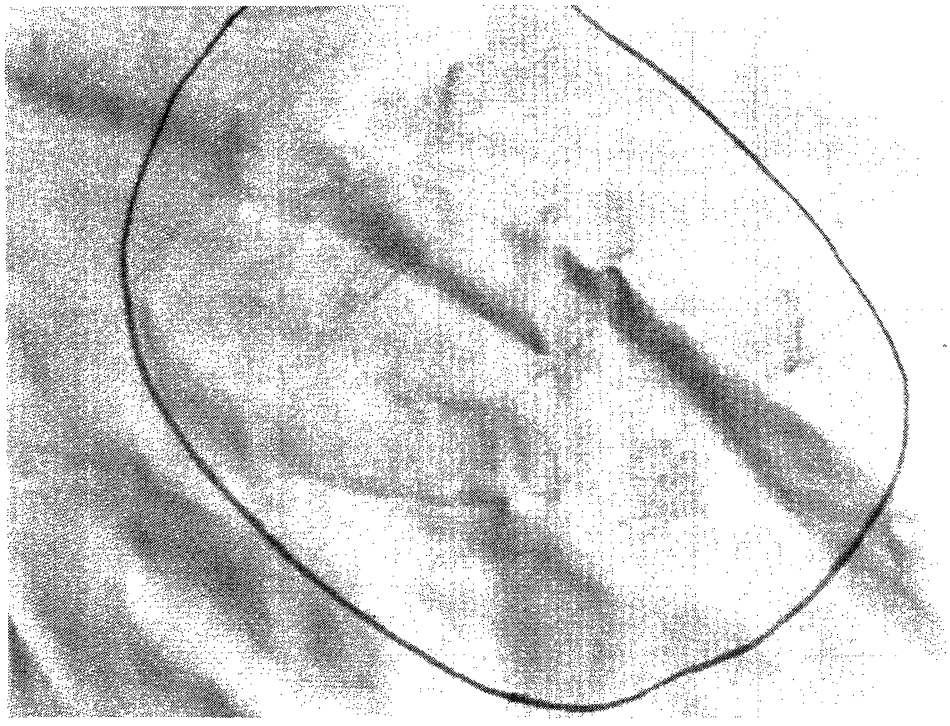

Figure 10. Section of airbag material after a slap abrasion event, showing markings transferred from the subject's leg.

abrasions because of a rougher texture due to larger-diameter fibers. Table 5 presents a comparison of test results from deployments with 420-D and 840-D airbags for two distances. Because no 840-D tethered airbags were available, the data are for tests with untethered airbags with both 320- and 350-kPa inflators.

The rankings suggest that the 840-D airbags are less injurious than 420-D airbags under similar test conditions. However, a potentially important confounding variable is not addressed by these data. The 840-D airbags were packaged in an airbag module that was different from those used with the 420-D airbags. Although a quantitative comparison of the airbag module covers has not been made, it is possible that the module cover of the 840-D airbags influenced the airbag kinematics in such a way that injury severity was reduced. With this in mind, the data do not support a conclusion that a significant difference in skin-injury potential exists for the two airbag fabrics. The pre-test hypothesis is not supported, in that these data do not suggest that a finer-weave fabric will produce fewer or less severe injuries than a coarser-weave fabric.

Table 5
Comparison of Results from 840-D and 420-D Airbags:
Injury Rankings for Untethered Airbags (33 = Most Severe)

Distance	Inflator Capacity	420-D	840-D
225 mm	320-kPa	20 27	15
	350-kPa	29 33	25
300 mm	320-kPa	4.5 4.5	4.5
	350-kPa	31 23 22 11	9

Distance from the Module. Airbag deployments with human volunteers were conducted with the subject's leg at distances of 225 to 400 mm from the surface of the undeployed airbag module. For each of the 60-L airbag configurations tested, injury severities were observed to decrease with increasing distance from the airbag module. Figure 11 shows a plot of injury rankings versus distance for each of the 60-L airbag configurations. In each plot, the most severe injuries were observed at 225 mm, and injury severity generally decreased with increasing distance.

The type of injury observed also varied with distance. At distances of 250 mm and less, wing abrasions were produced by all airbag configurations. At distances of 300 mm and greater, stamp abrasions were produced by tethered airbags with 350-kPa inflators, and slap abrasions were produced by untethered airbags with 350-kPa inflators. No abrasions were produced with either tethered or untethered airbags with 320-kPa inflators at distances of 300 mm or greater.

Inflator Capacity. Airbags with 350-kPa inflators produced more severe injuries at all distances than identical airbags with 320-kPa inflators. The effect is clearly shown in Figure 12 for the 300-mm distance. At 225 mm, the effect is less pronounced, but the rankings for tests with 350-kPa inflators were consistently higher than for tests with 320-kPa inflators, indicating more severe injuries. Quantitative experiments subsequently conducted (see Section 3) showed that the reason for this difference was that the 350-kPa inflators produce higher airbag fabric velocities throughout the deployment than do the 320-kPa inflators, resulting in more severe impacts of the airbag fabric with the skin.

Tether. The airbag tether substantially reduces injury severity for airbags with 350-kPa inflators at distances of 300 mm and greater. This is consistent with the excursion limit that the tether imposes on the airbag. At 300 mm, the injuries produced by the tethered airbags with 350-kPa inflators are stamp abrasions, which are generally less severe than the slap abrasions produced by the untethered airbags at the same distance. At distances greater than 300 mm, the tethered airbags produced no injuries,

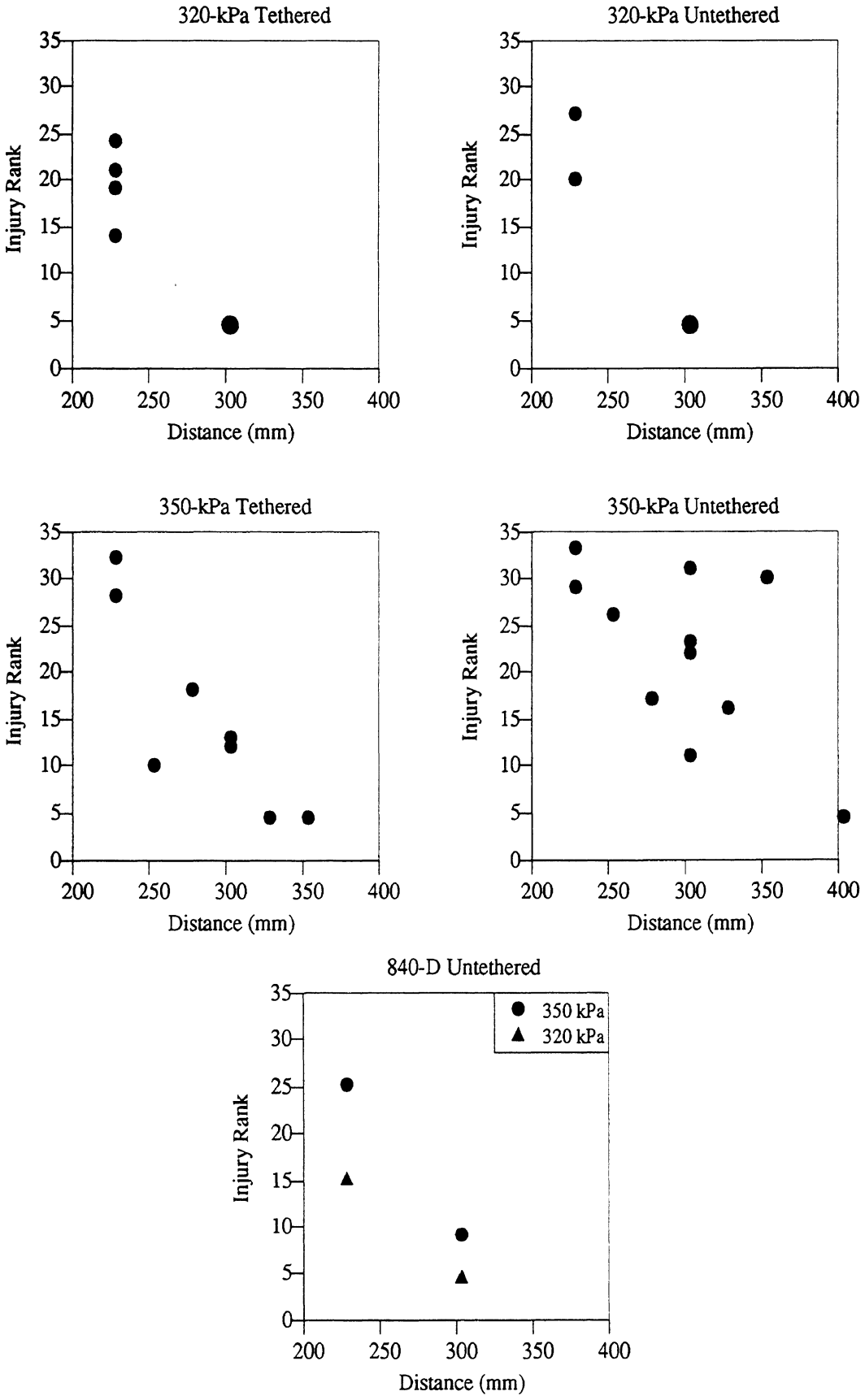

Figure 11. Injury rankings versus distance for human-subject tests with 60-L airbags.
(Larger symbols signify two tests.)

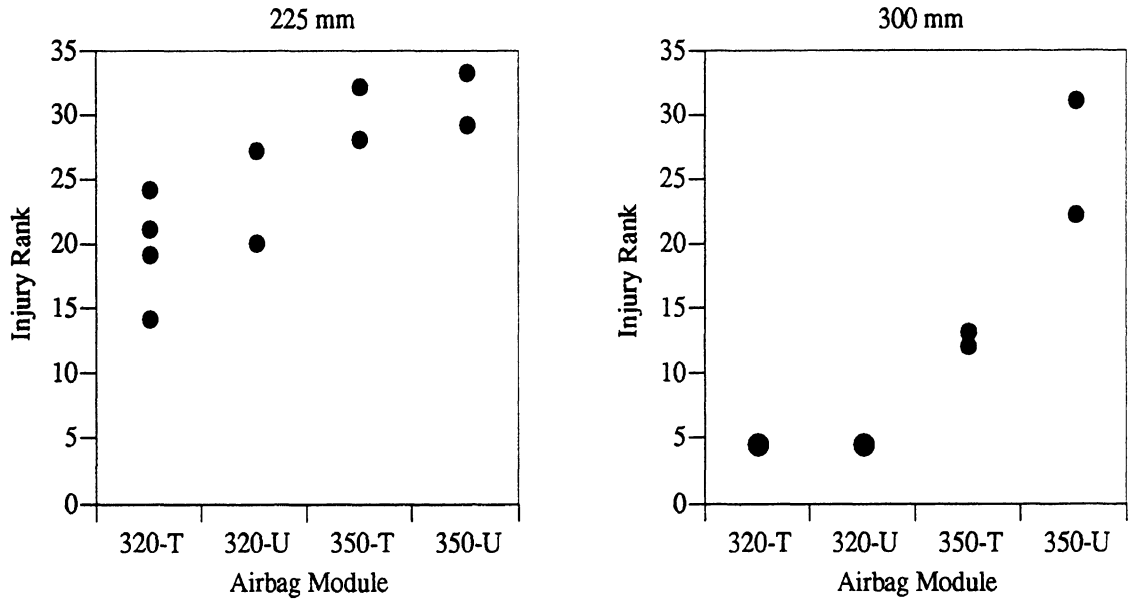

Figure 12. Injury rankings for four airbag configurations at 225 and 300 mm.
(Larger symbols signify two tests.)

while the untethered airbags with 350-kPa inflators produced slap abrasions of substantial severity for distances up to 350 mm from the airbag module. Thus, the airbags with 350-kPa inflators are capable of producing skin injury throughout the entire excursion of the airbag, corresponding to about 300 mm for the tethered airbags and 350 mm for the untethered airbags.

Summary of Factor Effects. Of the four airbag design and deployment factors investigated, three were observed to produce effects supporting the pre-test hypotheses. While the findings regarding airbag fabric were not conclusive, the 420-D fabric did not appear to reduce injury compared with the 840-D fabric.

Fabric — More severe injuries were produced by airbags with 420-D fabric than by airbags with 840-D fabric. However, confounding caused by different module covers for the two fabric types may be responsible for the observed difference in injury severity.

Distance — Abrasions were more severe for shorter distances to the module cover. The type of abrasion differed with distance: wing abrasions were observed at 225 mm for all airbag configurations, stamp abrasions occurred for tethered airbags with 350-kPa inflators at 250 and 300 mm, and slap abrasions were produced by untethered airbags with 350-kPa inflators from 250 to 450 mm.

Inflator — Abrasions were more severe with 350-kPa inflators than with 320-kPa inflators for all test configurations. No abrasions were observed at distances of 300 mm or greater using tethered or untethered airbags with 320-kPa inflators.

Tether — Tethering eliminated abrasions at 300 mm and greater distances for airbags with 320-kPa inflators, and reduced abrasions at 300 mm and eliminated them at greater distances for airbags with 350-kPa inflators. Because untethered airbags with 320-kPa inflators did not produce abrasions at 300 mm, tethering eliminated more abrasions with the 350-kPa inflators than with the 320-kPa inflators.

2.3.4 Tests with 40-L Airbags

Six human-volunteer tests were performed with 40-L, untethered airbags constructed of 420-D fabric. Each of these modules was fitted with a 190-kPa inflator. The tests were conducted at 25-mm intervals between 200 and 375 mm from the module.

Skin abrasions with a severity greater than ARS 1 (*i.e.*, with bleeding) were observed only for the test at 200 mm, as shown in Figure 13. The injury was classified as a wing abrasion because the high-speed film of the deployment showed that a swinging

fold of airbag fabric struck the leg in the area of injury, and because the abrasion caused by the seam (visible in Figure 13) was typical of wing abrasions. The abrasions in this test were less severe than in any of the tests with 60-L airbags.

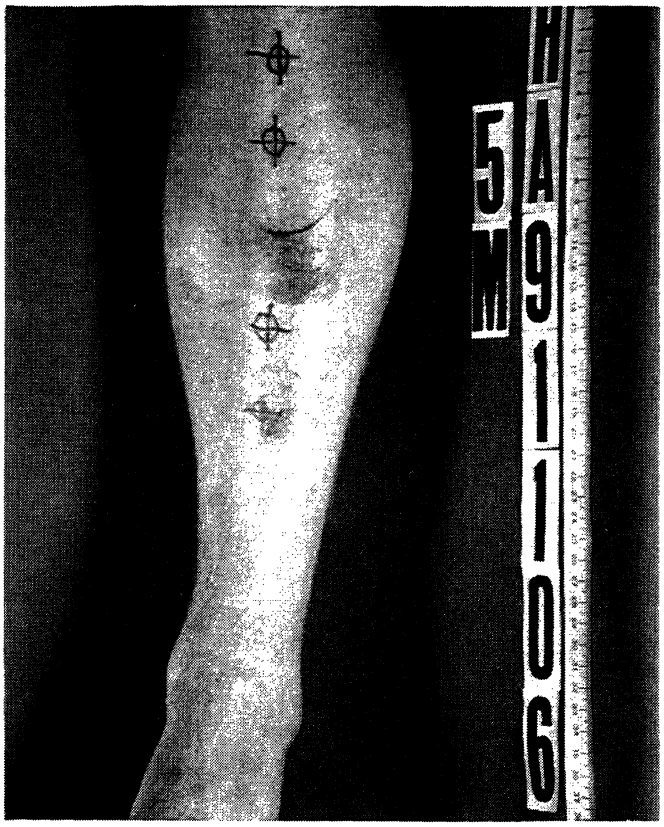

Figure 13. Post-test photo of ARS 3 injury produced by 40-L airbag at 200 mm.

2.3.5 An Experimental Fold Technique

One test was performed with a tethered, 420-D, 60-L airbag, using a 320-kPa inflator and an experimental fold technique developed to test the findings of this study with regard to abrasion mechanisms. The rationale behind the experimental fold technique is described in Section 3.6. The airbag was deployed into a subject's leg positioned 225 mm from the module, duplicating a test condition used for four other deployments with tethered airbags, 320-kPa inflators, and the standard fold technique.

No abrasion greater than ARS 1, (*i.e.*, no bleeding) was observed in this test. Subsequent quantitative analysis of the kinematics and surface impacts produced by the experimental fold indicated that the fold was successful in reducing the severity of the airbag kinematics that cause abrasion, resulting in minimal or no abrasion in this test with a human volunteer (see Section 3.6 for a description of the kinematics).

2.3.6 Healing of Abrasions

All skin abrasions resulting from airbag deployments healed completely. ARS 1 and 2 injuries, with epidermal damage only, were minor in severity and not of cosmetic significance. ARS 1 injuries required no treatment and left no permanent marks, such as scarring or pigmentation. ARS 2 injuries, in which epidermal breakdown was not at first visible, but then became apparent over the first 24 hours in the form of weeping of serum onto the skin surface and superficial crusting or eschar (scab) formation, did not require specific treatment other than a protective dressing. These injuries healed within a few days, leaving no permanent marks.

ARS 3, 4, and 5 injuries all have the potential to cause permanent scarring or pigmentation changes in the skin, and require specific medical treatment to facilitate healing and to minimize the risk of infection. Scarring may occur whenever the dermal layer of the skin is injured more than superficially, and permanent pigmentation changes, similar to a tattoo, may occur as a result of the accumulation of blood in the tissue, with subsequent deposition of blood pigments.

ARS 3 and 4 injuries were treated using the method of moist healing. This was achieved in most cases with an occlusive dressing, such as Duoderm®, but can also be achieved by moist gauze dressings changed two or three times a day. Immediate occlusion of the wound surface with an occlusive polyurethane or hydrocolloid dressing material (or most types of gauze) after simple cleansing with mild soap and water relieves pain and speeds healing by preventing eschar formation and promoting the repair of the

surface wound by facilitating the growth and migration of keratinocytes that cover and close the open wound surface. In one case, a ARS 4 injury, moistened gauze dressings were used initially, followed by an occlusive dressing, because of the large amount of exudate from the wound. ARS 3 and 4 wounds will also heal if untreated, but healing is slower and the risk of both wound infection and scarring is greater than if the wounds are treated with moist dressings or occlusion. ARS 3 injuries healed in five to ten days under an occlusive dressing.

The deepest injury observed, rated as ARS 4, required between two and three weeks to heal. In this case, and in several others in which there was hemorrhage into the superficial soft tissues, long-term, possibly permanent, pigmentation changes developed. This change in the appearance of the skin results from the taking up of blood pigments containing iron by the skin tissue, analogous to tattooing. Pigmentation change was an unanticipated result of airbag-induced abrasion. Whether it might occur after airbag-induced abrasion to the face or neck is unknown. In general, pigmentation change after injury is more commonly observed on the lower extremities, where removal of pigment is less efficient, than on the upper surfaces of the body, and is not commonly seen on the face or chest.

3.0 QUANTITATIVE ASSESSMENT OF ABRASION MECHANISMS

3.1 OVERVIEW

As described in the previous section, the abrasions observed in tests with human volunteers were divided into three types: wing, stamp, and slap abrasions. Each of these abrasion types was observed in particular test configurations and each appeared to be caused by a particular type of airbag fabric interaction with the skin. For example, wing abrasions were associated with contact between a flap of unfolding airbag fabric and the skin. Quantitative data were needed to understand the combination of factors necessary to cause abrasion, and which factors controlled the severity of the abrasion for each of these abrasion types.

Initially, this problem was to have been examined through use of a test fixture that could produce carefully controlled abrasion events on a test subject. Normal force, lateral velocity, and fabric roughness were to be controlled and varied to determine the effect of each factor on abrasion incidence and severity. However, kinematic analysis of airbag deployments with human volunteers indicated that the fabric velocities during abrasion events were so high that constructing a laboratory apparatus that could operate in the same velocity range was impractical. Local fabric velocities in excess of 150 m/s (340 mph) were measured in areas of the deployment envelope where abrasion occurred.

Further, test data from experiments with surrogate materials suggested that the abrasion mechanism assumed in the concept of the abrasion machine might be insufficient to describe some airbag-induced abrasions. Specifically, the concept of the abrasion machine was based on the assumption that abrasions were due to shear stresses produced by lateral motion of the airbag fabric relative to the skin while the fabric exerted pressure on the skin. Under this assumption, variations in the lateral velocity and

the fabric roughness would be important in determining abrasion severity. However, experimental data indicated that surface pressure of the fabric on the skin was of principal importance, and that the pressure levels were so high and durations of application so short that the type of machine envisioned for duplicating the injury mechanisms involved in the human volunteer tests was unsuitable.

Consequently, quantitative assessment of airbag abrasion mechanisms focused on measurement of the parameters associated with injury mechanisms during actual deployments. An abrasion event was assumed to be sufficiently described by the kinematics of the fabric during the deployment and the surface pressure of the fabric against the skin. The characteristics of the airbag fabric and the skin were assumed to be constants. The evidence from human subject testing with different airbag fabrics suggested that fabric roughness was not an important factor, and intersubject and intersite skin variability was assumed to be less important than fabric movement and surface pressure in determining abrasion severities.

Two types of quantitative data were collected: airbag fabric velocity measurements, obtained by analysis of high-speed films of deployments, and surface pressure measurements on contacted surfaces, obtained through use of an Instrumented Leg Form (ILF). Data from these two sources provided an effective description of airbag-induced abrasion mechanisms.

Quantitative investigations focused primarily on wing abrasions for several reasons. Wing abrasions presented a wide range of abrasion severities including some of the most and least severe abrasions observed. They occurred in the most consistent and predictable manner, and they were produced by all airbag configurations. Additionally, airbag fabric motions responsible for this type of injury were easiest to observe through high-speed film analysis. The findings from analysis of wing-abrasion events were later found to apply to the stamp and slap abrasions as well.

Deployments were conducted with a target surface shaped similar to the lower leg located in the deployment envelope. Most tests were performed using the Instrumented Leg Form (ILF) as the target surface located 225 mm from the airbag module (see Section 3.3). Other tests were performed with the ILF located 300 mm from the module. These distances were chosen to investigate the airbag motions contributing to wing abrasions (225 mm) and stamp and slap abrasions (300 mm). Table 6 summarizes the types of quantitative tests performed. The sum of the numbers in Table 6 is greater than the total number of quantitative tests performed (56) because more than one type of data was collected in many tests. For example, in many of the tests with the ILF, airbag fabric velocities were also measured.

Table 6
Summary of Tests for Quantitative Assessment of Abrasion Mechanisms

Type of Test/Measurement	Number of Deployments
Fabric Velocity	24
ILF Development	12
ILF Data Collection	13
ILF and Prescale	14
Prescale on Test Fixture	8
Total	56

3.2 AIRBAG DEPLOYMENT KINEMATICS

All but one of the airbag configurations tested with human volunteers utilized what is referred to as the "standard" fold technique, also called an "accordion" fold technique. When an airbag folded in this way deploys, two flaps of material swing outward from the module, as depicted in the photo series in Figure 14. These flaps are called "wings" in this report because of their flapping movement as the airbag deploys. The fabric in the wings comprises the top and bottom portions of the airbag in these tests,

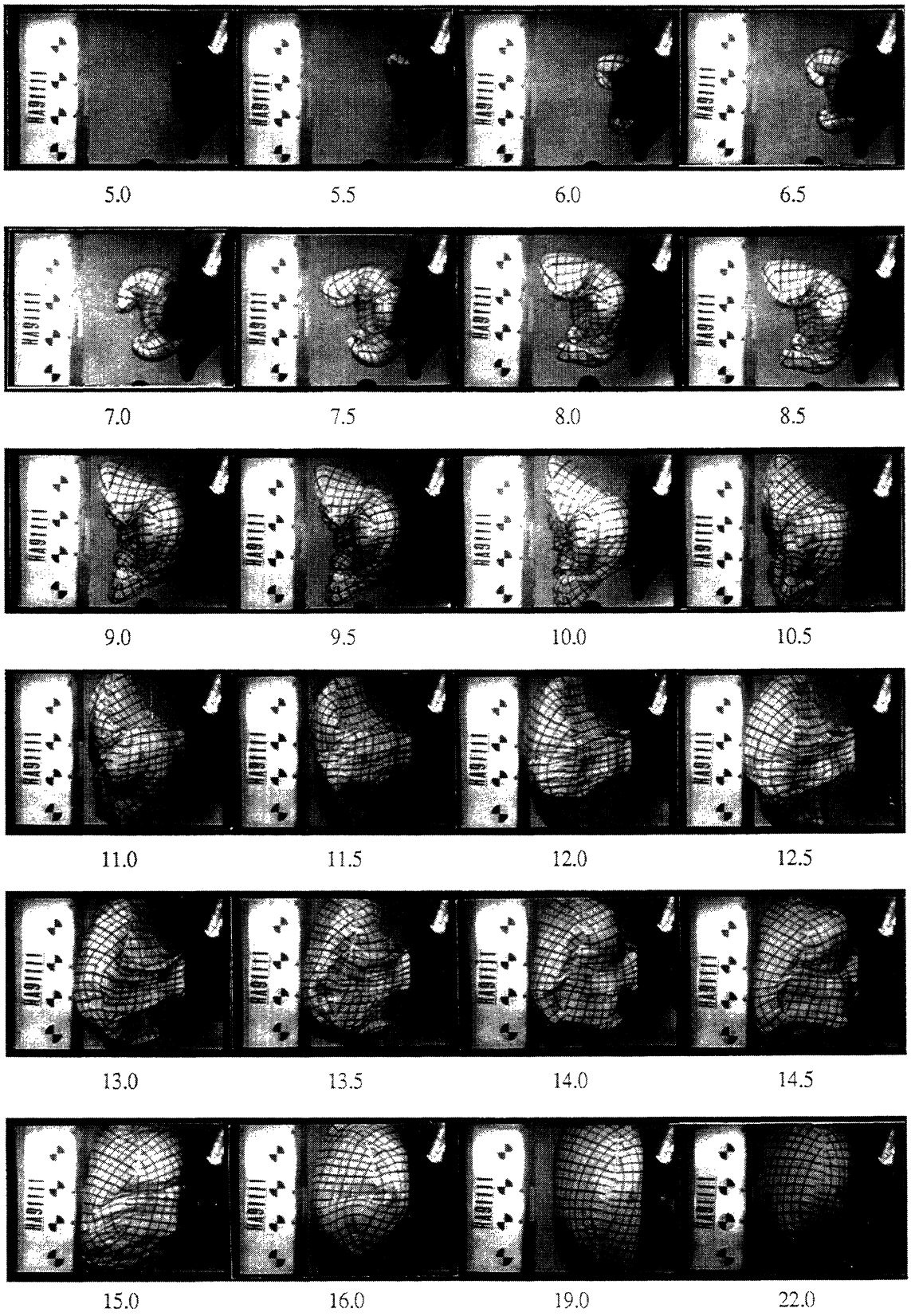

Figure 14. Photo series from high-speed film depicting airbag kinematics. Photo labels indicate the number of milliseconds elapsed after inflator trigger.

which would be the left and right sides of the airbag, respectively, if the airbag were deployed from a neutral steering-wheel orientation. In the early phases of the airbag deployment, the wings are at the leading edge of the deploying airbag.

The fabric at the center of the airbag deploys after the wings with this fold technique, traveling over 400 mm for untethered airbags and approximately 300 mm for tethered airbags. The airbag reaches its furthest excursion prior to completely filling. After reaching its maximum volume, the airbag fabric oscillates forward and backward. This can result in multiple strikes of the fabric against a subject's skin if the subject is located near the outer edge of the deployment envelope. These oscillations are much more pronounced with untethered airbags than with tethered airbags.

3.3 VELOCITY MEASUREMENTS

Several airbag deployments were conducted specifically for the purpose of quantifying fabric velocity. High-speed films were taken at 3000 or 6000 frames per second from the side view. Targets of known geometry were placed on the test fixture approximately in the vertical plane of the center of the module to facilitate quantitative analysis of the film. In several tests, the airbag fabric was marked with a 25-mm grid prior to deployment. This grid allowed specific points on the airbag to be tracked in the high-speed films. Films were analyzed using a Lafayette 403 film analyzer and manual digitization methods. The velocity of a point on the fabric was calculated by dividing the displacement of the point in the plane of the film in two consecutive frames by the elapsed time between frames. Film distances were expressed as actual distances by reference to targets of known geometry in the film frame. No attempt was made to compensate for parallax or the relative distance of points from the camera since the measurement errors in the digitizing process were potentially larger than possible errors from these sources.

Describing the kinematics of airbag deployment is complex because of the flexible nature of the airbag material and the explosive nature of the deployment. Additionally, measurement of fabric velocity must be done indirectly, such as through film analysis. In this analysis, only the fabric motions directly affecting abrasion mechanisms were measured. Three velocities of interest were defined as shown in Figure 15:

Leading Edge	The horizontal (axial) speed of the portion of airbag fabric furthest from the plane of the steering wheel (one dimension).
Seam Velocity	The speed of a portion of airbag fabric near the airbag seam at the uppermost edge of the airbag (leftmost with the wheel oriented in the neutral position), measured both horizontally and vertically (two dimensions).

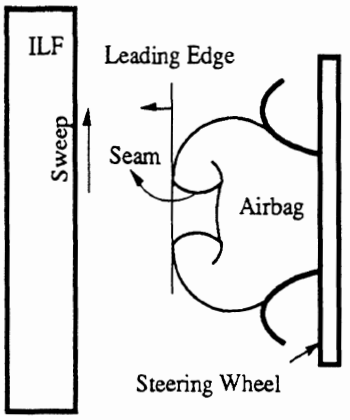

Figure 15. Definition of airbag fabric velocities.

Sweep Velocity — The vertical speed of a portion of airbag fabric in contact with the target surface (one dimension).

The leading-edge velocity was measured horizontally along the axis of the steering wheel and airbag module in the direction of the deployment. These values do not represent the velocity component of any individual portion of airbag fabric because the portion of airbag fabric that has deployed the furthest changes quickly. Rather, these values are a general indication of the closing speed between the airbag and a target in the deployment envelope.

Seam velocities refer to the speed in a vertical plane parallel to the deployment axis of portions of airbag fabric near the seam. The standard fold technique results in a section of the seam being approximately at the "tips" of the wings. The velocity of this portion of airbag fabric was considered important because marking-pen targets from human volunteers had transferred onto these portions of airbag fabric from areas of the skin that had sustained abrasion (see Section 2.5.2).

Sweep velocities refer to the speed of the airbag fabric while in contact with the target surface. These values were used to assess the effect of airbag fabric scraping against the skin on abrasion severity. Because the target surface in each of these tests was oriented vertically, perpendicular to the deployment axis, all sweep velocity values represent vertical speeds.

Because of the interest in the wing abrasion mechanism, most velocity tests were carried out with the target surface located 225 mm from the module cover prior to the deployment. At this range, one of the wings is at the leading edge throughout the deployment, the seam velocity is approximately the speed of the tip of a wing, and the sweep velocity is the vertical speed of the wing tip as it moves while in contact with the target surface. In most of these tests, the upper wing (left side of the airbag if the wheel

was in the neutral position) was the leading edge of the airbag during the period of the deployment prior to initial contact with the target surface. Consequently, all velocity measurements for these tests were made using the upper wing only.

3.3.1 Velocity Data

Figures 16, 17, and 18 show seam, leading-edge, and sweep velocities for four different airbag configurations. The thicker lines are estimates of the mean velocity visually fit to the data. As such they cannot be compared statistically, but effectively demonstrate the velocity relationships among the airbag configurations. The velocities were calculated from high-speed films of tests with the ILF located 225 mm from the airbag module.

Seam velocity data are important for assessing injury mechanisms because the seam velocity is the velocity of the portion of fabric responsible for wing abrasions. At 225 mm, the seam is approximately at the leading edge of the airbag deployment. The seam velocity peaks at about 170 m/s at a distance approximately 125 mm from the airbag module for airbags with 350-kPa inflators and 150 m/s for airbags with 320-kPa inflators. The inverted-U shape of the velocity curves (Figure 16) reflects the swinging and unfolding motion of the wings during the early phases of the deployment. The velocity of the airbag seam decreases prior to impact of the tip of the airbag wing with the target surface at 225 mm.

The shapes of the leading-edge velocity plots also are due to the sweeping motions of the airbag wings. As shown in the photo series in Figure 14, the leading edge is initially comprised of fabric from the back side of the airbag. As the wing unfolds, the fabric at the leading edge is progressively closer to the airbag seam, until at 225 mm the seam is at or near the leading edge. Since the leading-edge velocity was measured only horizontally, the velocity drops dramatically at distances beyond about 200 mm as the wing begins to swing upward. The leading-edge velocity is lower than the seam velocity

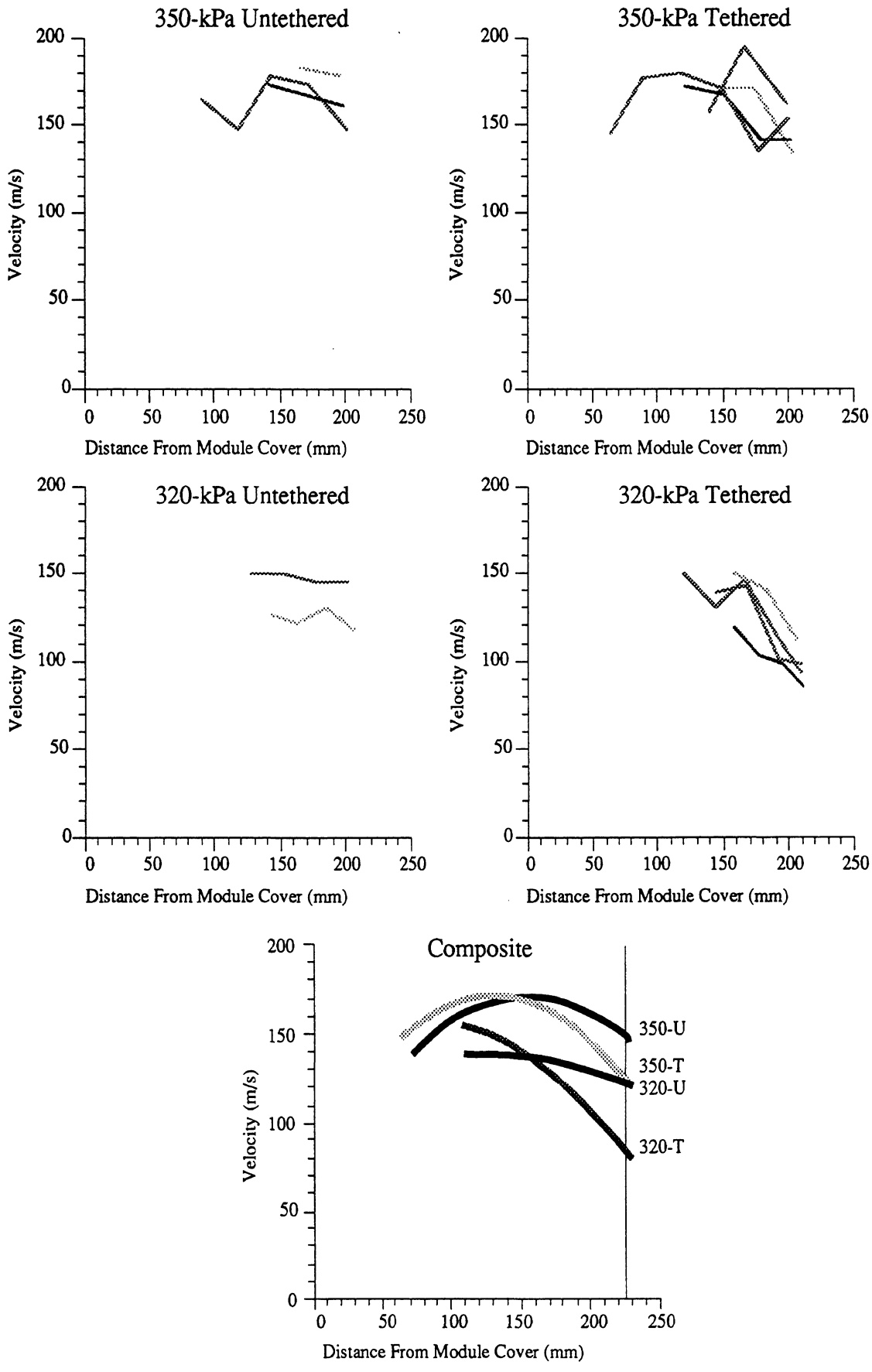

Figure 16. Seam velocities for 60-L airbags.

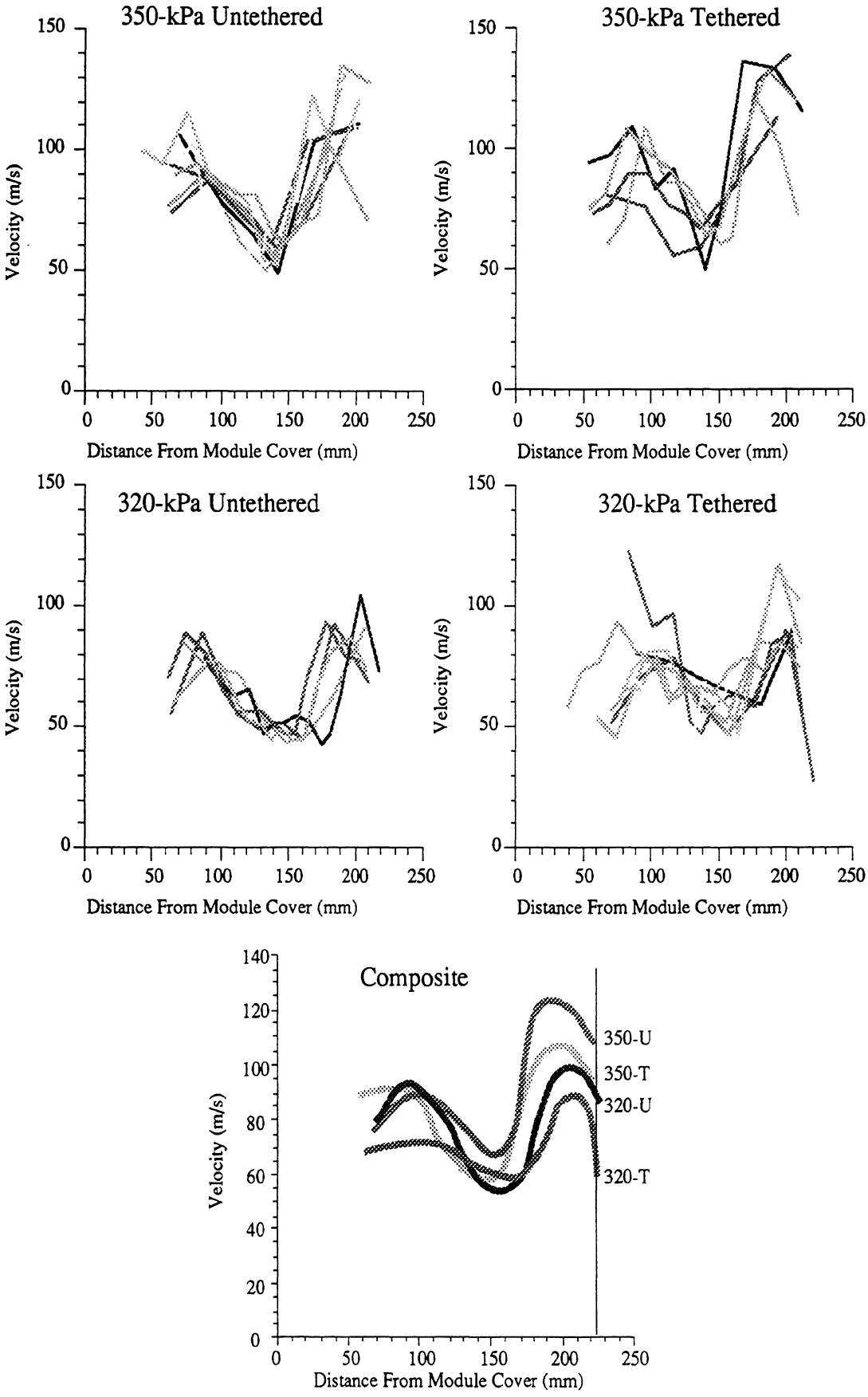

Figure 17. Leading-edge velocities for 60-L airbags.

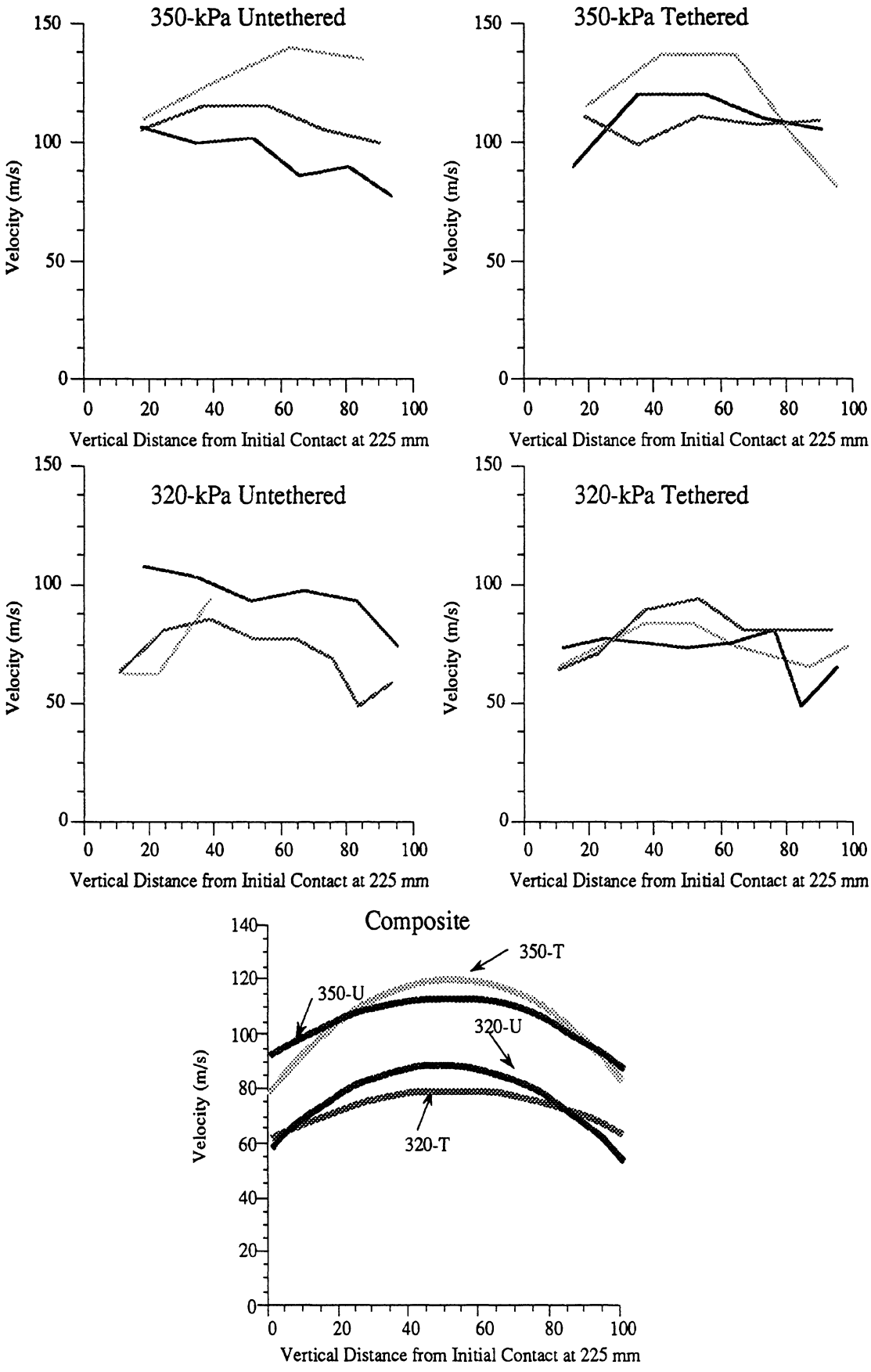

Figure 18. Sweep velocities for 60-L airbags.

even when the seam velocity is at the leading edge because the seam velocity was measured in two dimensions rather than one and the seam moves upward as well as horizontally as it approaches 225 mm.

The sweep velocities are fairly constant through 100 mm of vertical travel along the target surface. Again, airbags with 350-kPa inflators have higher sweep velocities than airbags with 320-kPa inflators. An important observation from these data is that the velocity of the airbag fabric along the skin is at approximately the same level over a much larger portion of skin than the area in which injuries were observed. A typical wing abrasion has a vertical dimension of about 30 mm, while the high-velocity sweep of the airbag fabric over the leg continued over a much larger area. This suggests that high-velocity fabric movement in contact with the skin is not sufficient to cause injury in the absence of high surface pressure.

The seam, leading-edge, and sweep velocities are well correlated across airbag configurations so that the relative levels of these velocities for the various module configurations are similar, as shown in Figure 19. Functionally, the airbag inflator

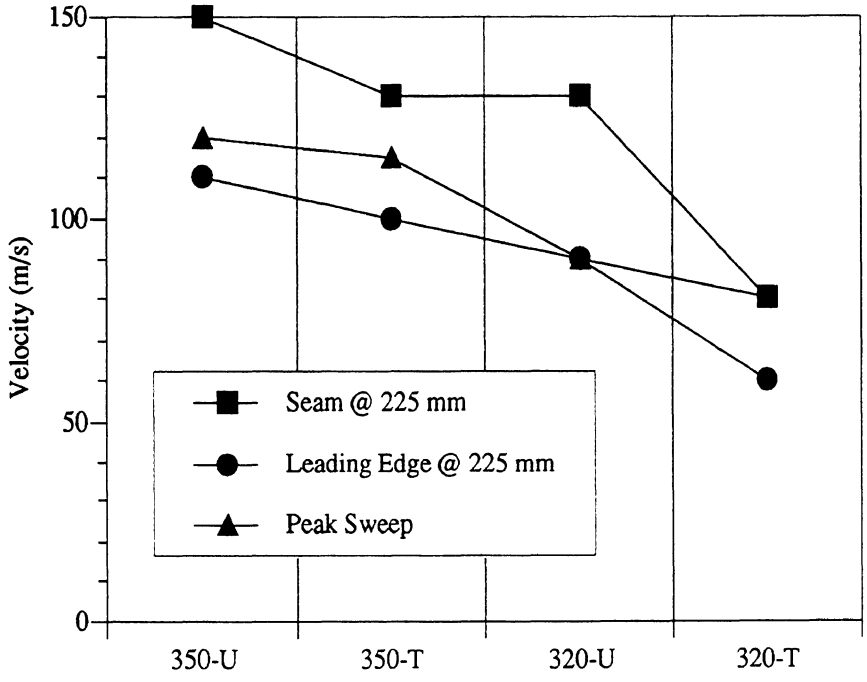

Figure 19. Relative levels of seam, leading-edge, and sweep velocities among different airbag module configurations.

capacity is the primary determinant of fabric velocity, while the presence of tethering can affect the kinematics in minor ways at distances less than the length of the tether to produce slightly different velocity characteristics.

It is also interesting to note that seam velocity values from the 40-L airbags with 190-kPa inflators are comparable to those of the 60-L airbags with 320-kPa inflators at 225 mm. However, no injury was observed in the single human volunteer test conducted with a 40-L airbag at 225 mm. A small ARS 3 injury was observed at 200 mm with the 40-L airbag. These data indicate that other factors in addition to airbag fabric velocity, including airbag kinematics and the mass of the fabric involved in a portion of the unfolding airbag, may affect the abrasion potential of the airbag. For example, comparable wing motions with the smaller 40-L airbag occurred closer to the airbag module cover than was the case with the larger airbag, reducing the envelope in which abrasion could be produced.

Attempts were made to measure velocities associated with stamp and slap abrasions at a distance of 300 mm from the module. However, the uneven motion of the airbag fabric made velocity analysis difficult. Often the fabric that initially contacted the target surface at 300 mm was hidden from the side-view camera at the time of contact. However, the results of the more thorough analysis of the wing abrasion mechanisms can be generalized to the slap and stamp abrasions, as discussed in Section 3.5.

3.3.2 Velocity and Injury Severity

Figure 20 shows injury rankings for human-volunteer tests at 225 mm (Section 2.5.1) plotted against the estimated seam velocity at 225 mm from Figure 16. The seam velocity is used because injuries produced by the seam were characterized by a distinct mark made by the airbag seam. In general, higher velocities are associated with more severe injury. The nature of the relationship is difficult to describe exactly because of variability in both the injury severity assessment and the velocity measurement.

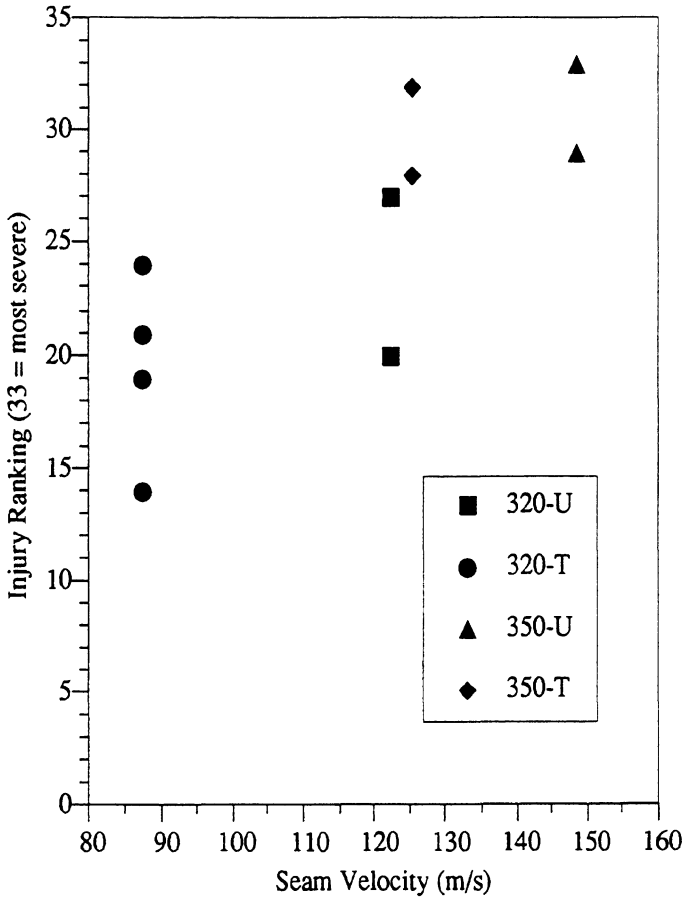

Figure 20. Injury ranking versus seam velocity.

Because of the ordinal nature of the injury rankings, it is not possible to extrapolate this curve to predict a fabric velocity for which injury would not occur. Additionally, the mass of fabric incorporated into the fold at the time of contact may play a role in determining the severity of the impact. However, the tethered airbags with 320-kPa inflators consistently produced ARS 3 or greater injuries at 225 mm with fabric velocities of approximately 85 m/s at contact between the airbag and the skin, indicating that reducing the velocity below this level is necessary to eliminate injury.

3.4 PRESSURE MEASUREMENTS ON TARGET SURFACES

Airbag fabric velocity measurements provided information on one component of the interaction between the fabric and the skin. The second component of interest was the pressure between the airbag fabric and the skin while the fabric was in contact. In the

early stages of the investigation, it was hypothesized that higher pressures would result in higher frictional forces applied to the skin when airbag fabric moved relative to the skin. Later, however, the data indicated that motions of the airbag fabric along the surface of the skin, and hence frictional forces, were less important than the velocity of the fabric normal to the skin immediately prior to impact. This conclusion was reached as a result of surface pressure measurements made with an Instrumented Leg Form, designed for this application, and Fuji Prescale, a pressure-sensitive plastic film.

3.4.1 Instrumented Leg Form

When the focus of the quantitative measurement of abrasion mechanisms was shifted from an abrasion-producing apparatus to measurements of the pressures and velocities produced by actual deployments, instrumentation to measure the pressures exerted by the airbag fabric on a target surface during a deployment became necessary. An Instrumented Leg Form (ILF) was designed to measure surface pressures exerted on a shape similar to a human leg. The design of the ILF was complicated by the explosive nature of the event to be measured. In the final design, the ILF was suspended above the test buck to isolate the instrumentation from the impact shock and mechanical noise associated with the deployment. Signal processing was hampered by the need to observe data at frequencies up to 10 kHz. This precluded low-pass filtering of the transducer signals at typical cut-off frequencies (*e.g.*, 200 Hz), necessitating other methods to eliminate mechanical and electrical noise from the system.

The successful ILF design is shown in Figure 21. Kistler 903A piezo-electric load cells were located behind rigid aluminum disks of slightly smaller diameter than the corresponding holes in the front of a three-sided leg form. The leg form was attached to the test buck, while the load cells and mounting structure were suspended from above the buck and carefully positioned so that the disks on the front of the load cells were flush with the front of the leg form. When an airbag was deployed into the front of the leg form, the load cells measured the force applied to the known area of each disk. Because

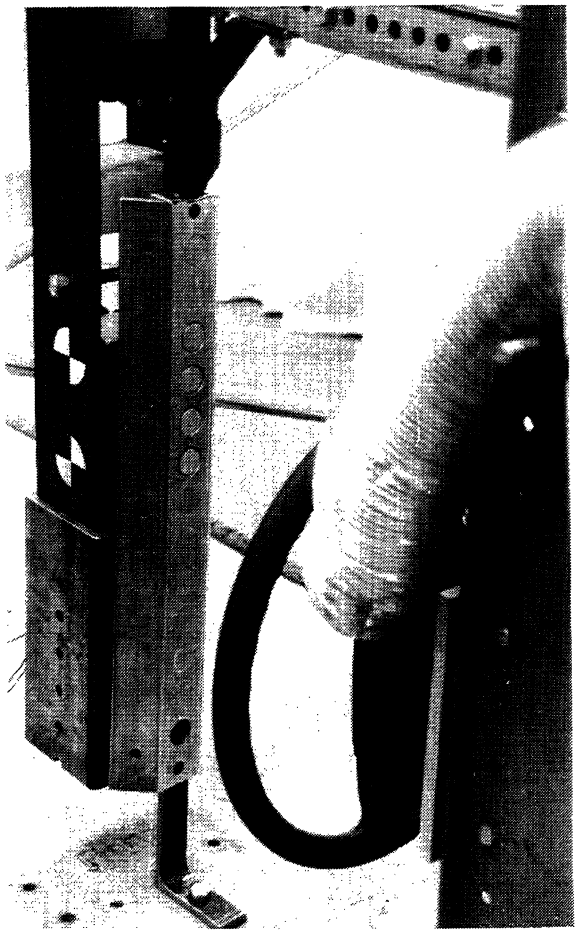

Figure 21. Instrumented Leg Form (ILF).

there was no mechanical connection between the leg form and the load cells, the signal was protected from the explosive impact of the airbag with the leg form except through forces exerted on the load cell disks. The load cells were mounted on heavy, high-density polyurethane blocks that minimized resonance.

At the time that the ILF was being designed and tested, it was not fully understood why mechanical resonances in the load cell mounting structure were so often excited. Testing with the final, more successful design indicated that an extremely strong, short duration impulse at the initial moment of contact of the airbag with the leg form was responsible for exciting oscillations (ringing) even at very high frequencies.

The surfaces that the ILF presented to the airbag were made of smooth aluminum, and were designed not to deform when struck by the airbag. This contrasts with the response of human skin, which presents a higher coefficient of friction and a more yielding surface. However, the understanding of abrasion mechanisms provided by surface pressure data suggests that these are not significant disadvantages to the measurement technique.

3.4.2 ILF Surface Pressure Data

Signals from the load cells were amplified by Kistler 1404 charge amplifiers and sampled between 33 and 100 kHz by a GW Instruments analog-to-digital converter interfaced with a Macintosh IIx microcomputer using software written for this application. Up to three load cells were sampled during each test.

Figures 22 and 23 show data collected during deployments with the ILF located 225 mm from the airbag module. Two characteristics of these data are particularly important. First, as previously noted, a very high pressure spike was generated when the airbag fabric initially struck the ILF. This was observed in the ILF data when a load cell disk was located in the area initially struck by the airbag. The magnitude of this pressure spike could not be determined precisely with the ILF because of limitations in both the ILF hardware (frequency response of the load cell assembly) and data acquisition system (throughput limited to 100 kHz).

The second important characteristic of these data is the relatively low pressure exerted by the airbag during the remainder of the deployment after the initial strike by the airbag fabric. These pressure levels were generally less than 1 kg/cm^2 (14 psi), peaking at the point of maximum inflation of the airbag at about 25 ms into the deployment. Pressure levels during this period of the deployment were generally higher for the

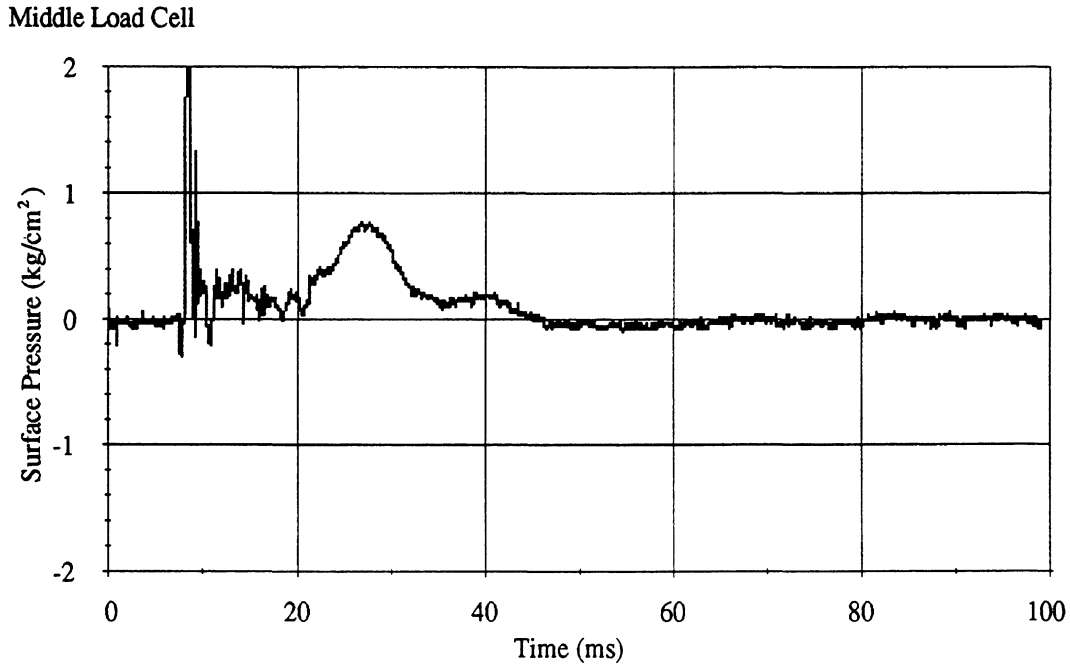

Figure 22. Data from ILF for a deployment at 225 mm with a tethered airbag and 350-kPa inflator.

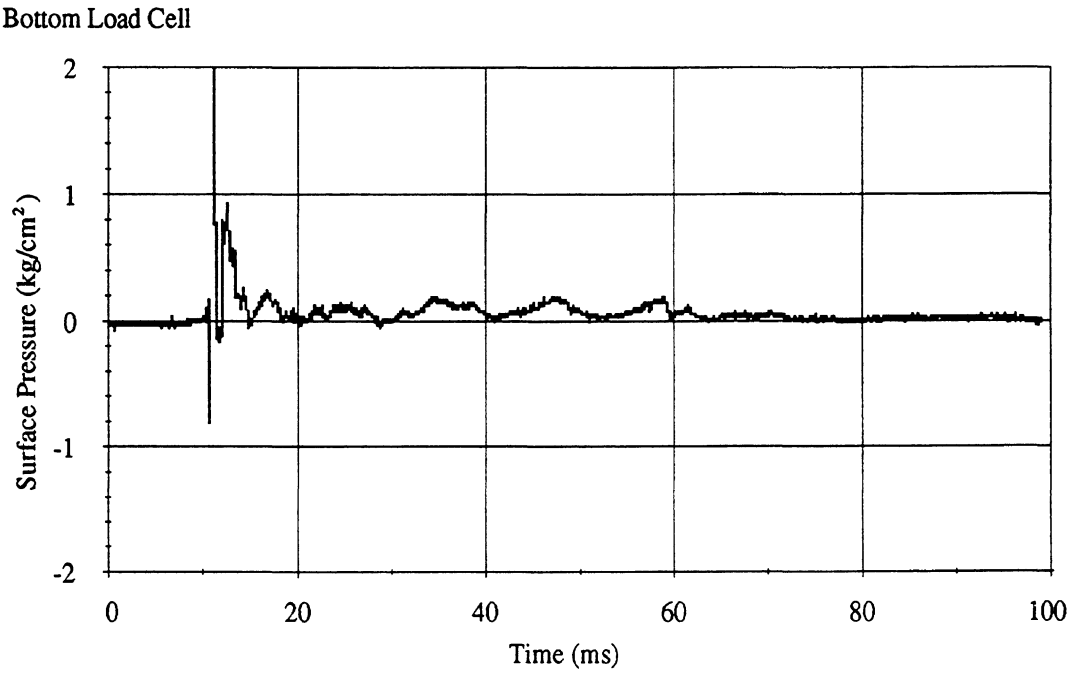

Figure 23. Data from ILF for a deployment at 225 mm with an untethered airbag with a 320-kPa inflator.

350-kPa inflator than for the 320-kPa inflator. Pressure fluctuations corresponding to the periodic axial oscillations of the airbag during the later stages of the deployment are also apparent in these data.

Based on data collected with the ILF, the magnitude of the initial spike was believed to be at least 10 times greater than the peak pressure level during the remainder of airbag contact. However, subsequent data collection with pressure-sensitive film showed the initial peak pressure to be as much as 100 times higher than pressure levels during the remainder of airbag contact.

3.4.3 Application of Fuji Prescale Film to Surface Pressure Measurement

The limitations of the ILF system precluded effective determination of the surface pressures produced by the initial impact of the airbag fabric. However, wing abrasions observed with human subjects were located at the point of initial contact of the airbag fabric with the skin, suggesting that the surface pressures at that point were important for understanding the injury mechanisms. A method of determining the magnitude of the peak surface pressure was developed using Fuji Prescale film.

Fuji Prescale is a pressure-sensitive film that uses microencapsulation technology to produce a response image related to the magnitude of the applied pressure. Figure 24 shows a schematic of the technology. The plastic film surface is evenly coated with

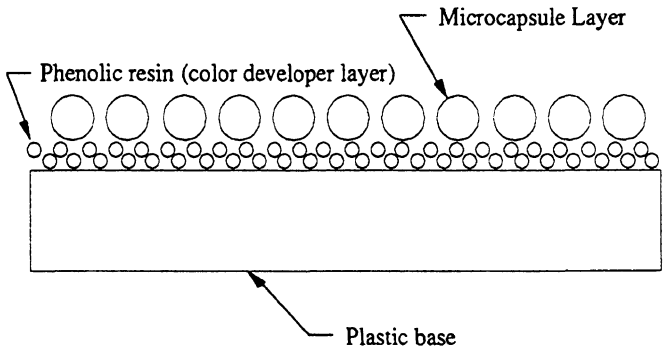

Figure 24. Schematic of microcapsule technology.

microcapsules containing a color-forming material that reacts with a surrounding color developer when the microcapsules are ruptured. The intensity of the color change varies with applied pressure and can be related to pressure magnitudes through use of an appropriate calibration. The Fuji system is designed to provide an even and reproducible graduated color change over a range of applied pressures. When exposed to a time-varying pressure, the film indicates the highest pressure applied. Although the material is available in a range of sensitivities and one- and two-sheet designs, the single-sheet, medium sensitivity (MS) film was found to be most appropriate for this application. The MS film has a useful pressure range from about 100 to 500 kg/cm^2 (1400 to 7000 psi).

Prescale Calibration. Since the film is slightly sensitive to the duration of the applied pressure, a calibration procedure was developed utilizing a pressure pulse duration more similar to that produced by airbag impact than that used in the calibration supplied by the manufacturer. Figure 25 shows the calibration device designed to apply carefully controlled pressure pulses to the film. A sample of film was held between a rigid platform and a 10-mm-diameter post. Both surfaces were polished steel. Pressure pulses of approximately 1-ms duration (at the base of the pulse) were produced by dropping the weighted arm onto the calibrator assembly. A 5-mm-diameter piece of synthetic foam rubber at the point of impact provided control over the duration of the pulse. The pressure level applied to the film was measured by a piezo-electric load cell located beneath the film platform, and the signal was recorded with a digital storage oscilloscope. The load cell was calibrated in a static mode and checked dynamically using a drop test with a known mass and an accelerometer.

Various pressure levels over the range of the film were obtained by varying the weight on the calibrator arm, changing the size of the foam rubber pad, and varying the height from which the calibrator arm was dropped. An effort was made to keep all of the calibration pulses approximately 1 ms in duration. Application of different pressure levels produced circular "dots" on the film ranging from light pink to bright red, corresponding to low and high peak pressures, respectively, as shown in Figure 26.

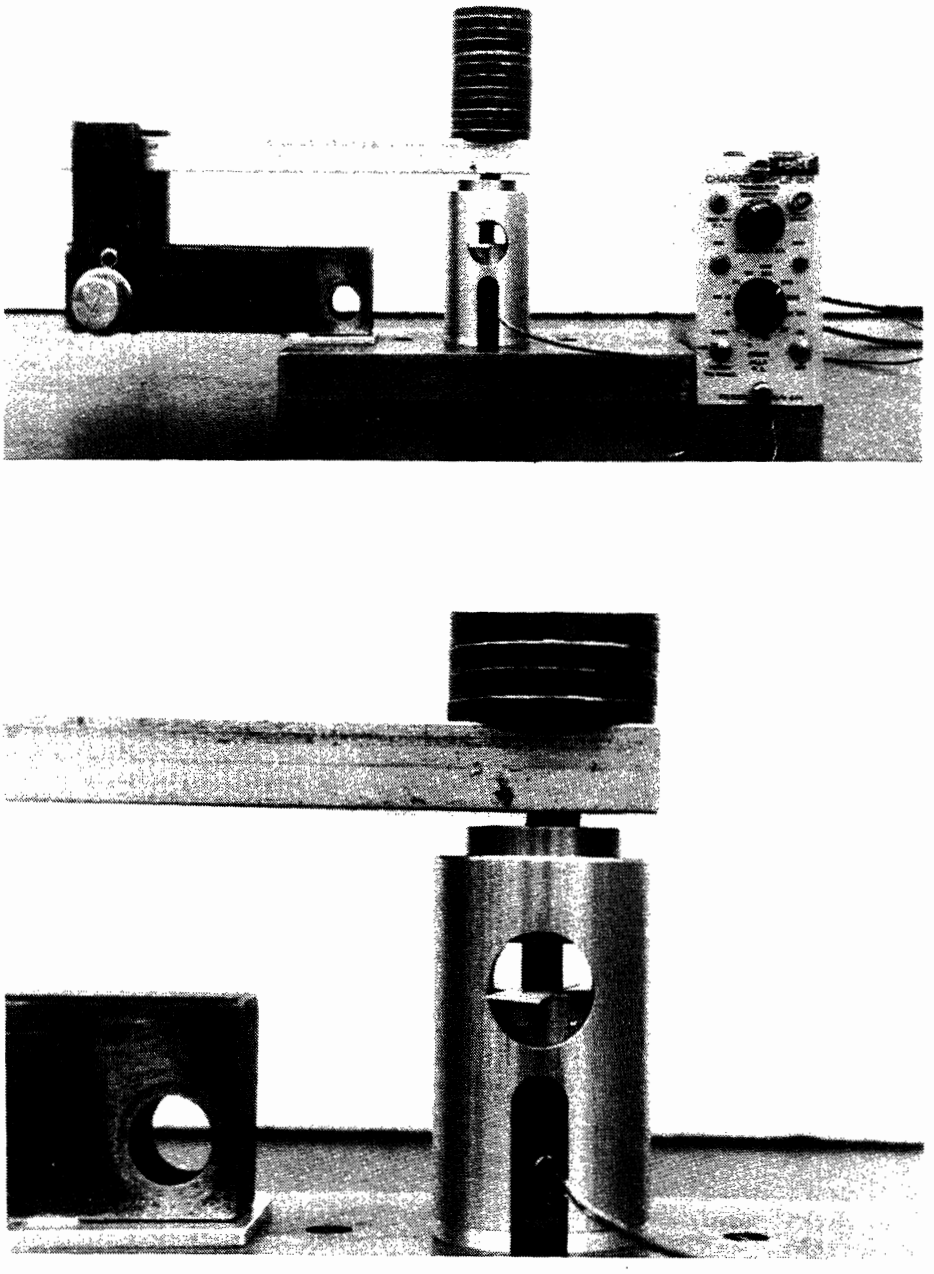

Figure 25. Device for calibration of Fuji Prescale film.

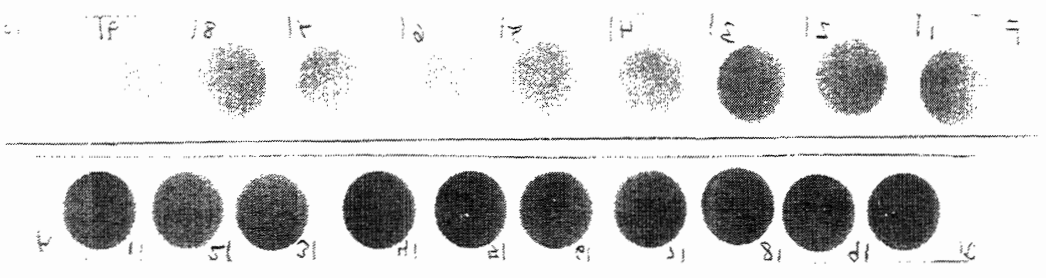

Figure 26. Circular "dots" made on Prescale film by calibrator.

To relate the color density to the magnitude of the applied pressure, the film samples were digitized using an 8-bit, 600-dpi (dots per inch) flatbed scanner in greyscale. This method assigns a value from 0 (lightest) to 255 (darkest) for each pixel of the image. A pixel is the smallest element of a digital image. At 600 dpi, one pixel represents an area 0.0017 x 0.0017 inches or 0.04 x 0.04 mm. The pixel values for each calibration dot were averaged, using an area slightly smaller than the dot to eliminate edge effects. These mean pixel values were plotted versus the measured peak pressure for each trial and a polynomial curve was fit to the data. Figure 27 shows a calibration curve for this material obtained using a Microtek 600 ZS scanner and Image 1.41 analysis software on a Macintosh IIci microcomputer.

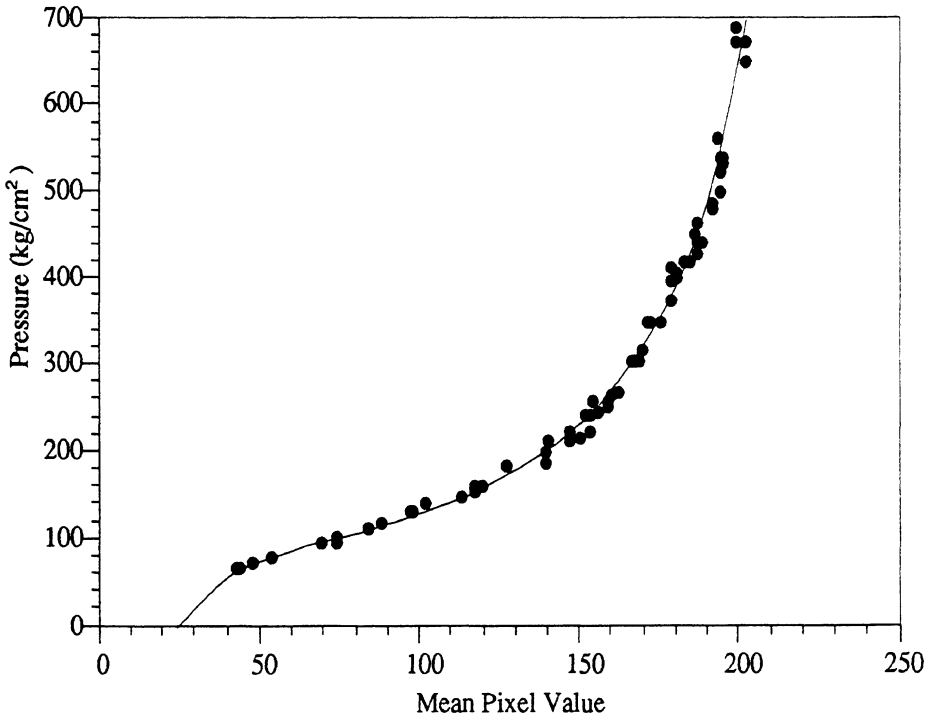

Figure 27. Calibration curve for Prescale film relating pixel density to applied pressure.

Conditions and Limitations of Prescale Film Measurements. Important limitations to the accuracy and precision of the Prescale film were addressed in these experiments. Because the color change is produced by a chemical reaction on the surface of the film, the response of the film can be affected by temperature and humidity, particularly the latter. To minimize these effects, calibration trials were carried out in the

same laboratory as the airbag tests. Since color-producing chemical reaction is also time dependent, requiring several minutes to develop completely, scanning of Prescale images was conducted at a uniform interval of time after exposure. The precision of the Prescale film is rated by Fuji at ±10% although better results can be obtained by carefully controlling the temperature, humidity, and scanning interval. The accuracy of the film measurement technique is dependent on the suitability and accuracy of the calibration procedure.

The most significant limitation of this measurement technique is the unknown nature of the pressure pulse produced by impact of the airbag fabric with the Prescale film during testing. Testing with the ILF indicated that the pulse is less than one millisecond in duration when the airbag is deployed into a rigid aluminum plate. Discrepancies between the duration of the calibration pulse and duration of the impact of the airbag with the film will produce errors in the peak surface pressure measurement. If the impact event is of shorter duration than the calibration pulse, the Prescale film analysis will produce peak pressure measurements less than the actual values.

3.4.4 Peak Surface Pressures During Airbag Fabric Impact

After a reliable calibration was obtained, Prescale film was used to measure the peak pressures on the surface of the ILF during impact of the airbag fabric with the ILF. Tests were conducted as before, except that a 50 x 170-mm piece of Prescale film was fastened to the front of the ILF using adhesive tape. The microcapsule coating was placed against the ILF, so that the plastic backing of the film would protect the microcapsules from shearing, due the airbag fabric motion, while allowing response to surface pressure.

The airbag was deployed, striking the ILF and Prescale film and producing an image on the film matching the pattern of peak surface pressure. The Prescale film was removed from the target surface and scanned by the same procedures used for the calibration. The calibration curve generated previously was imported into the software so that pixel values could be interpreted directly as pressure levels.

A total of 22 tests were conducted using Prescale film on the surface of the ILF or a test fixture specially designed for these measurements (see Reed and Schneider 1992 for a description of the test fixture). Figures 28 and 29 show Prescale images produced by four different module configurations with the ILF located 225 mm from the airbag module. The patterns of peak surface pressure are apparent as red marks on the white film. The 25-mm circular marks visible on the film correspond to the edges of the sensor disks over which the film was placed. The film images were immediately noted to be very similar in shape and size to the wing abrasions observed with human subjects in similar deployments. Most apparent is the line of dots produced by impact of the airbag seam, which closely matches similar patterns of injury seen with wing abrasions. The density of the color change in the Prescale image, as well as the area of the image, is well correlated with the severity of injury measured by the ARS and injury ranking. The darker, larger images were produced by airbags with 350-kPa inflators that produced more severe abrasions than airbags with 320-kPa inflators.

Pressure and Abrasion Patterns. The similarity between the patterns of peak surface pressure produced by the airbags deployed into a rigid target surface and the injury patterns observed with human skin suggests that high surface pressure is a primary cause of airbag-induced abrasion. Several hypotheses were formulated on the basis of these observations. First, airbag-induced abrasions (ARS 3+) were believed to be caused by high-velocity impact of the airbag fabric with the skin producing very high local surface pressures that damaged the epidermis and dermis. Second, high surface pressure due to airbag fabric impact was believed to be both necessary and sufficient for ARS 3+ abrasions. That is, sufficiently high surface pressures are capable of producing injury

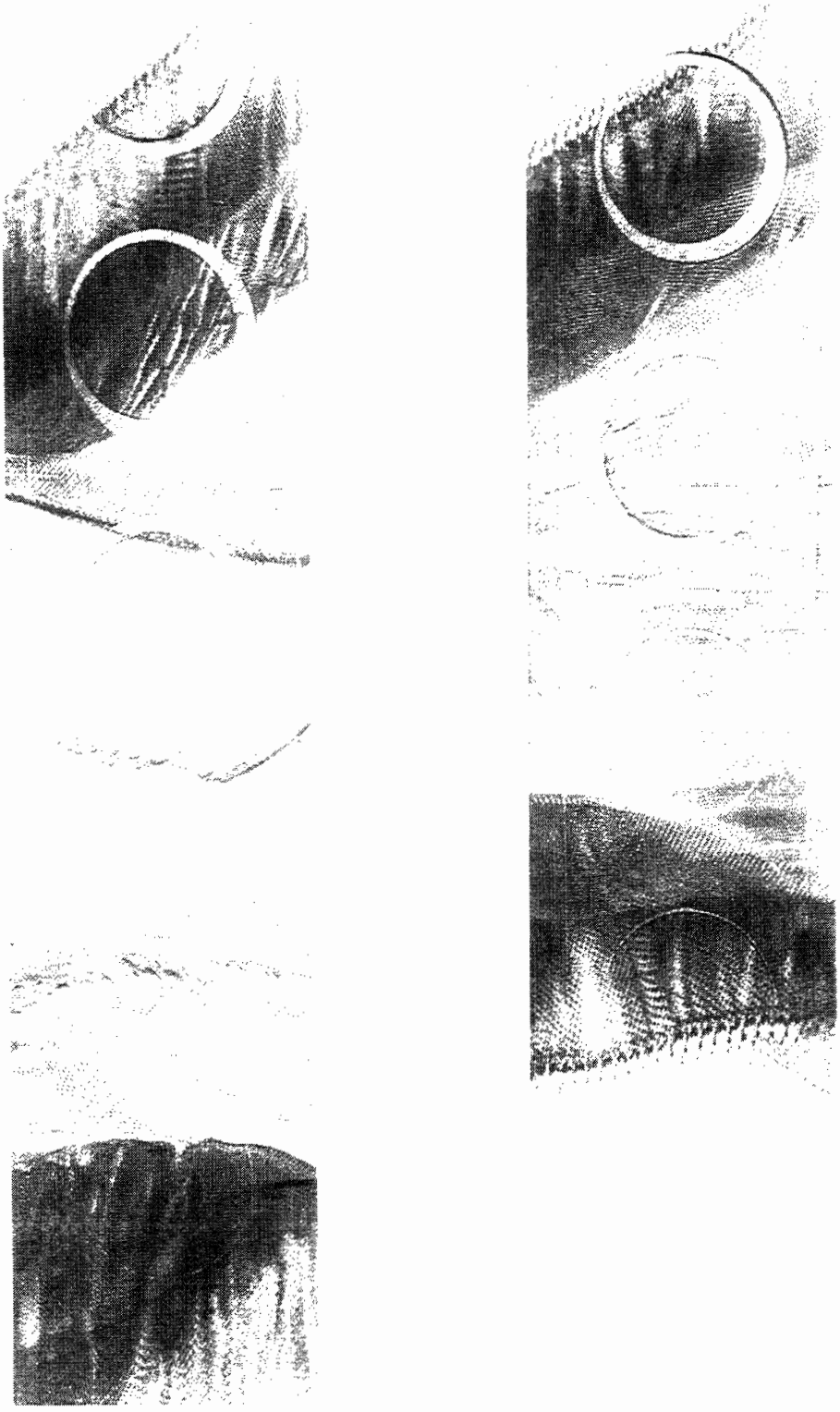

Tethered Untethered

Figure 28. Prescale images produced by deployments of tethered and untethered airbags at 225 mm with 350-kPa inflators (actual size).

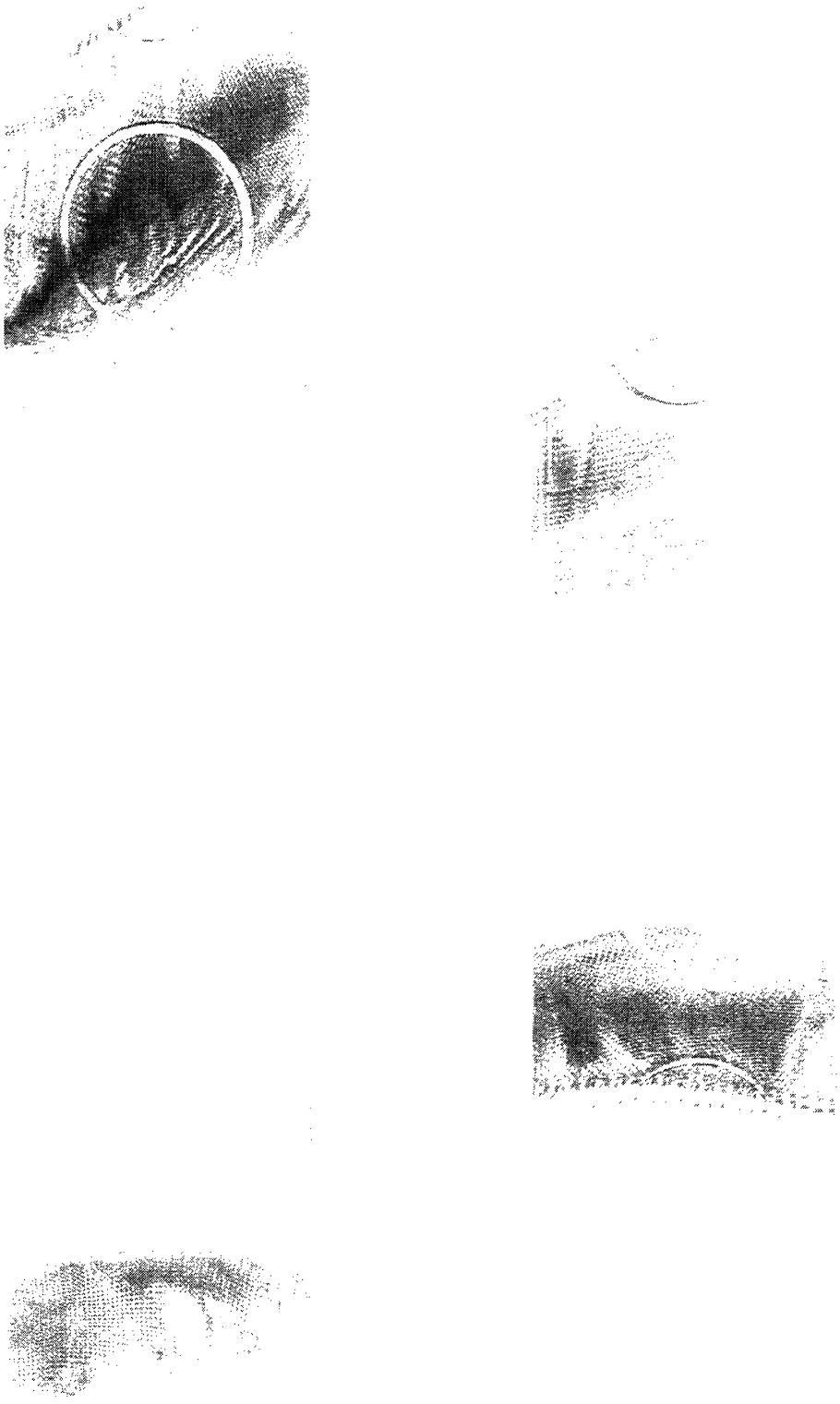

Tethered Untethered

Figure 29. Prescale images produced by deployments of tethered and untethered airbags at 225 mm with 320-kPa inflators (actual size).

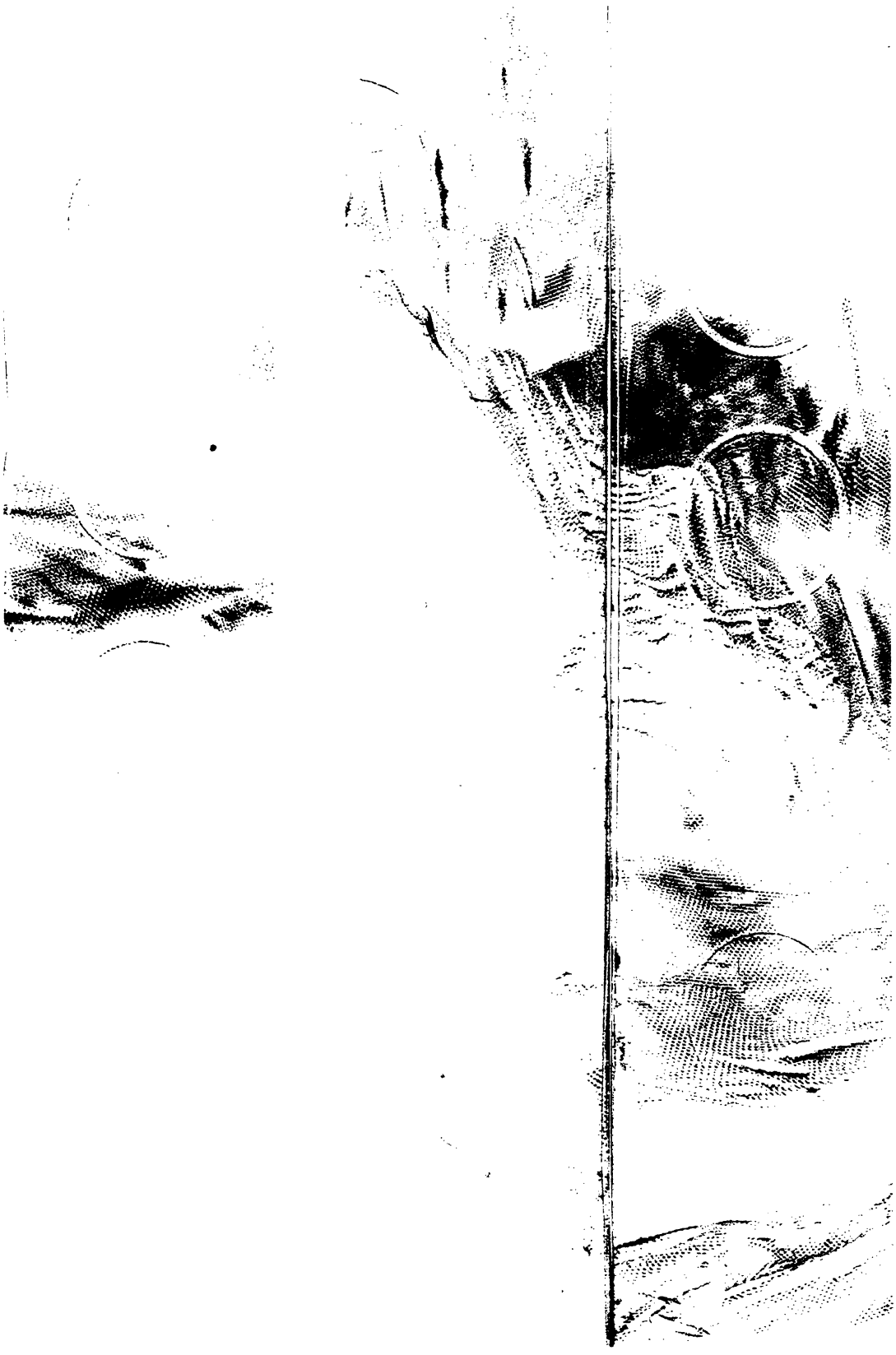

Tethered Untethered

Figure 30. Prescale images produced by deployments of tethered and untethered airbags at 300 mm with 350-kPa inflators (actual size).

even in the absence of other factors, while other factors (*e.g.*, lateral airbag fabric movement) could increase the severity of an injury that was primarily due to high surface pressure.

These hypotheses were explored by testing airbags that produced stamp and slap abrasions with human volunteers. Stamp abrasions were known to be produced by airbag fabric motions largely perpendicular to the skin surface, as evidenced by the skin target markings that transferred to the fabric without smearing (see Figure 9). Slap abrasions had characteristics similar to both stamp and wing abrasions, in that there were areas of the injury for which the epidermis was removed and other areas where it was largely intact.

Figure 30 shows Prescale images obtained with the target surface located 300 mm from the airbag module, using tethered and untethered airbags with 350-kPa inflators. The images are again very similar to the patterns of abrasion obtained for similar tests with human skin, demonstrating that the pattern of peak surface pressure matches closely the pattern of injury for all three abrasion types.

Surface Pressure Level Corresponding to the Abrasion Threshold. The total area of the Prescale film showing a color change after a deployment was larger than the area of injury to human skin in a comparable deployment, indicating that the response threshold of the film was lower than the injury threshold for human skin. This characteristic of the Prescale allowed fairly accurate determination of the surface pressure on a rigid target that corresponded to the injury threshold for human subjects.

The Image 1.41 software used for this analysis allows dynamic thresholding to be applied to the image. The threshold level can be adjusted between 0 and 255, corresponding to the range of pixel values from white to black. The software displays only those pixels that exceed the threshold value, which in this case corresponds to those areas of the image exceeding a particular surface pressure level. For each Prescale

image, the threshold level was adjusted until the area exceeding the threshold value was judged to be equal to the area of injury in corresponding deployments with human subjects. The process was necessarily subjective, because the precise area of injury for each test with human skin was not known, and because the area of injury and the Prescale image varied somewhat among tests with identical airbag configurations.

Figures 31 and 32 show matched pairs of human abrasions and thresholded Prescale images. The threshold level that most consistently produced acceptable matches corresponded to a pressure level of 175 kg/cm^2 (2490 psi). Expressing this level in terms of human skin response, an airbag fabric impact capable of producing a pressure level of 175 kg/cm^2 or higher on a rigid target surface was sufficiently severe to cause ARS 3+ abrasions to human skin.

Surface Pressure Levels on Human Skin. Although the surface pressure levels produced by airbag fabric impacts on a rigid surface were well correlated with human skin abrasions occurring in similar deployments, the same surface pressures might not be produced in impacts with skin supported by compliant subcutaneous tissue. The Prescale surface pressure measurements had led to the hypothesis that high surface pressures during the initial impact of the airbag fabric with the skin were the primary determinant of each of the abrasion mechanisms. In three tests with human volunteers, an attempt was made to verify if (1) similarly high surface pressures occurred on impacts with human skin, and (2) high surface pressure alone was capable of producing ARS 3+ injury without shear (scraping) applied by the airbag fabric.

In each of these tests, the front of the subject's leg was covered with a thin backing sheet of polyethylene film and pieces of Prescale film were placed over the plastic. The objective was to shield the skin from direct contact with the airbag, thereby eliminating scraping by the airbag fabric while simultaneously recording the peak surface

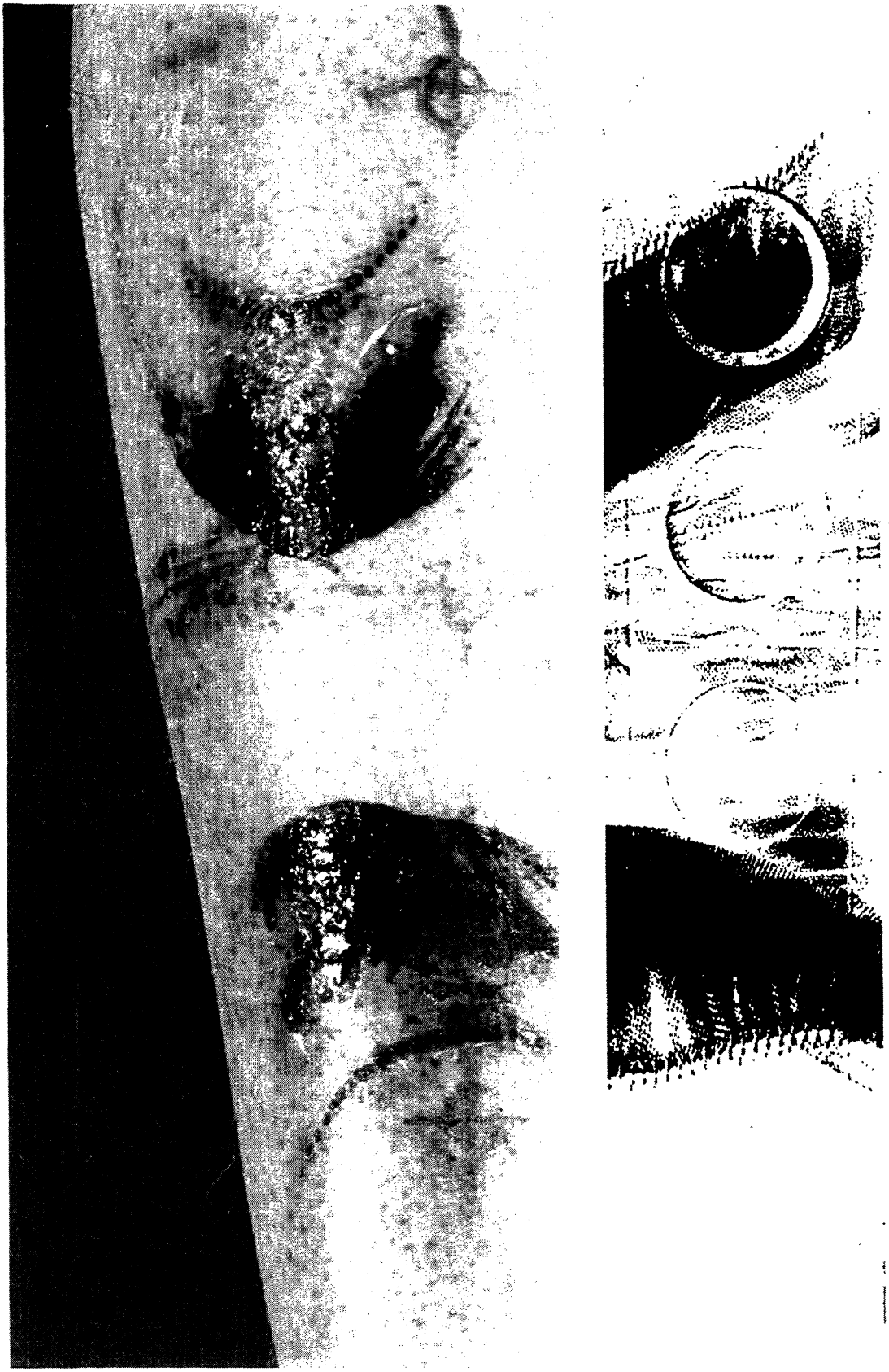

Figure 31. Abrasions and a thresholded Prescale image obtained with 350-kPa inflators and untethered airbags.

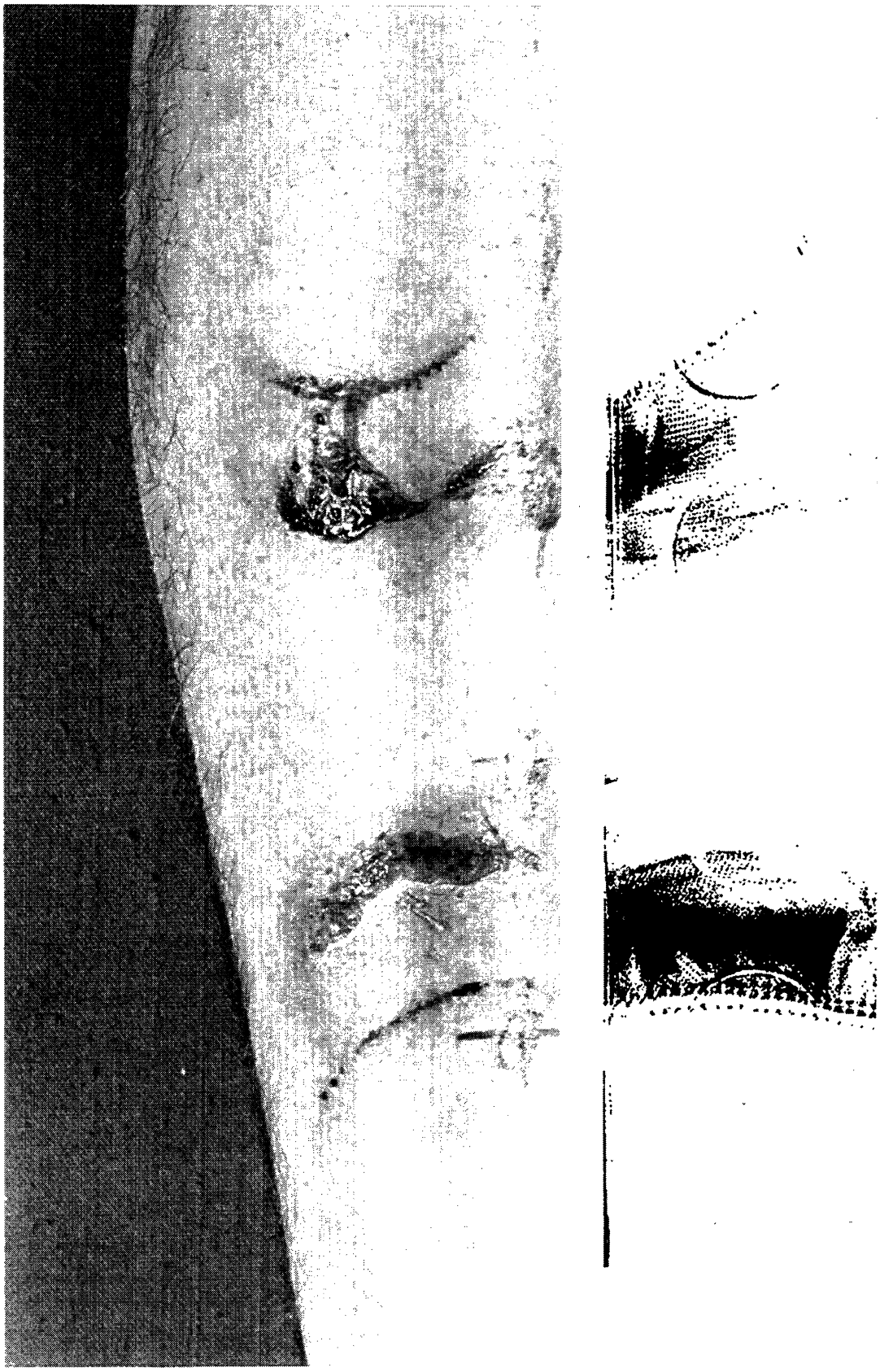

Figure 32. Abrasions and a thresholded Prescale image obtained with 320-kPa inflators and tethered airbags.

pressure with the Prescale film. Because the plastic film could not be accurately molded to the curved surface of the subject's leg, the Prescale and backing sheet were not in firm contact with the subject's leg over some areas of the skin.

Figures 33 and 34 show pre- and post-deployment photographs from two tests. The airbag configurations tested used 350-kPa inflators, which produced the most severe injuries in the previous testing. A third test, using a tethered airbag with a 320-kPa inflator, did not produce any injury or significant marking on the Prescale. These tests demonstrated three important aspects of the airbag abrasion mechanisms.

1. High surface pressures are produced by airbag fabric impact with the skin. In both tests shown in Figures 33 and 34, the Prescale film showed markings that indicate surface pressures in excess of 200 kg/cm^2. In test HA9102, much of the microcapsule coating was removed from the Prescale film by the deformation of the subject's leg and the film that occurred during the deployment, making a thorough assessment of the pressure levels impossible. Enough microcapsule coating remained to observe high pressure levels, although the peak magnitude of the pressure was not measured accurately due to the damage to the film.

2. High surface pressure alone can cause abrasions that closely resemble stamp abrasions. Although the skin was shielded from the scraping action of the airbag by two sheets of plastic, skin injury to the epidermis and dermis resulted in the area initially impacted by the airbag fabric. A close-up photo of one injury shows a laceration of the epidermis in a small area and a much larger area where the blood began immediately to pool beneath the epidermis (Figure 34). An examination of the subject several days later showed that the epidermis was, in fact, necrotic and that damage extended into the dermis (ARS 3). The extent of the injury, however, was reduced by the relative rigidity of the plastic sheets that covered the skin. In a typical, unprotected deployment, abrasions produced by the airbag seam were clearly evident on the subject's skin. In test HA9109, the seam

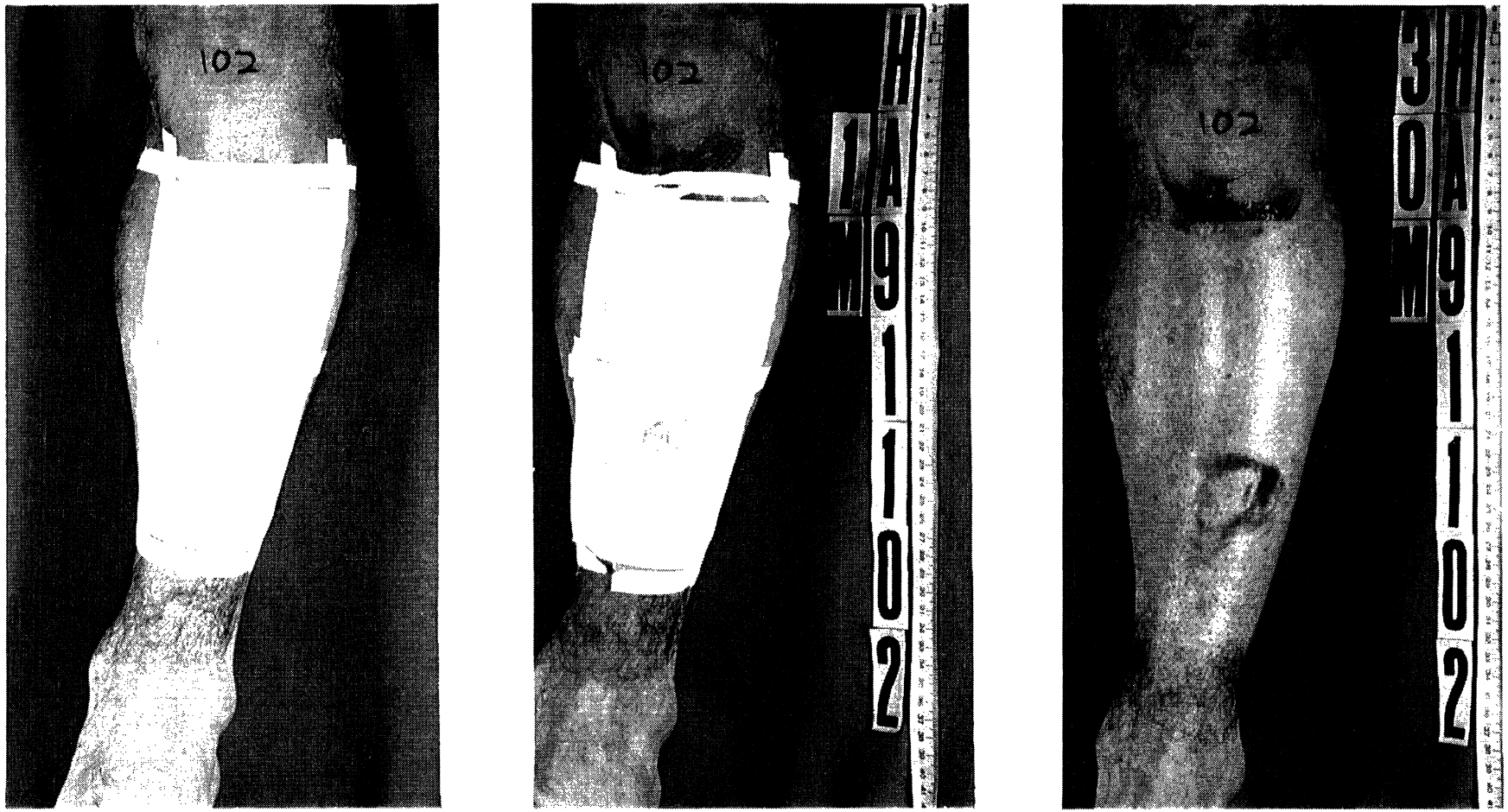

Figure 33. Photographs of a test with Prescale film placed over the surface of a subject's leg prior to deployment of an untethered airbag with a 350-kPa inflator at 225 mm.

Figure 34. Photographs of a test with Prescale film placed over the surface of a subject's leg prior to deployment of a tethered airbag with a 350-kPa inflator at 225 mm.

marks are evident on the Prescale film as they were in tests with the ILF. That these abrasions are not evident in the skin protected by the plastic sheets indicates that the film distributed locally high pressures, resulting in lower pressure levels applied to the skin. These lower pressure levels reduced the severity of the abrasion below the level of injury that would have been produced if the surface pressure impulse had been applied directly.

3. The scraping action of the airbag fabric contributes to the severity of wing abrasions, although high surface pressures are necessary for wing abrasions to occur. In test HA9102, the upper wing of the deploying airbag impacted high on the subject's leg at the upper edge of the plastic shield while the lower wing impacted onto the Prescale film and backing. Although injuries from the upper wing were more severe in previous tests with this airbag configuration, the difference in the two injuries demonstrates the effect that the scraping action of the airbag fabric can have on an abrasion. At the site of the bottom wing impact, where the skin was protected by two layers of plastic, the injury is of similar depth but the epidermis is intact. This is analogous to the stamp abrasions observed in previous testing. Because the damage extends into the dermis, the epidermis is shed during the healing process. However, the epidermis provides a barrier to infection as long as it remains intact, so an abrasion of similar depth but with the epidermis intact should be considered marginally less severe than one in which the epidermis was removed.

These tests with Prescale over human skin confirmed the hypotheses regarding abrasion mechanisms formulated as a result of tests with the ILF. Although surface pressure levels on the skin during airbag fabric abrasion events are high, the actual levels could not be confirmed effectively for comparison with data from the rigid structure because of difficulties using the film on a deformable surface. The leg tissue deforms considerably subsequent to the initial impact of the airbag fabric. This resulted in serious damage to the Prescale film in one case. When the film is mounted such that it is more

securely protected against damage, it acts to distribute the surface pressures applied to it, thereby affecting the event that it was intended to measure. In short, the Prescale is designed to be applied to a rigid surface that human tissue does not provide. Because of the difficulty in applying the Prescale film to the skin, further quantitative testing with human subjects was not performed.

Surface Pressure Levels on a Compliant Substrate. Additional tests to compare the Prescale data from the rigid target surface with a more compliant surface were conducted using Prescale film mounted to a 5-mm-thick piece of soft KRATON substrate material produced as part of the effort to develop an abrasion-predictive material (see Section 4). The KRATON substrate feels similar to human flesh on handling. Substrate and Prescale film were placed on the rigid static test fixture (see Reed and Schneider 1992) for two deployments at 225 mm. The resulting Prescale images were found to differ significantly from images obtained with the rigid target surface, shown in Figure 35. The peak pressure levels observed in tests with the substrate were lower than those measured with the Prescale film placed directly on a rigid target surface for the same airbag module configurations. The surface pressure levels recorded for an airbag with a 350-kPa inflator deployed into a layer of substrate are roughly equivalent to the surface pressures produced by the impact of an airbag with a 320-kPa inflator into a rigid target. This suggests that airbag fabric impact probably produces lower peak surface pressures with human skin than with the rigid target surface.

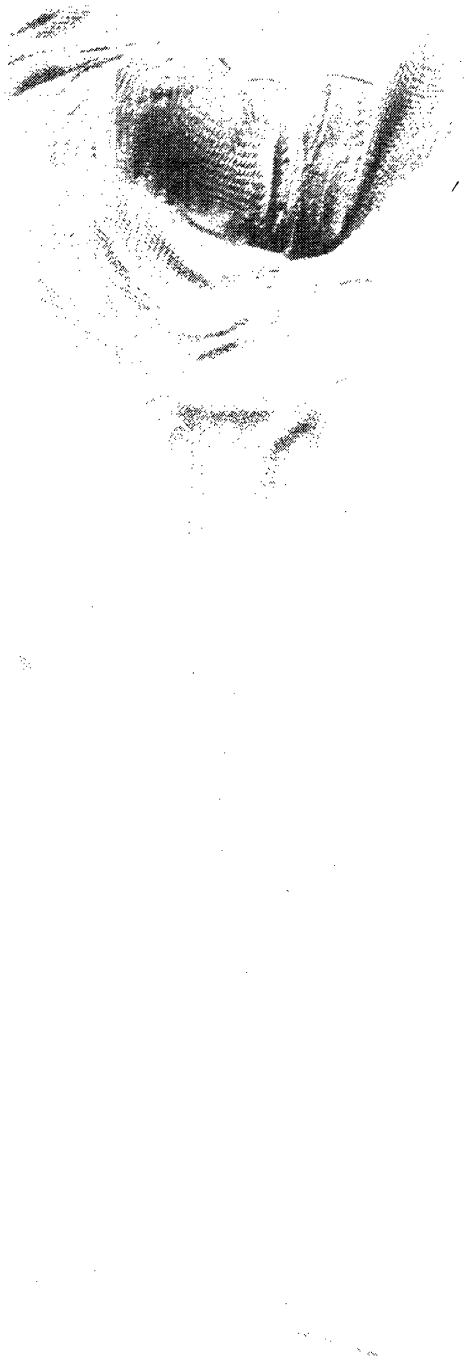

Figure 35. Prescale image obtained from a deployment with Prescale film applied over a compliant substrate (350-kPa inflator, tethered airbag, 225 mm).

However, the rigid-surface pressure measurements remain a valid tool for examining the relationship between airbag fabric impact severity and abrasion severity for several reasons:

1. The patterns of peak surface pressure on a rigid surface and the patterns of abrasion sustained by human skin positioned similarly in the deployment envelope are very similar in shape and area.

2. Airbag fabric impacts that produce higher rigid-surface pressure levels produce more severe abrasions, meaning that the magnitude of the rigid-surface pressure is correlated with the severity of abrasion.

3. Areas of airbag fabric impacts that result in rigid-surface pressures below a threshold level of approximately 175 kg/cm^2 do not cause ARS 3+ injuries to human skin.

Consequently, it was concluded that measurements of rigid-surface pressures during airbag fabric impact can be effectively used to predict the occurrence and severity of airbag-induced abrasion, even though the surface pressure levels may not correspond in magnitude to the surface pressures experienced by the skin.

3.5 SUMMARY OF INJURY MECHANISMS

Airbag-induced skin abrasions were found to be caused primarily by airbag fabric impacting the skin at high velocity, producing high surface pressures that damaged the epidermis and dermis. Lateral movement of the airbag fabric relative to the skin was found to affect the severity of the abrasion by removing skin layers, but even high-velocity movement of the airbag fabric across the skin did not cause abrasion in the absence of high surface pressures, which were produced only during the initial impact of the airbag fabric with the skin.

By comparing surface pressure measurements taken in test configurations identical to those in which wing, stamp, and slap abrasions occurred, the pattern and severity of each abrasion type were found to be correlated with the pattern and level of application of high surface pressure. Image analysis of the Prescale pressure data recorded on rigid target surfaces showed that airbag fabric impacts producing peak surface pressures exceeding approximately 175 kg/cm^2 produced abrasion with human skin. Pressure data collected using human skin and skin surrogates suggest that the actual skin surface threshold for injury with airbag fabric impact is probably lower, since a compliant substrate material was observed to attenuate the surface pressure during airbag fabric impact.

These observations differ from the injury mechanisms hypothesized prior to this study. Abrasions were assumed to occur when airbag fabric was drawn rapidly across the skin while pressure was maintained between the fabric and the skin. That is, the mechanism of injury was thought to be "scraping," the mechanism typically associated with familiar abrasion events (*e.g.*, sliding on rough, firm ground). However, the pressure levels between the airbag fabric and the skin during most of the deployment were found to be less than 1 kg/cm^2, apparently below the level that could produce abrasions due to lateral fabric movement. Instead, abrasions occurred only at points of high-velocity fabric impact when the airbag fabric struck the skin while traveling in excess of 80 m/s. The patterns of high surface pressures generated by the impacts were found to correspond well with the patterns of injuries to human skin. These high pressures were both necessary and sufficient for skin abrasion to occur. When these impact-generated pressures occurred without substantial lateral fabric motion, stamp abrasions were observed. When the airbag fabric struck the skin while moving laterally relative to the surface, the epidermis was removed as it was damaged and the more severe wing or slap abrasions resulted. In the case of the wing abrasions, although the airbag fabric wing continued at high velocity for up to 100 mm across the skin surface, abrasions were noted only where the high surface pressures were recorded, at the initial points of airbag fabric impact.

A level of surface pressure less than that required for a stamp injury, but greater than the 1-kg/cm^2 level generally present during the deployment, might produce an abrasion in conjunction with lateral motion of airbag fabric across the skin. However, such pressure levels did not appear to occur in the static deployments in this study. In actual crash situations, loading of the occupant against the airbag may produce sufficiently high surface pressures to cause this type of abrasion, although the resulting abrasions would likely be less severe than those observed in the static tests because the injury would be produced by scraping away the skin layers, beginning with the relatively tough outer epidermis. The impact-induced injuries observed in this study can affect the dermis without removing the epidermis, effectively crushing the skin layers without removing them and producing an injury much more quickly. This was the case with the stamp abrasions and the abrasions observed in tests with the skin protected by plastic.

3.6 EXPERIMENTS WITH AN ALTERNATIVE AIRBAG FOLD TECHNIQUE

An experimental airbag fold technique was developed to determine if airbag packaging could influence the airbag kinematics sufficiently to reduce or eliminate abrasion. Since results of quantitative testing (see above) demonstrated that abrasions were caused by impacts of high-speed airbag fabric with the skin, one method of reducing the potential for skin abrasion would be to reduce the incidence of high fabric velocity in the airbag deployment envelope. The experimental fold was therefore designed to reduce the peak fabric velocities, primarily by eliminating the sweeping "wing" action that was responsible for the most severe injuries observed in testing with human volunteers.

A theoretically optimal fold for reducing fabric velocities would position each section of airbag fabric in the module in the same position relative to the other fabric sections as it would be when fully deployed. This would result in each section of fabric travelling the least distance as the airbag filled, thereby resulting in the lowest fabric velocities for a given fill time. Although this theoretically optimal fold could only be

achieved with a flexible material (*e.g.*, in the manner of a latex balloon), the principle of reducing the travel distance for each section of airbag fabric can be applied to the design of a fold technique for current airbag fabrics.

In particular, the experimental fold in this study was designed to (1) place the airbag fabric from the center of the front of the airbag in the same position in the module, namely, outermost, and (2) eliminate to the extent possible the sweeping "wings" observed with the accordion fold technique used with the other airbags in the study. Because the actual folding technique used is less important than the principles employed in the design of the fold, the details of the technique will not be presented here. Rather, the effect of the experimental fold technique on the deployment kinematics and the incidence of abrasion are discussed.

Figure 36 shows a frame from a high-speed film of a deployment with the experimental fold, along with a frame from the same time in a deployment with an identical airbag and inflator with the standard fold technique. With the experimental

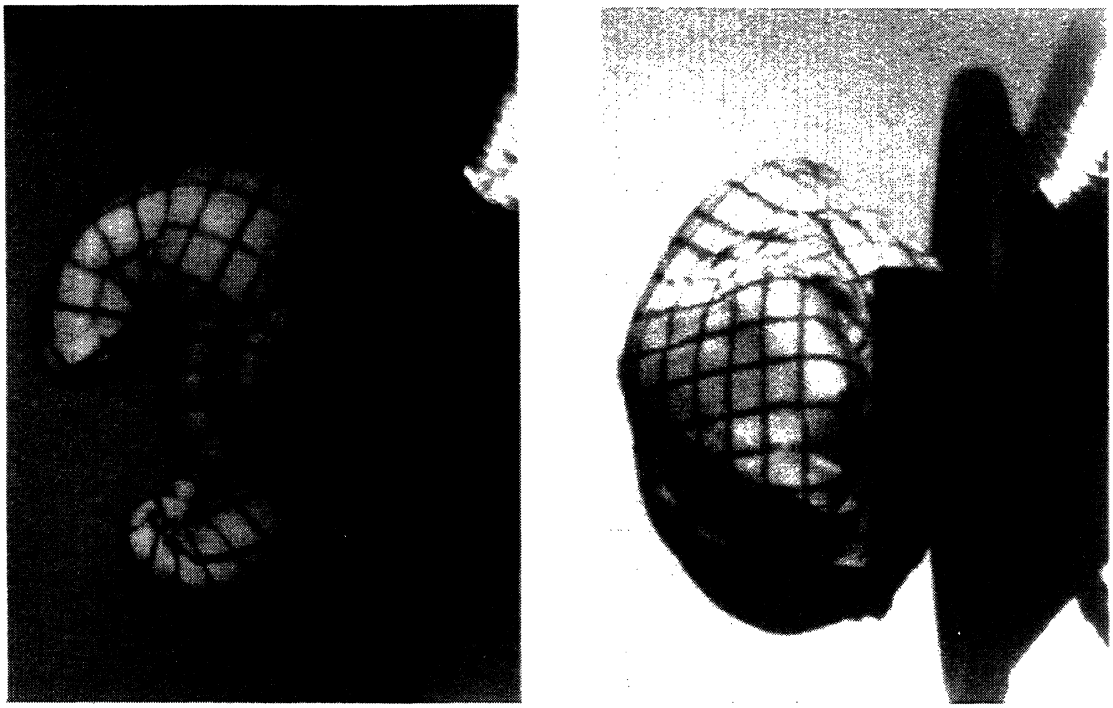

Standard Fold Experimental Fold

Figure 36. Film frames from high-speed film of deployments with standard and experimental fold techniques.

fold, the sweeping wings have been eliminated, and the center of the airbag is the first part of the airbag to exit the module. The peak fabric velocities were reduced, as shown in Figure 37, particularly for distances between 175 and 225 mm from the module.

In a test with Fuji Prescale film on the static test fixture (see Section 3.4.4 for procedures), the surface pressure levels due to airbag fabric impact were below those associated with skin injury. Figure 38 shows Prescale images from a deployment with a standard fold airbag and an identically configured test with the experimental fold. Quantitative analysis of the image showed no areas in which the pressure levels exceeded 175 kg/cm^2, the level for which skin abrasions are expected. In a subsequent test with a human volunteer, no abrasion was observed with the experimental fold, while in similar tests with the standard fold, ARS 3 abrasions were produced (see Section 2.3.5). The experimental fold was found to reduce fabric velocities and fabric impact forces, and thereby eliminate abrasion in this limited series of tests.

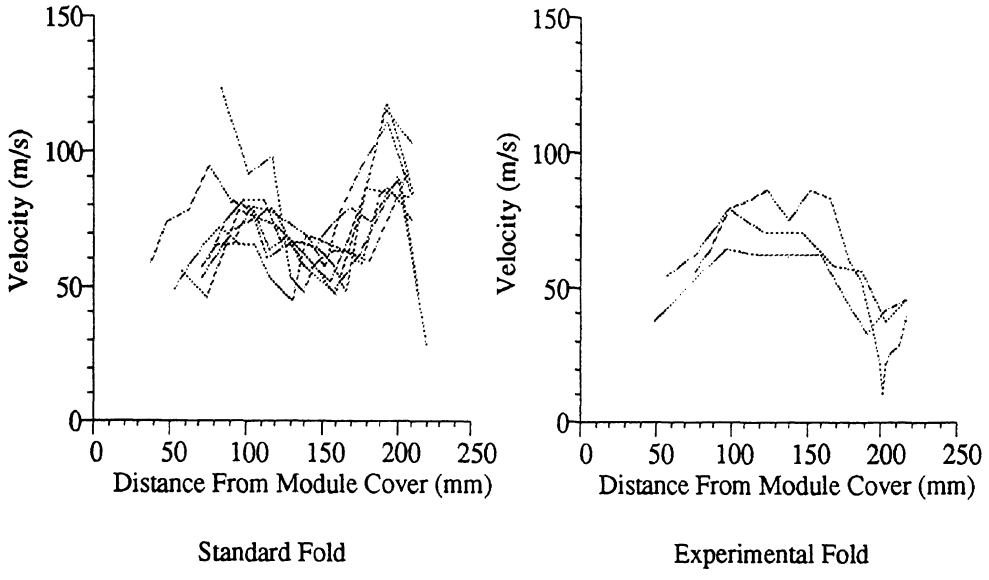

Figure 37. Comparison of leading-edge velocities from standard and experimental folds for tethered airbags with 320-kPa inflators.

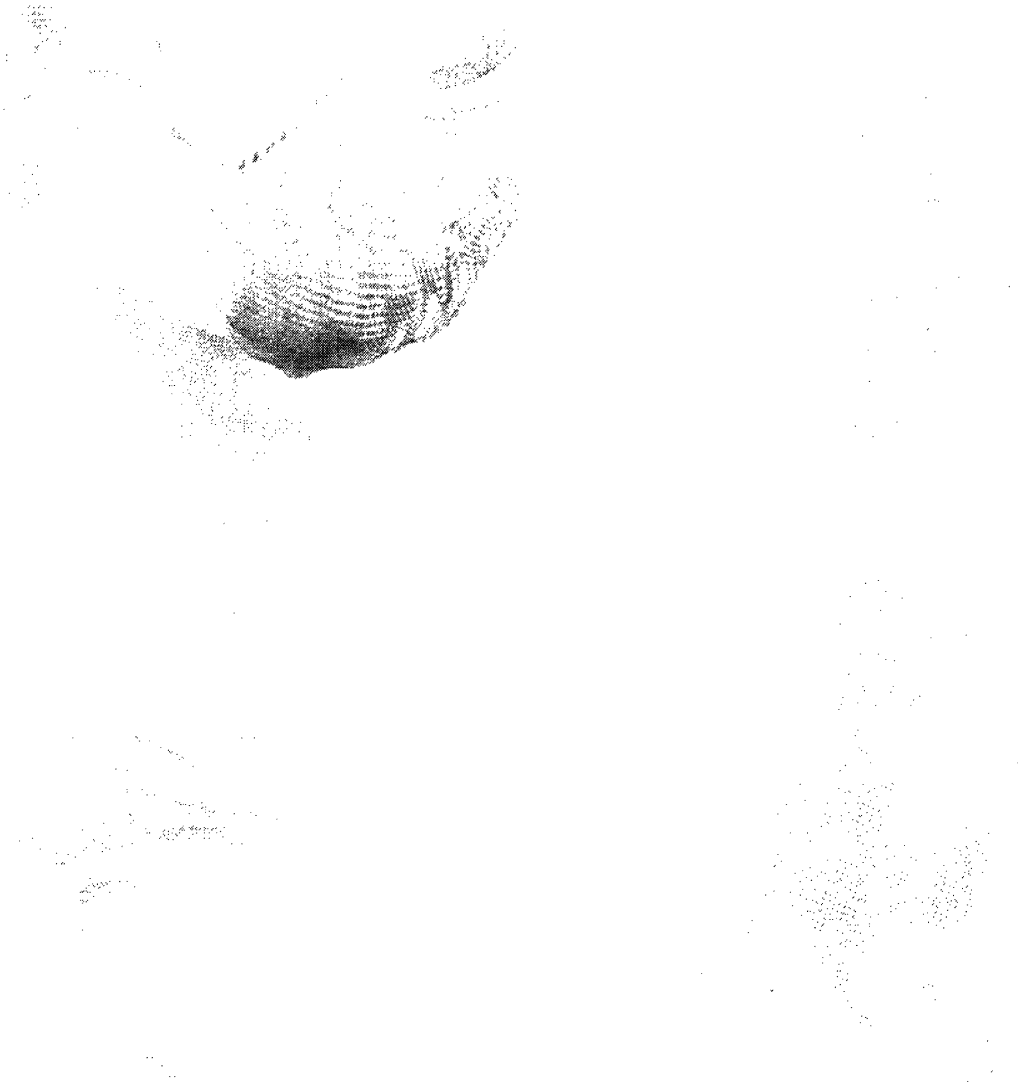

Standard Fold Experimental Fold

Figure 38. Prescale images produced by deployments of tethered airbags with 320-kPa inflators into a rigid target surface at 225 mm using the standard and experimental fold techniques.

4.0 INVESTIGATIONS OF ABRASION-PREDICTIVE MATERIALS

4.1 OVERVIEW

An important goal of this study was to develop a material that would respond to airbag fabric contact in a way that could be used to predict abrasion in human skin. This "surrogate skin" was to be used on test dummies to assess abrasion potential in dynamic tests with airbags. However, in the course of the study, the results from testing with human volunteers, quantitative measurements of injury mechanisms, and tests of candidate surrogate materials suggested that static laboratory testing with an abrasion-predictive material on a cylindrical target surface provides a sufficiently effective means for evaluating an airbag's abrasion potential.

Evaluation of candidate materials was performed by applying the material to a prosthetic lower leg and deploying an airbag into the material, as shown in Figure 39. The prosthesis was used to hold the material in a shape similar to the shape of the tibia

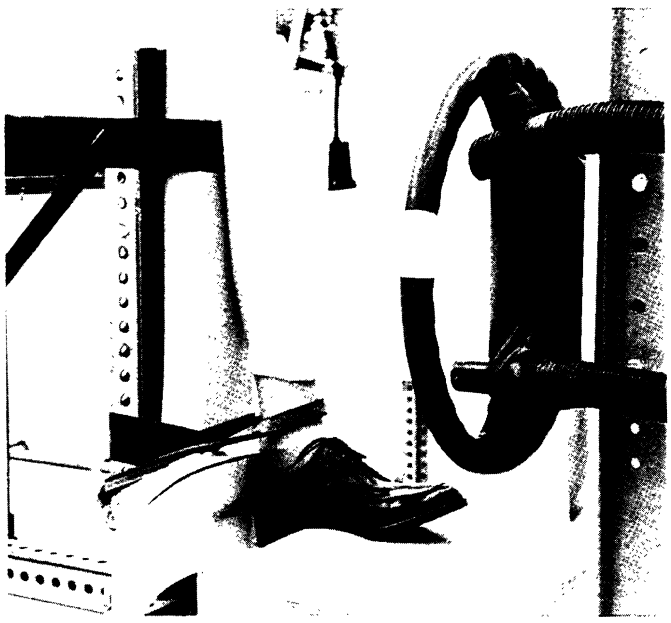

Figure 39. Prosthetic leg used in testing of candidate materials.

region. Most tests of candidate materials were performed with the surface of the material 225 mm from the airbag module to duplicate the test configuration for which wing-type abrasions were observed with human skin.

The initial approach was an attempt to develop a "skin" that would react to the airbag fabric in a way qualitatively similar to human skin, *i.e.*, show a range of "injuries" from scraping of the epidermis to subsurface bleeding. Several materials were tested that demonstrated promising qualitative responses. Later in the study, as more information was obtained regarding the injury mechanisms with human skin, efforts were directed toward more quantitative systems using materials that responded to particular levels of surface pressure. Collectively, all of the candidate materials are referred to as Abrasion-Predictive Coatings (APCs) rather than as surrogate skin materials, because some of the systems do not resemble human skin, although they provide important response characteristics that can be related to skin tolerance.

Although several APCs were explored and developed that could ultimately be used on an irregular surface such as a dummy face, the best results were obtained using a pressure-sensitive film that was more readily adapted to a cylindrical form. This geometrically simpler target surface was also believed to produce less intertest variability than would be the case with a dummy face, and the cylindrical surface approximated the shape of the human tibia region, the only skin area for which human response data were available for comparison with the surrogate materials.

4.2 QUALITATIVE APPROACHES

4.2.1 Layered Systems

Wing-type abrasions are characterized by arc-shaped areas of injury, often with a distinctive line of small abrasions caused by the airbag seam. Initial APC efforts attempted to obtain a similar appearance in materials exposed to similar deployments. In tests with human skin, the epidermis and upper layers of dermis were removed while the

more compliant lower layers of dermis and subcutaneous tissue remained but showed subsurface bleeding. Consequently, an approach was sought that would simulate the differing characteristics of the skin layers.

A substrate layer comprised of a copolymer gel was used to simulate the compliant, lower layers of the dermis and subcutaneous tissue. These layers are flexible to the touch and account for the substantial mobility of the upper skin layers. The gel layers were produced by dissolving styrene-isoprene and styrene-butadiene (KRATON 1101 and 1104) in heavy mineral oil at approximately 110 °C. The resulting solution was poured onto flat molds and heated in an oven at approximately 120 °C until the mixture had flowed in the mold to an even thickness. During cooling, physical cross-bridges are formed in the solution, making the material soft but resilient. The consistency of the material was varied by changing the amount and proportions of copolymer dissolved in the solution. The resulting sheets of substrate material felt flesh-like to the touch, although the surface was sticky and mineral oil tended to leach out of the surface unless it was covered with another material.

The stiffer, thinner epidermis was more difficult to simulate than the flexible lower layers of tissue. The requisite material had to be very thin and durable enough not to respond to low-level rubbing, as with the fingers, but able to be torn and removed the way human skin is by airbag deployments. After trying many different surface coatings, including paints and thin layers of plastic, thin tissue paper was found to provide the most biofidelic response. Applied to a layer of substrate, the tissue paper was tough enough to withstand moderate amounts of handling. When exposed to an airbag deployment, the paper showed surface disruptions and tears very similar in shape and area to the abrasions experienced by human subjects. Figure 40 shows an example of layered paper on substrate following a deployment of an untethered airbag with a 350-kPa inflator at 225 mm. Other types of paper were also tested, including rice paper and various art papers. However, thin tissue paper provided the best response.

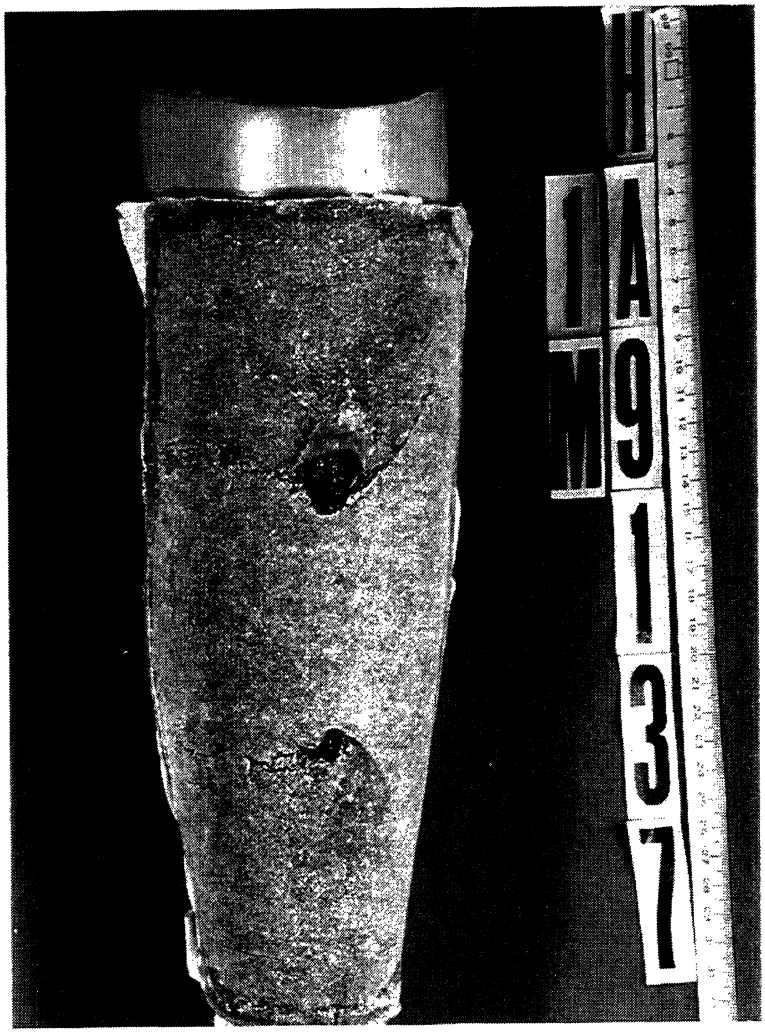

Figure 40. Layered paper on substrate following a deployment at 225 mm.

The performance of the paper can be explained by physical similarities between the composition of paper and the physiology of the epidermis. The epidermis consists of epithelial cells layered together in a laminated structure. This layering of tissue is grossly similar to the structure of fibers in paper, suggesting that the failure modes might be similar. In fact, the qualitative response of some types of thin paper to airbag deployments was remarkably similar to epidermis.

While some success was achieved, there are several limitations to this layered, qualitative approach for predicting abrasion to human skin. Foremost is the failure of this system to respond appropriately to two of the injury types observed with human subjects. Although the layered paper and substrates responded well to wing abrasions,

stamp and slap abrasions did not produce comparable responses. This is due to the airbag actions responsible for the respective injury types and the inability of the layered APC to respond to normally directed force. As previously noted, stamp and slap abrasions result almost exclusively from high surface pressure impulses to the skin (Section 3.4). Although the severities of wing abrasions are also mediated by high surface pressure, substantial lateral velocity of the airbag material also applies shear force to the surface. This explains the more complete removal of epidermis from the area of wing abrasions as compared with the other abrasion types, and also explains the response of the paper during wing abrasion events. It is apparent from manual manipulation of the paper/ substrate materials that human epidermis is much stronger in tension than are the papers used in the layered systems, yet shape and extent of the surface damage during a deployment is similar to that of epidermis. This apparent contradiction results because the human skin tissue responds to both high surface pressure and shear, yielding damage in the dermis and epidermis, while the paper/substrate combination responds only to the shear stress component, showing a similar level of damage in a weaker material. The surface pressure impulse is believed to damage the skin such that the epidermis is more easily torn and detached from the lower layers, whereas no similar effect is observed with the paper/substrate systems.

The layered qualitative systems are also limited by the difficulty of tuning the system to match the damage threshold to the human injury threshold. Because abrasion potential must be inferred from the apparent damage to the surface, it is important that the size and extent of the damage correspond directly to the human skin injuries that would be expected. This is accomplished by varying the properties of the paper, the adhesion between the paper and the substrate, and the properties of the substrate. Although the latter two parameters can be controlled fairly easily, the properties of the paper are difficult to modify without appropriate laboratory and prototyping facilities. Although several paper companies assisted in the development effort by providing samples of current products, the physical characteristics of a particular paper could not be adjusted without considerable expense.

4.2.2 Scratch-Off Coatings

Other qualitative methods for indicating abrasion events were also investigated. One material of interest was a scratch-off coating similar to those used for instant lottery tickets and other game pieces. In commercial applications, the material is printed onto coated paper using an offset process. The toughness of the coating is varied by controlling the surface of the stock, the composition of the material, and the thickness of the coating. Samples of varying compositions were obtained and tested by manual means and found to present a potentially useful response to shear. However, as with layered systems, the scratch-off coatings do not respond to surface pressure, and consequently cannot indicate stamp and slap abrasions appropriately.

4.3 QUANTITATIVE APPROACHES

The results of quantitative investigation of abrasion mechanisms indicated that surface pressure was the most important factor determining the occurrence and severity of injury, with a very large surface pressure impulse being associated with abrasion and even higher levels of pressure corresponding to progressively more severe injuries (Section 3.4). These findings suggested that abrasion could be effectively predicted by measuring the pattern and magnitude of peak surface pressure during an airbag deployment.

Even prior to these findings, some evidence from tests with APC candidate materials indicated marked correlation between surface pressure and abrasion. Tests with certain types of papers coated with microencapsulated dyes had shown markings after deployments very similar to injury patterns. At the time of testing, it was hypothesized that the shearing action of the airbag fabric was rupturing the microcapsules to produce the image. However, in several experiments, a thin layer of plastic that initially covered the microcapsule surface was not removed prior to testing, yet an almost identical image was produced that was very similar to injury patterns. The implications of these results were not understood until after the injury mechanisms were more fully described.

4.3.1 Microencapsulated Dyes on Paper

Several kinds of paper readily available in offices are coated with small microcapsules that, when ruptured, release chemicals that produce a color change. This technology, frequently applied to carbonless, multiple-copy forms, is similar to that used in Fuji Prescale film, described in Section 3.3. Microcapsules containing a reactive chemical are embedded in a layer of developer. When the capsules are ruptured, the chemical is released and a color change results. For business forms, the color change is typically to black or blue, but other colors are possible. These microcapsules, between 5 and 20 μm in diameter, require considerable pressure to rupture. The apparent ease with which they are ruptured by a ball-point pen is the result of the application of a modest force through the very small area at the tip of the pen.

It was hypothesized that while these papers were designed to respond to normal force, the microcapsule layers would also be susceptible to rupture due to shear, and consequently could be used to record abrasive shear events. In the early stages of the search for an APC, several different types of single-sheet microcapsule-coated papers were obtained from manufacturers and tested by placing a sheet on the front of the prosthetic leg and deploying an airbag, as was described for the other candidate materials. Figure 41 shows the image resulting from a test with one type of paper. The pattern of response was similar to the pattern of injury seen in similar tests with human skin. At the time of testing, the paper response was believed to have been produced by reaction to shear stresses imposed by the airbag fabric sliding across the surface of the paper.

The response of one brand of pressure-sensitive paper (Kimberly-Clark) was found to be very similar to injury patterns for all three abrasion types (wing, stamp, and slap) but there were some limitations to use of this product as an APC. The response threshold of the paper was not adjustable and could not indicate a range of responses (*i.e.*, corresponding to a range of abrasions from minor to severe). Ideally, if the threshold corresponded exactly to the human threshold, the paper would give a binary indication of

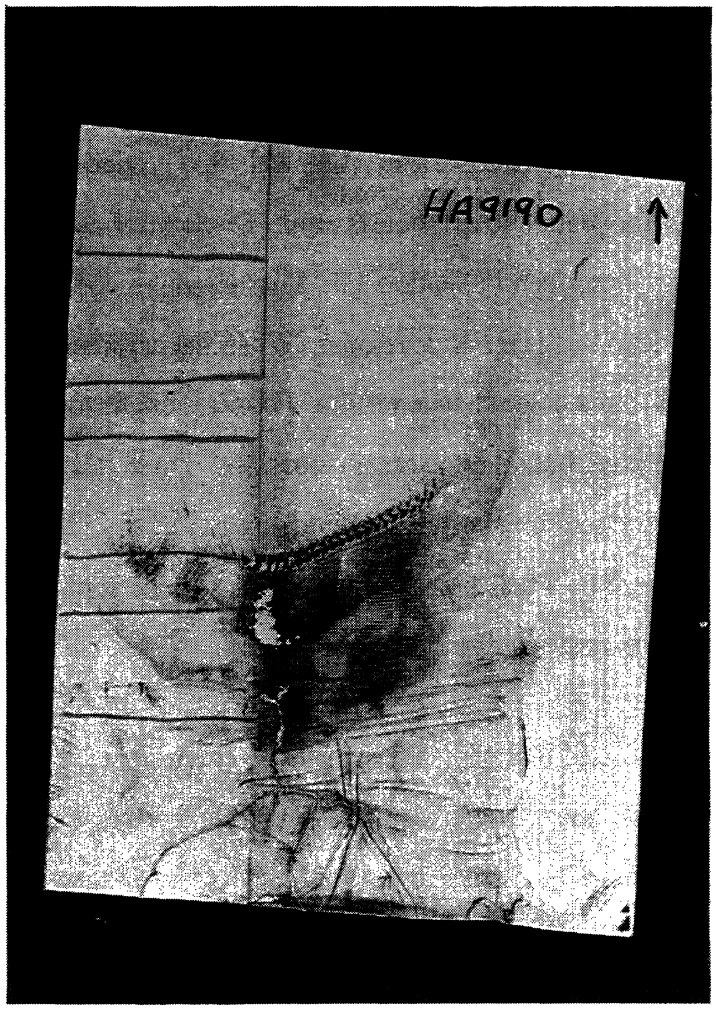

Figure 41. Microcapsule-coated paper following a deployment at 225 mm.

injury potential (*i.e.*, likely/not likely). However, if the match was not exact, then certain events to which the paper would respond would not produce injury with human skin, or vice versa.

4.3.2 Fuji Prescale Film

Shear Measurement. Another type of microcapsule material also showed a potentially useful response to airbag deployment forces. Samples of Fuji Prescale film (see Section 3.4) obtained from the manufacturer were glued to the surface of the prosthetic leg and airbags were deployed into them. Prescale film is made with a microcapsule technology similar to the pressure-sensitive papers except that Prescale uses

a polyethylene film instead of paper for a substrate. Although the manufacturer markets Prescale as a calibrated tool for measuring pressure (normal force), the microcapsule layer also shows a reaction to shear or scraping, if the force is applied to the microcapsule side of the film. In these first tests with Prescale film, the samples were mounted to the prosthetic leg so that the microcapsule layer was exposed to the airbag fabric, since the intention was to record a shear event. The film responded to the airbag deployment in an area and pattern corresponding to injuries seen with human skin. However, the action of the airbag fabric removed much of the microcapsule layer from the film base.

Pressure Measurement. Quantitative assessment of abrasion mechanisms demonstrated that high surface pressure was the primary mediator of abrasion incidence and severity (Section 3.4). Some of the data leading to this conclusion were collected through use of Fuji Prescale film, previously evaluated as a potential shear-sensitive APC. The quantitative measurement experiments described in Section 3 demonstrated that Prescale film could be used to predict the occurrence of all three types of abrasions, making the film the leading APC candidate material.

The important difference between the first APC Prescale tests and subsequent testing was the orientation of the film relative to the airbag fabric. Initially, when shear was believed to be the primary cause of injury, the film was mounted so that the microcapsule layer was exposed to the airbag fabric. The microcapsules responded, but the surface was damaged during the fabric impact so that analysis of the resulting image was impossible. After the important role of surface pressure in abrasion mechanisms was observed, Prescale tests were performed with the film backing toward the airbag so that the microcapsules were protected. The microcapsule layer still responded to pressure but was not damaged by the airbag fabric.

Prescale film has several advantages over other APC candidates. Most important, it shows a range of responses corresponding to a range of applied pressures. The medium-sensitivity type of film used in these tests begins to respond at pressures below

the level producing injury in human skin for airbag exposures and continues to respond with increasing image density for pressure levels producing injuries up through ARS 4 (see Section 2.5.1 for ARS definitions). Airbag fabric impacts can be evaluated in terms of the possible occurrence of abrasion and also the severity. The film is also commercially available and standardized to ensure consistent calibration among lots.

One limitation of the film as an APC is that it cannot be used on irregular surfaces because of the stiff film backing. This precludes use of the film on large irregular areas, such as a dummy face, although small pieces of the film (10–20 mm) could be placed on particular areas of interest. However, this is not regarded as a substantial limitation because of the effectiveness of test procedures that have been developed for assessing airbag skin injury potential using a simple cylindrical target surface (see Section 4.2.4). Since this type of static deployment is believed to be sufficient for abrasion assessment, an irregular-surface APC is not considered necessary, although two candidate materials have been investigated.

4.3.3 Irregular-Surface APCs

Two microcapsule-based systems for measuring abrasion events on irregular surfaces were developed as part of the APC research effort. Both function in the same manner as the pressure-sensitive paper systems described in Section 4.2.1. One system, supplied by Moore Research, Inc., consists of two aqueous solutions, one containing the microcapsules and a second containing the developer. The solutions are mixed together in an appropriate proportion and then coated onto a surface. When dry, the material responds in the same manner as pressure-sensitive paper, producing a sharp black image when subjected to high pressure. A second system, provided by MicroScent, Inc., is a single solution containing both the microcapsules and the developer. Also aqueous-based, the solution forms a pale blue coating when dry that turns bright blue when subjected to high pressure.

There are several difficulties encountered when working with these materials. First, the aqueous solutions are difficult to apply to nonporous surfaces and an even layer of the material, which is essential for consistent performance, is difficult to achieve on an irregular surface. Second, the surface of the material can easily be damaged by light scraping or handling. When these materials are used in commercial products, they are printed on flat, porous paper stock, avoiding these problems. If an irregular-surface APC should become necessary for future airbag abrasion assessments, one of these coatings or a similar microcapsule system could be used to provide a suitable APC with some additional development effort.

4.3.4 Airbag Assessment Test Procedure

Based on results of the APC testing described above and investigations to assess the abrasion mechanisms described in Section 3, a test procedure was developed using Prescale film as an APC to evaluate the injury potential of airbags. This procedure is described in detail in a separate report entitled *Assessing the Skin Abrasion Potential of Driver-Side Airbags* (Reed and Schneider 1992). In brief, the Prescale film is attached to the surface of a 100-mm-diameter rigid cylinder that acts as a target surface. The cylinder is oriented appropriately relative to the airbag module and the deployment is carried out. The image on the Prescale film resulting from the airbag fabric impact is then analyzed using digital techniques similar to those described in Section 3.3 of this report. Skin injury is predicted for areas of the deployment envelope in which peak pressures in excess of 175 kg/cm^2 on the target surface are measured.

5.0 CONCLUSIONS AND DIRECTIONS FOR FUTURE RESEARCH

5.1 EFFECTS OF DESIGN AND DEPLOYMENT FACTORS

Driver-side airbag configurations similar to those in contemporary passenger cars were found to produce skin abrasions in human volunteers under certain test conditions. The incidence and severity of the abrasions were mediated by several factors.

1. *Inflator capacity* had a strong effect on the injury potential of the airbags. Higher-capacity inflators caused more severe abrasions and abrasion over a wider region of the deployment envelope than lower-capacity inflators.

2. *Airbag tethering* eliminated or strongly reduced the severity of abrasions occurring with untethered airbags at distances greater than the length of the tether (about 250 mm).

3. The *distance* between the target surface and the airbag module was also an important determinant of abrasion severity. In general, deployments with the subject's skin closer to the module resulted in more severe abrasions, although for untethered airbags with higher-capacity inflators, relatively severe abrasions were observed over the full extent of the airbag's excursion.

A finer weave *airbag fabric* was not found to reduce the incidence or severity of abrasion. In fact, the data show a trend toward greater severity for the finer weave fabric than for the coarser weave fabric. However, because of the small number of tests and because the two types of airbags were packed in different modules, these findings are not regarded as conclusive. Nevertheless, the data do not support the hypothesis that finer-weave airbag fabric results in fewer or less severe injuries.

5.2 INJURY MECHANISMS

Quantitative measurements of airbag fabric velocity and target surface pressure during deployments were used to describe the abrasion mechanisms. High fabric velocities, frequently in excess of 80 m/s (262 ft/s), were found to produce high surface pressures on the impacted surface. The pattern of these surface pressures corresponded very closely to the pattern of injury to human skin in similarly configured deployments. The data suggest that high surface pressures caused by impact of airbag fabric moving at high velocity are necessary and sufficient to cause abrasion.

The quantitative data do not support the hypothesis that the abrasions observed with the human subjects were caused by lateral movement or "scraping" of the airbag fabric over the skin, although such movement is believed to contribute to the severity of an abrasion. In test configurations that produced a high-velocity fabric movement over a 100-mm-long area of skin, injury was observed only at the point of initial contact, where surface pressure measurements indicated that the peak pressures during the abrasion events were up to 100 times higher than during the remainder of the fabric motion. Further, airbag fabric impacts without substantial lateral motion were observed to cause a type of abrasion in which the skin was damaged but not removed ("stamp" abrasions). Similar abrasions were also observed when the skin was protected from the scraping action of the airbag fabric with a flexible sheet of plastic. These findings may explain why the rougher airbag fabric did not produce more severe abrasions, since it is the high surface pressures generated by the impact of high-velocity airbag fabric, and not the surface scraping, that determines the incidence of abrasion.

Based on these findings, a laboratory procedure was developed to determine the abrasion potential of airbags without the use of human volunteers. This procedure is discussed in detail in a separate report (Reed and Schneider, 1992). Fuji Prescale film, a pressure-sensitive material, is placed on a rigid, 100-mm-diameter cylinder positioned in the airbag deployment envelope. When the airbag is deployed, peak surface pressures on

the target surface are recorded on the Prescale film. The experimental data suggest that airbag fabric impacts that result in a peak surface pressure on the rigid target surface in excess of 175 kg/cm^2 (2500 psi) will produce abrasion with immediate surface or subsurface bleeding in human skin.

Surface pressure measurements with human skin and flesh-like surrogate materials indicate that the surface pressures on the human skin during abrasion events are probably slightly lower than those measured on the rigid target surface. Uncertainty about the actual levels of surface pressure on the skin remains because of difficulties in the measurement procedure. However, pressure levels in excess of 175 kg/cm^2 (2500 psi) were measured on human skin over the site of stamp-type abrasions.

5.3 EXPERIMENTAL AIRBAG FOLD TECHNIQUE

In a small number of tests, an experimental airbag fold technique incorporating the findings of this study was shown to reduce the incidence of abrasion by reducing peak airbag fabric velocities. The lowered velocities resulted in lowering of peak surface pressures on a rigid target surface below the levels associated with skin abrasion. In a test with a human volunteer, the experimental fold did not produce abrasion under test conditions for which the standard airbag fold caused abrasions with immediate surface bleeding. These tests demonstrated that modification of the airbag fold is an effective means of reducing the abrasion potential of an airbag system.

5.4 DIRECTIONS FOR FUTURE RESEARCH

A more complete study of the threshold response of human skin to abrasion events should be conducted. It is particularly important to assess the variability among different types of skin (*e.g.*, young, old, male, female) and the interaction between lateral

velocity, impact pressure, and injury severity. These experiments should include consideration of alternative airbag fold techniques, since these will result in different kinematics and possibly different injury types or mechanisms.

Although a finer mesh airbag fabric appeared to be less important than other design factors in this research, other fabrics that may be used in airbags, such as uncoated fabrics, should be evaluated with respect to their potential to cause mechanical skin injury.

Further, since the severe impacts created by high-velocity airbag fabric are sufficient to cause skin injury, damage to other tissue, such as the cornea or sclera of the eye, might also result. A study needs to be made of the tolerance of eye tissue, eyelids, eye sockets, etc., to airbag fabric impact, to determine if design guidelines based on reducing skin abrasion are adequate, or if other changes are desirable to reduce airbag-induced injuries further.

REFERENCES

Box, G.E.P (1978) *Statistics for experimenters*. John Wiley and Sons, New York.

Digges, K.H., Roberts, V., and Morris, J. (1989) *Residual injuries to occupants protected by restraint systems*. SAE Paper no. 891974.

Huelke, D.F., Roberts, J.V., and Moore, J.L. (1992) Air bags in crashes: clinical studies from field investigations. To be published in *Proc. of the 13th International Technical Conference on Experimental Safety Vehicles*. U.S. Department of Transportation, National Highway Traffic Safety Administration, Washington, D.C.

Kikuchi, A., Horii, M., Kawai, A., Kawai, S., Komaki, Y., and Matsuno, M. (1975) Injury to eye and facial skin (rabbit) on impact with inflating air bag. *Proc. 2nd International Conference on the Biomechanics of Serious Trauma*, pp. 289-296. Edited by J.P. Cotte and M.M. Presle. IRCOBI, Bron, France.

Reed, M.P., and Schneider, L.W. (1992) *Assessing the skin abrasion potential of driver-side airbags*. Report no. UMTRI-92-6. University of Michigan Transportation Research Institute, Ann Arbor.

Schneider, L.W., Johnson, G., Ostrom, M., Reed, M., Burney, R., and Flannagan, C. (1991) *Investigation of airbag-induced abrasions using deployments into human volunteers*. Final Report no. UMTRI-91-32. University of Michigan Transportation Research Institute, Ann Arbor.

Smith, G.R., Gulash, E.C., and Baker, R.G. (1974) *Human volunteer and anthropomorphic dummy tests of General Motors driver air cushion system*. SAE Paper no. 740578.

APPENDIX

PHOTOGRAPHS OF SUBJECTS' LEGS TAKEN 15 MINUTES AFTER TESTS WITH 60-LITER AIRBAGS, IN RANK ORDER OF INJURY SEVERITY

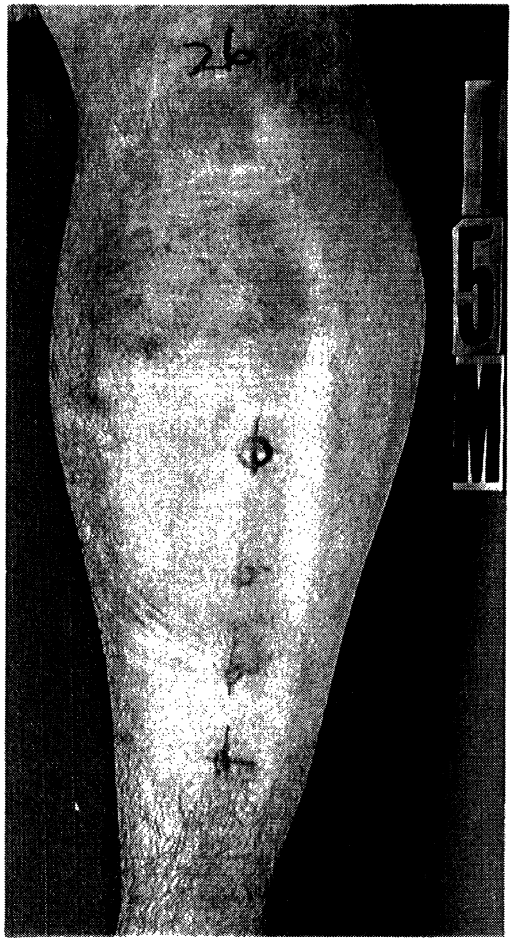

Test No. HA9126*
840 D 350 kPa 300 mm U.
ARS 3 Rank 9

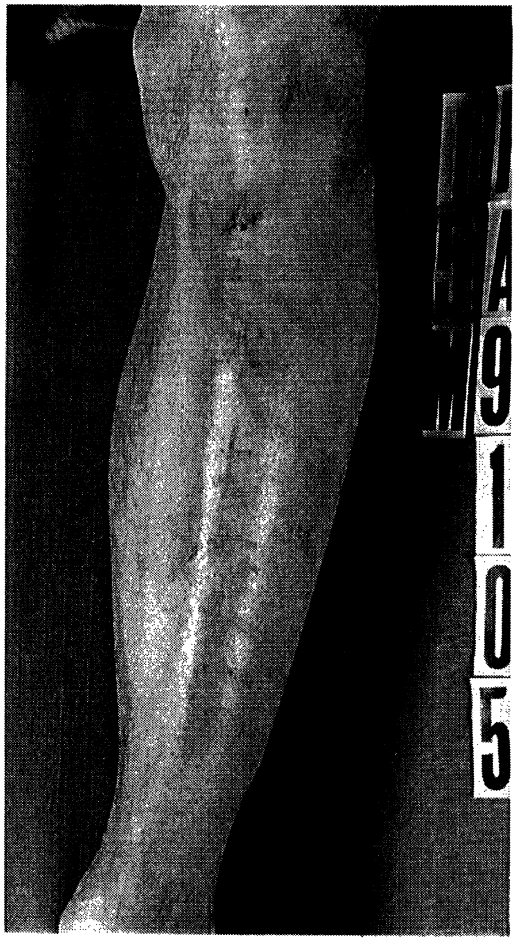

Test No. HA9105
420 D 350 kPa 250 mm T.
ARS 3 Rank 10

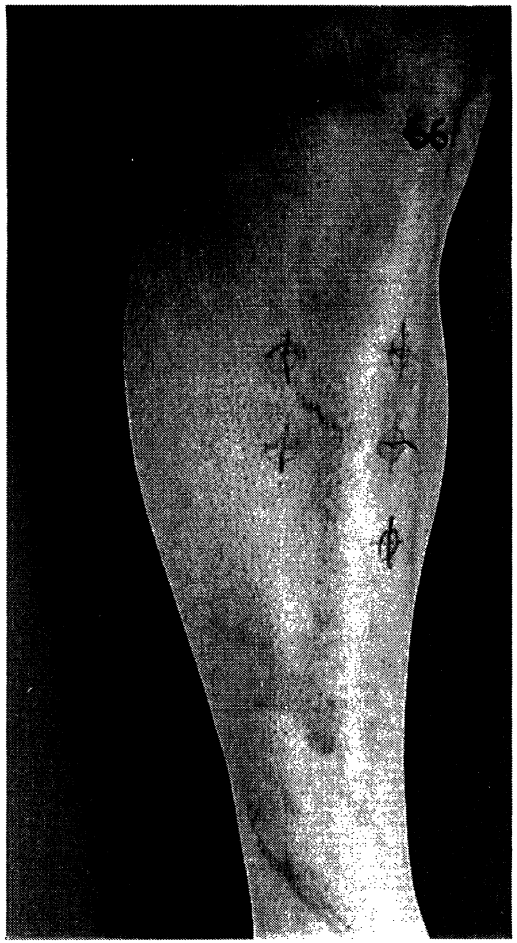

Test No. HA9166
420 D 350 kPa 300 mm U.
ARS 3 Rank 11

*840 D = Fabric Denier; 350-kPa = Inflator Capacity; 300 mm = Distance from module; U = Untethered; Tests below rank 9 are ARS 1 and are not shown.

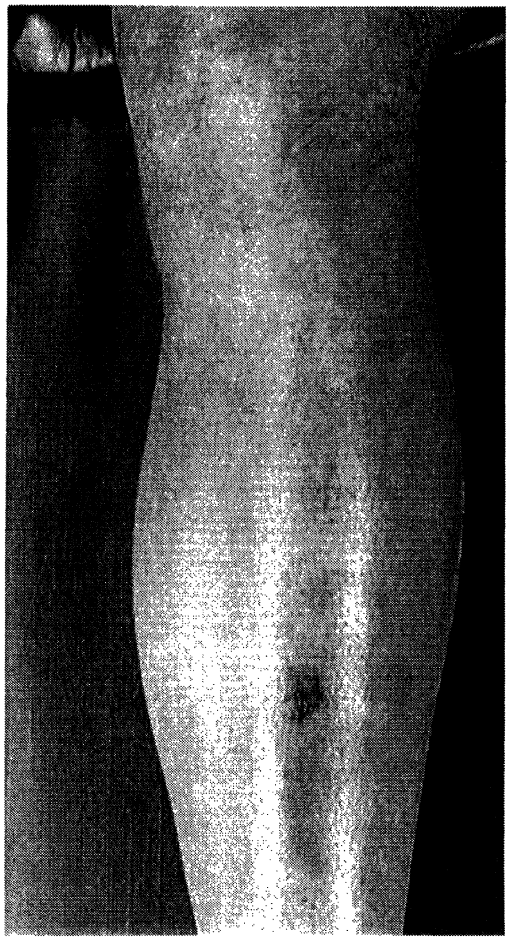

Test No. HA9109
420 D 350 kPa 300 mm T.
ARS 3 Rank 12

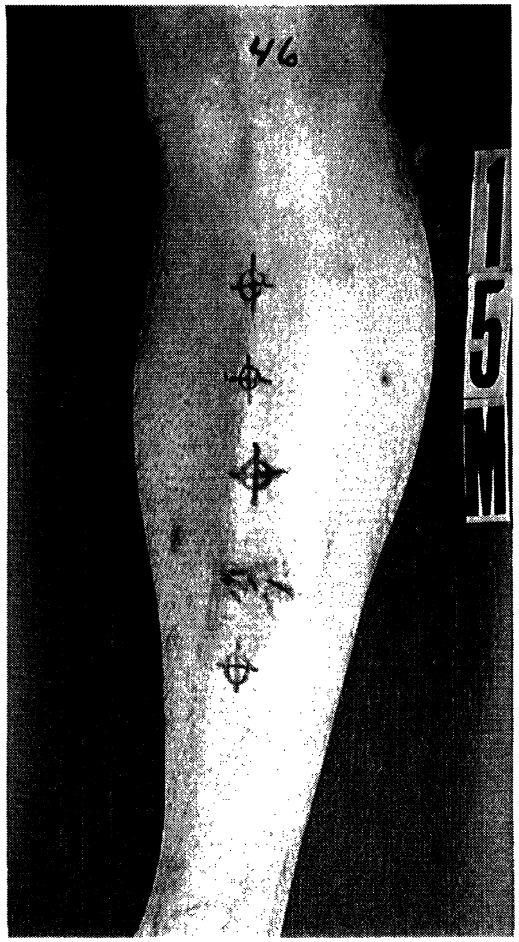

Test No. HA9146
420 D 350 kPa 300 mm T.
ARS 3 Rank 13

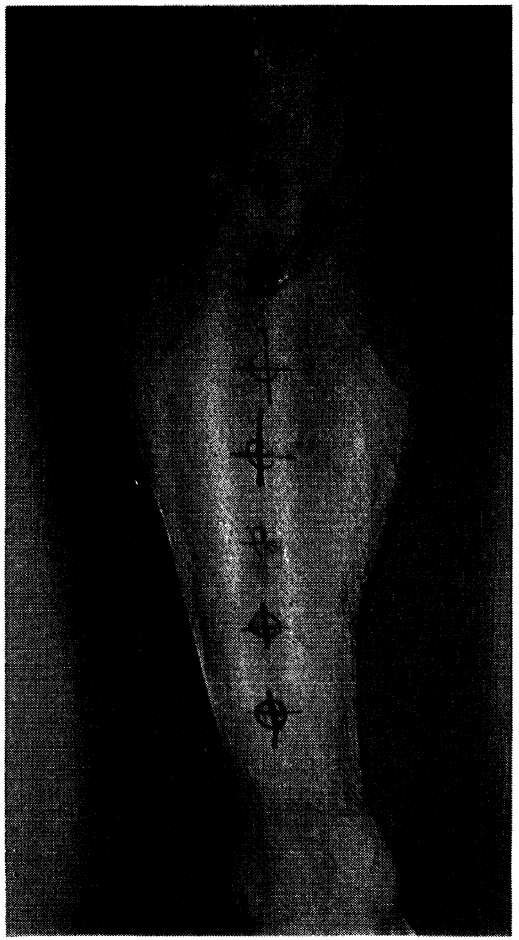

Test No. HA91110
420 D 320 kPa 225 mm T.
ARS 3 Rank 14

Test No. HA9155
840 D 320 kPa 225 mm U.
ARS 3 Rank 15

Test No. HA9123
420 D 350 kPa 325 mm U.
ARS 3 Rank 16

Test No. HA9125
420 D 350 kPa 275 mm U.
ARS 3 Rank 17

Test No. HA9124
420 D 350 kPa 275 mm T.
ARS 3 Rank 18

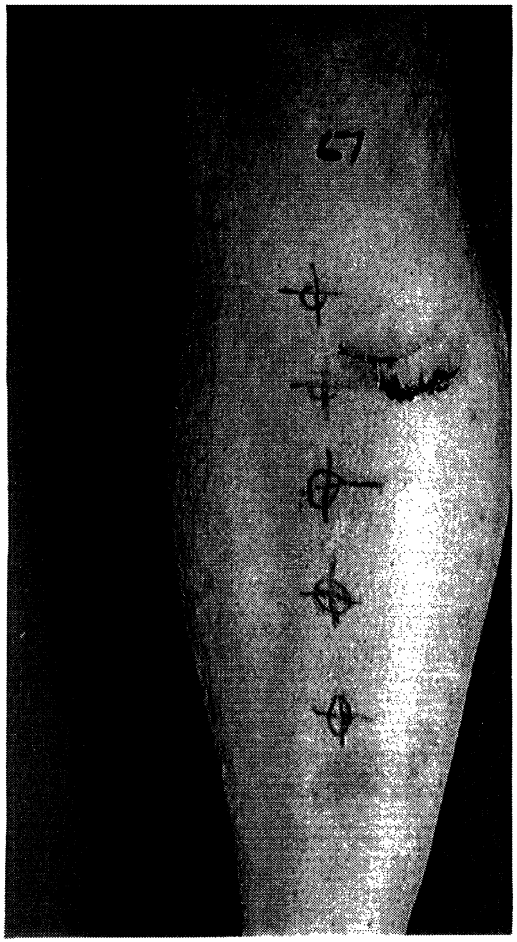

Test No. HA9167
420 D 320 kPa 225 mm T.
ARS 3 Rank 19

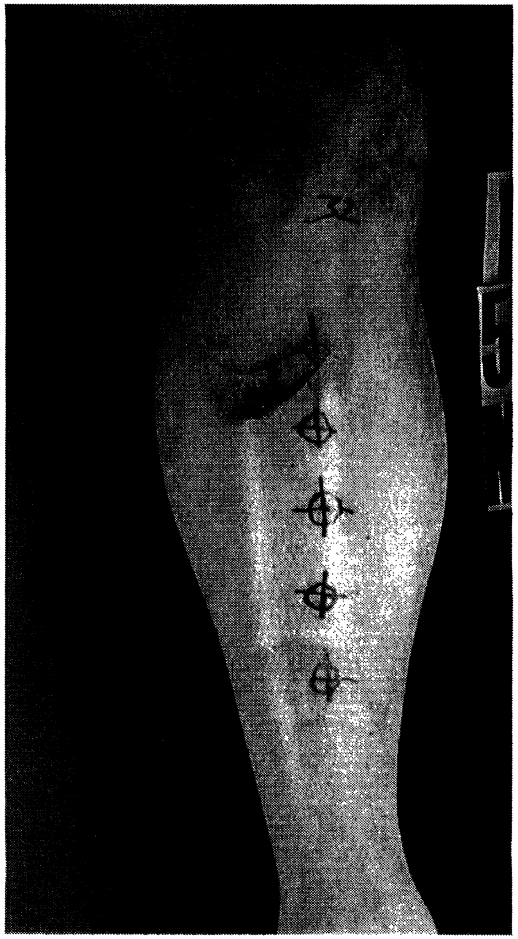

Test No. HA91132
420 D 320 kPa 225 mm U.
ARS 3 Rank 20

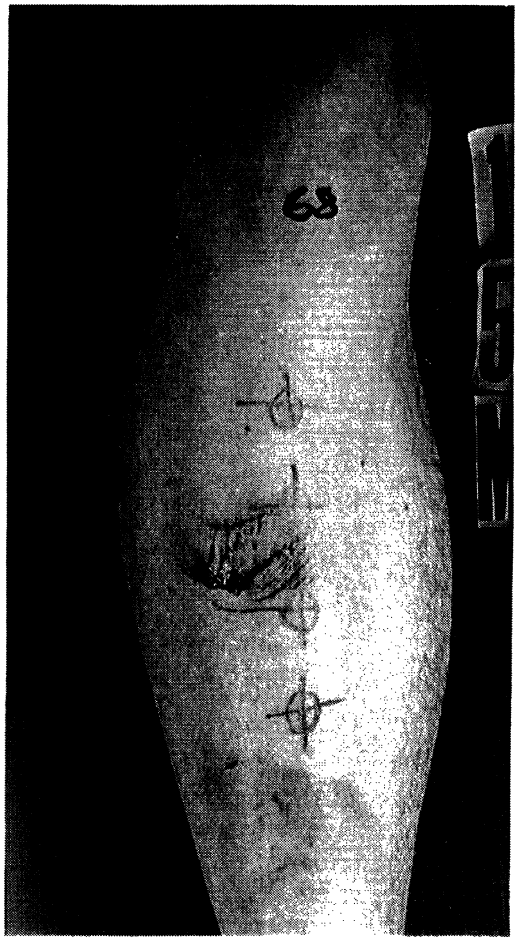

Test No. HA9168
420 D 320 kPa 225 mm T.
ARS 3 Rank 21

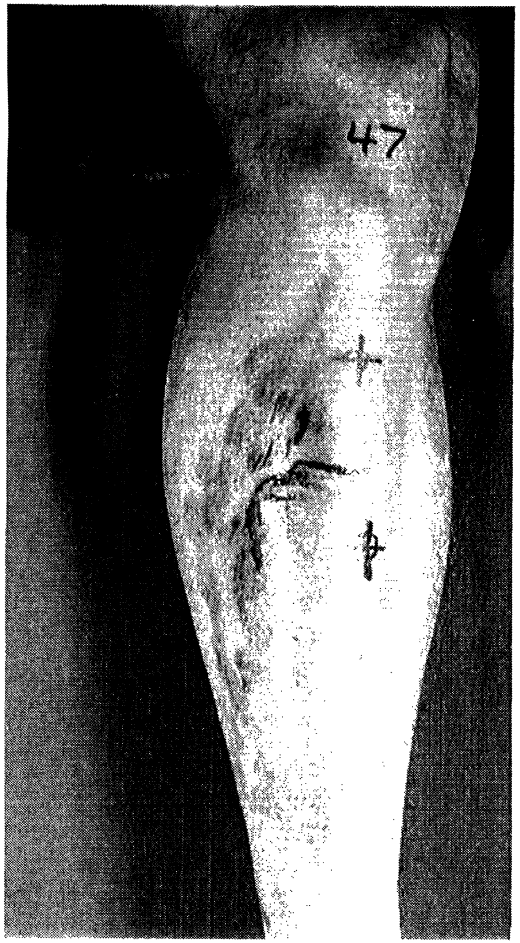

Test No. HA9147
420 D 350 kPa 300 mm U.
ARS 3 Rank 22

Test No. HA9165
420 D 350 kPa 300 mm U.
ARS 3 Rank 23

Test No. HA9152
420 D 320 kPa 225 mm T.
ARS 3 Rank 24

Test No. HA9154
840 D 350 kPa 225 mm U.
ARS 4 Rank 25

Test No. HA9106
420 D 350 kPa 250 mm U.
ARS 4 Rank 26

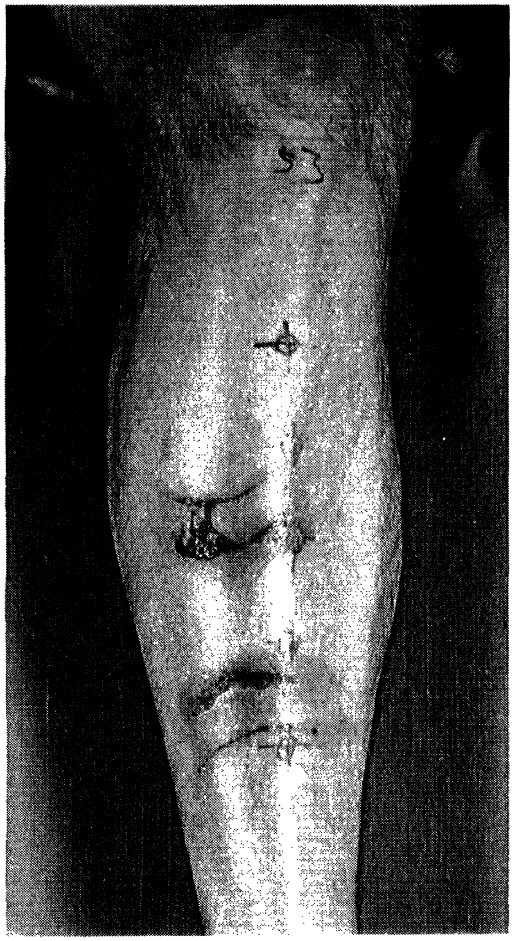

Test No. HA9153
420 D 320 kPa 225 mm U.
ARS 4 Rank 27

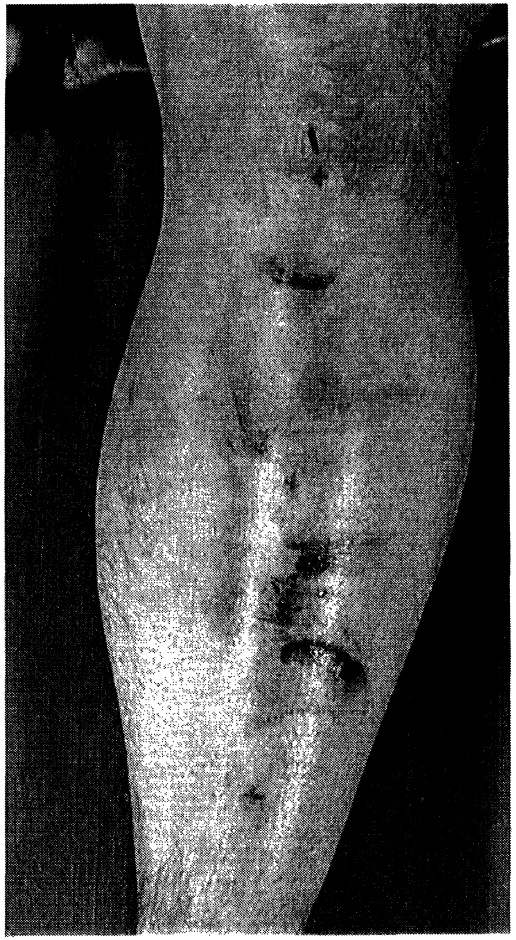

Test No. HA9107
420 D 350 kPa 225 mm T.
ARS 4 Rank 28

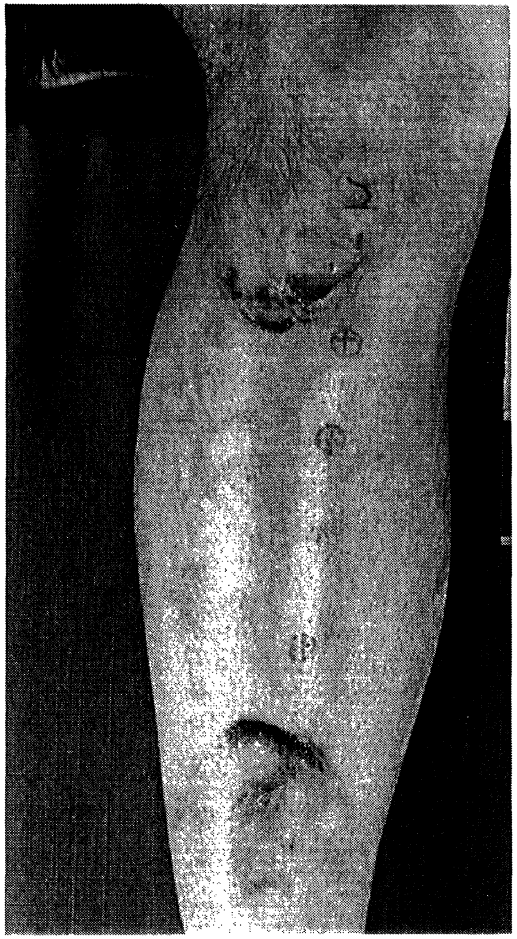

Test No. HA9108
420 D 350 kPa 225 mm U.
ARS 4 Rank 29

Test No. HA9112
420 D 350 kPa 350 mm U.
ARS 4 Rank 30

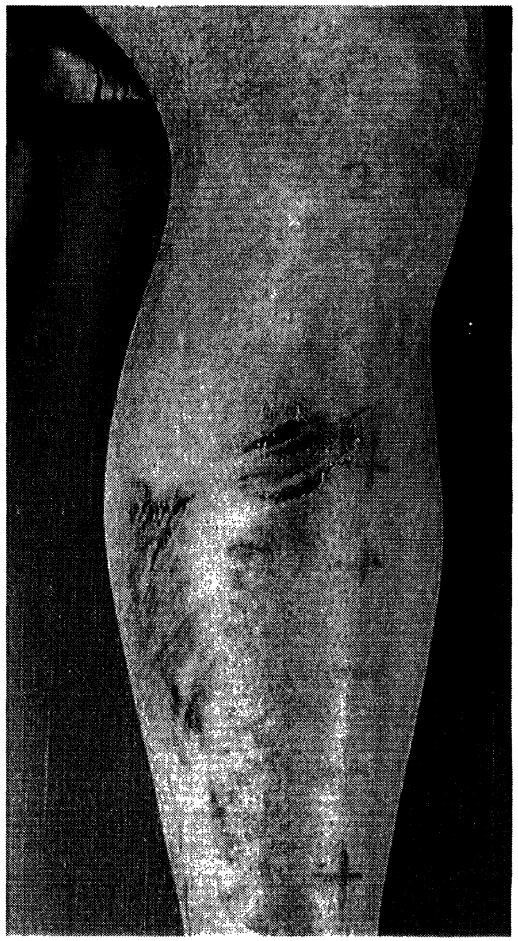

Test No. HA9110
420 D 350 kPa 300 mm U.
ARS 4 Rank 31

Test No. HA9150
420 D 350 kPa 225 mm T.
ARS 4 Rank 32

Test No. HA9151
420 D 350 kPa 225 mm U.
ARS 4 Rank 33

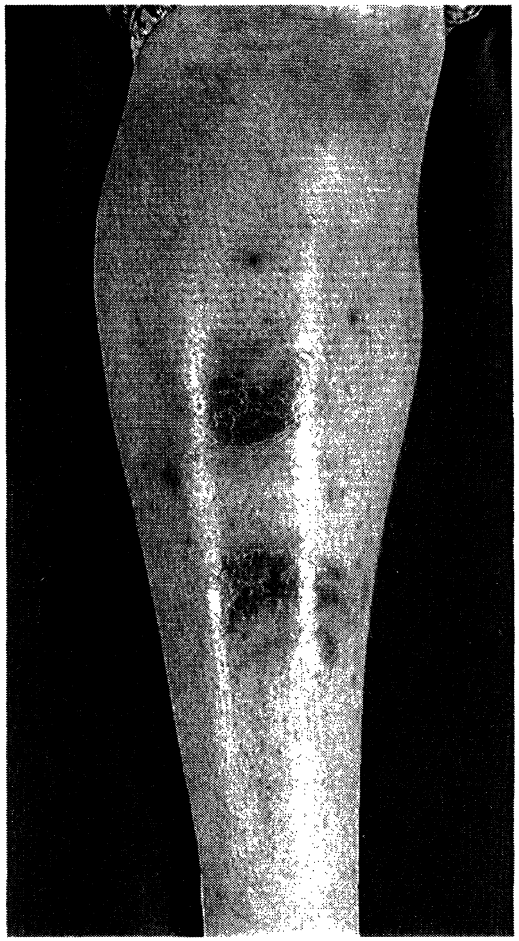

Test No. HA9151
420 D 350 kPa 225 mm U.
Three Weeks Post-Test

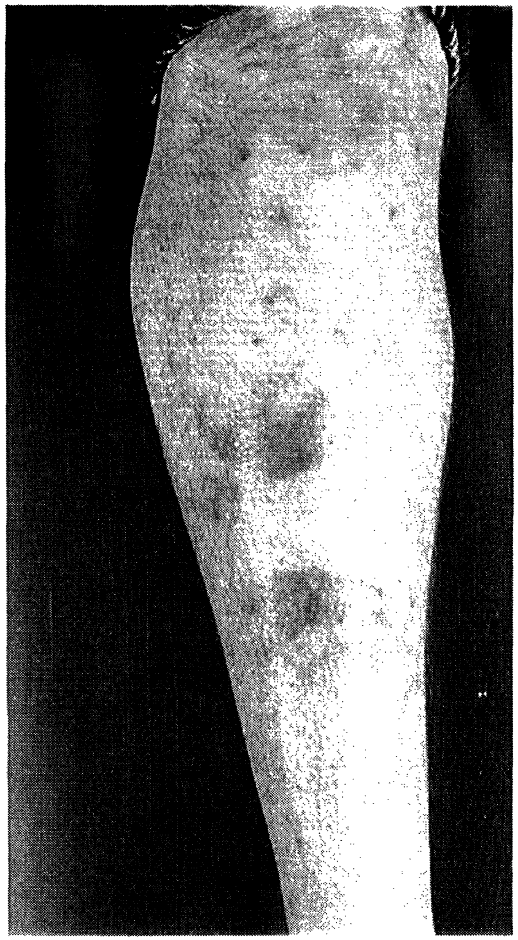

Test No. HA9151
420 D 350 kPa 225 mm U.
Eight Weeks Post-Test